Water-soluble photoswitchable supramolecular hosts based on the hemiindigo chromophore

by

Anton Kliuchynskyi

B.Sc., Taras Shevchenko National University of Kyiv, 2020

A Thesis Submitted in Partial Fulfillment of the

Requirements for the Degree of

MASTER OF SCIENCE

in the Department of Chemistry

University of Victoria

We acknowledge and respect the Lək^{w}əŋən (Songhees and Esquimalt) Peoples on whose territory the university stands, and the Lək^{w}əŋən and W̱SÁNEĆ Peoples whose historical relationships with the land continue to this day.

Water-soluble photoswitchable supramolecular hosts based on the hemiindigo chromophore

by

Anton Kliuchynskyi

B.Sc., Taras Shevchenko National University of Kyiv, 2020

Supervisory Committee

Dr. Fraser Hof, Department of Chemistry

Supervisor

Dr. J. Scott McIndoe, Department of Chemistry

Departmental member

Abstract

The constant search for new and unusual hosts is what pushing supramolecular chemistry forwards. The scope of their applications is immense: drug recognition and reversal, novel materials, catalysis, purification and separation of chemicals etc., not to mention a fundamental insight into chemical and biological systems that can be gained by studying them. Sulfonated calixarenes constitute an important family of such hosts. Their exceptional binding properties coupled with water-solubility, high stability and endless potential for synthetic modifications make them perfect candidates for study. There are numerous examples of those macrocycles, modified in a way that introduces a fluorescent chromophore, enabling them to be used as detectors for various guests. Yet, cases of them being able to change their properties upon irradiation with light – having a photoswitchable chromophore – remain particularly scarce. This work attempts to present such system – a pair of sulfonated calixarenes, calix[4] and calix[5]arene with a hemiindigo moieties installed on the upper rim. Here we demonstrate their synthesis, as well as a study into their photophysical and supramolecular properties. Various advanced NMR techniques such as DOSY and NOESY were used in conjunction to demonstrate differences in their aggregation.

Table of Contents

List of Figures

Supporting Information

List of Tables

List of Abbreviations

Å – Angstrom, 10^{-10} m

Abs - Absorbance

ATR-FTIR - Attenuated Total Reflectance Fourier Transform Infrared

MeCN – Acetonitrile

COSY – Correlated Spectroscopy

DAD – diode array detector

DNA – deoxyribonucleic acid

DMF – dimethyl formamide

DMSO – dimethyl sulfoxide

DOSY – diffusion-ordered spectroscopy

ESI – electrospray ionization

EXSY – exchange spectroscopy

HRMS – high-resolution mass spectrometry

HPLC– high-performance liquid chromatography

mM – millimole

μM – micromole

NMR – nuclear magnetic resonance

NOE – Nuclear Overhauser effect

NOESY – Nuclear Overhauser effect spectroscopy

PES – Polyethersulfone

ppm – parts per million

RNA – ribonucleic acid

TFA – trifluoroacetic acid

THF – tetrahydrofuran

UV-Vis – ultraviolet-visible

Acknowledgements

First I would like to thank people directly responsible for the very existence of this thesis: my immensely supportive and encouraging supervisor Fraser, HofLab – probably the most professional, yet easy-going collective I've ever encountered – Alok, Becky, Allison, Chelsea, Juan, Emma, Peter, Beena, Cleo, Baxter, Zoey, Kiara, Kirsty, Alana, Izzy, Ethan for all the scientific and psychological help they provided, and, of course, Seth, his contribution turned out to be a decisive one. I hugely appreciate the time spent here with you, guys.

I would give special thanks to Cornelia, Gus and Jesse, not only for letting me use their extremely very-well maintained equipment, but also for providing a fresh perspective on science. To Scott McInode, for allowing me to brag about Fraser. To Violeta Iosub, Kelli Fawkes and Michelle Mills, for trusting me to teach those fun courses. To Chris Bar, Ori and Eerik for always being so helpful and informative. To the whole staff of CHEM Department for being so considerate and understanding.

To Lily for the incredible moral support. To Yasin, for all those short chat breaks near certain bench. To Babak, for being around in the darkest hour. Of course, to Oleksii and Orysia for all the Discord sessions and movie nights. To Cossack for the gym guidance – it gave me the energy to finish this work. To Uliana. And to my family.

Chapter 1. Introduction

1.1 Structure and applications of calixarenes

The importance of supramolecular chemistry is hard to underestimate. From DNA complexes to molecular machines, from enzymatic catalysis to drug recognition – supramolecular chemistry can be found throughout nature and in the laboratory.[1–5] One of the focal points is the concept of "host-guest" interactions, where one molecule, usually with a concave binding surface (host), binds a smaller molecule (guest) through a collection of non-covalent interactions. Among these, one of the most studied families are the cup-like hosts called calixarenes (Figure 1.1).[6]

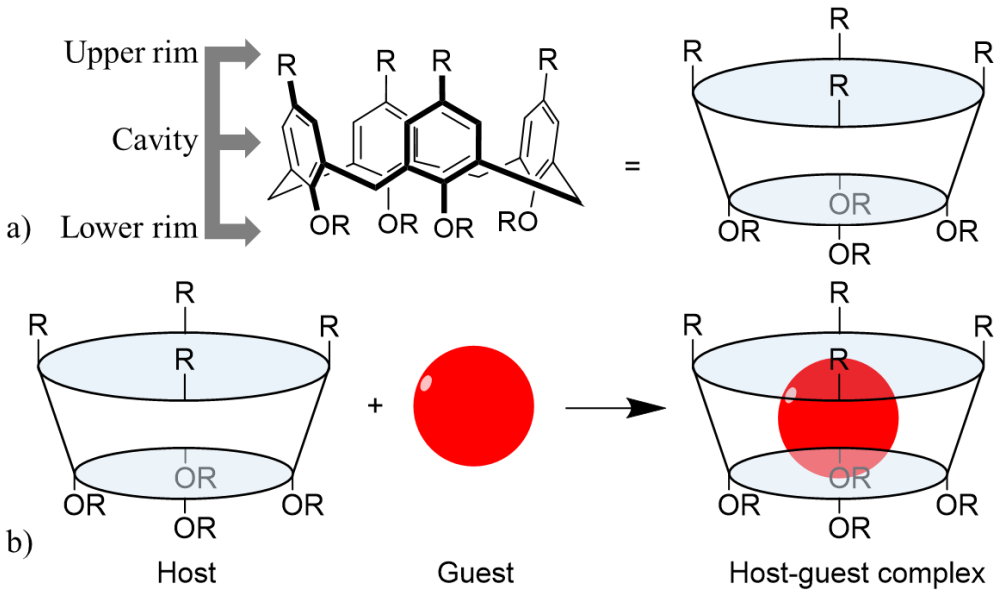

Figure 1.1 a) Parts of a calixarene: upper and lower rim allow modifications (R), aromatic cavity is responsible for primary binding; b) Guest enters the cavity forming a host-guest complex with a calixarene.

Calixarenes are macrocyclic compounds, consisting of 4-10 phenol units connected at the 2- and 6-positions by methylene bridges. The creation of a binding pocket lined by aromatic rings theoretically allows for efficient *endo*-complexation. However, simple unsubstituted calixarenes are usually outperformed by other macrocycles, such as cyclodextrins and crown ethers.[7] Furthermore, the poor water-solubility of simple calixarenes limits their use in biomedical applications. Therefore, extensive modifications of aromatic *para*-positions (usually referred to as the *upper rim*) and phenolic hydroxyls (referred to as the *lower rim*) (Figure 1.1a) are required to uncover their "almost unlimited potential".[6]

Therefore, modifications that increase water-solubility are of particular biomedical interest. This is generally achieved by installation of charged or neutral polar functional groups on either rim of the host molecule. In addition to solubility, they can form non-covalent interactions with corresponding sites on the guest. More importantly, they enhance the binding ability of the aromatic cavity due to the hydrophobic effect – tendency of nonpolar compounds to aggregate together in aqueous solutions.[8] Finally, modifications increase the utility of calixarenes in real-world applications, allowing them to be used aqueously and in biological fluids, for example, as chemosensors for drugs[4] and biomarkers[9] or as drug and poison reversal agents.[10]

Usually, enhanced solubility is achieved via installation of charged groups like sulfonates (**3**),[11] carboxylic acids (**5**),[12] phosphonates (**8**)[13] or amines (**4, 6**)[14] in the *para*-position of the aromatic ring. Such charged calixarenes have the added advantage of a particularly high affinity towards oppositely charged guests, for example, negatively charged *p*-sulfocalix[n]arenes have shown high affinity towards cationic molecules.[15] Examples of neutral molecules[16] as well as aforementioned charged groups,[17,18] but installed on the lower rim (**2**, **7**, **9**), also exist.

However, enhanced water-solubility is rarely enough to make calixarenes useful. Additional tuning of both rims is often required to reach the desired properties. As expected from phenols, lower-rim modifications are usually introduced by various esterifications or etherifications.[19] In contrast, the upper-rim modification chemistry is more versatile. It often relies on cross-couplings[20] or imine formation[21] to install various alkyl and aryl groups that would steer the affinity towards target guests or introduce certain physical properties, such as fluorescence.[22]

The aim of this Chapter is to give an overview of existing upper and lower-rim modifications of water-soluble calixarenes, along with their applications and synthetic routes. This will help to get a better impression of current scope of

functionalization and potential tools at our disposal in order to develop new synthetic procedures for novel calixarenes.

1.2 Solubilizing the calixarene

As previously mentioned, to enable most of their biomedical functionality calixarenes have to be made soluble in water. There are a plethora of methods to this end, most of which ultimately rely upon installation of charged groups on either rim. Many such groups are also able to form numerous hydrogen bonds and electrostatic interactions, thus achieving an additional desired property of guest engagement and recognition (Figure 1.2).

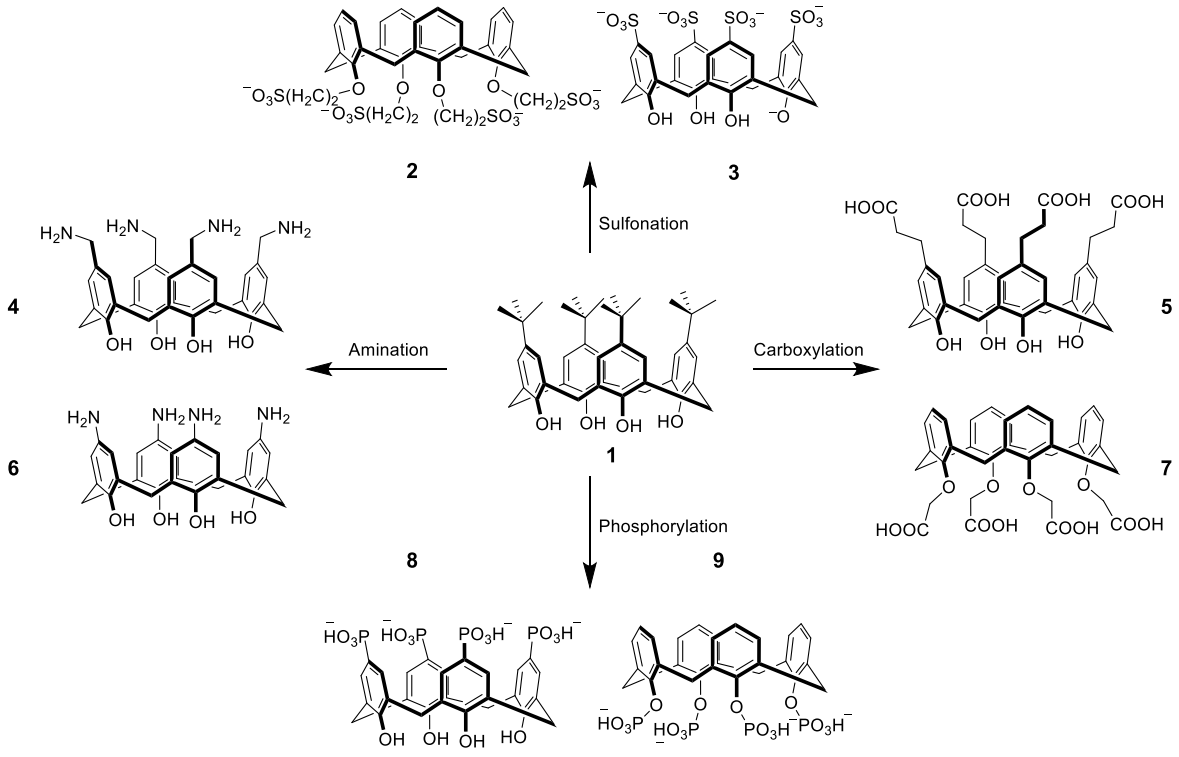

Figure 1.2. General routes towards water-soluble calixarenes.

1.2.1 Sulfonation

Sulfonation is the most widely used approach to calixarene solubilization. This is mainly due to its making highly soluble calixarenes, relatively simple preparation, and strong (yet not always selective) binding towards common guests, e.g. cationic drugs. There are four main sulfonation methods: direct, ipso-, chloro- and lower-rim via alkylation. Each methods has its advantages, disadvantages, and appropriate targets.[23]

Of these methods, direct sulfonation is the most popular. First developed by Shinkai et al.,[11] it consists of Friedel-Crafts dealkylation of 4-*tert*-butylcalix[4]arene **1** to calix[4]arene **10** followed by electrophilic aromatic substitutions *para* to the phenol groups to get 4-sulfocalix[4]arene **3**. This reaction is most often achieved in hot sulfuric acid (Figure 1.1).

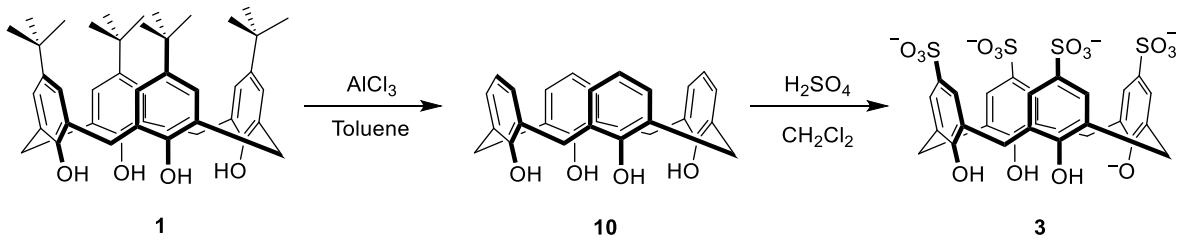

Figure 1.3. An example of direct sulfonation of calixarenes.

Ipso-sulfonation of 8-*tert*-butylcalixarene to 8-sulfocalix[8]arene gives an alternative approach, by not requiring a dealkylation step. Low solubility of *p*-H-calix[8]arene in commonly used solvents hinders its usage, especially in lower-rim alkylations and therefore, an alternative route is desired. This

approach is plagued by products of partial substitution and generally low yields and is preferable only in case of 8-*tert*-butylcalixarene **11** conversion to 8-sulfocalxi[8]arene **12** (Figure 1.4).[24]

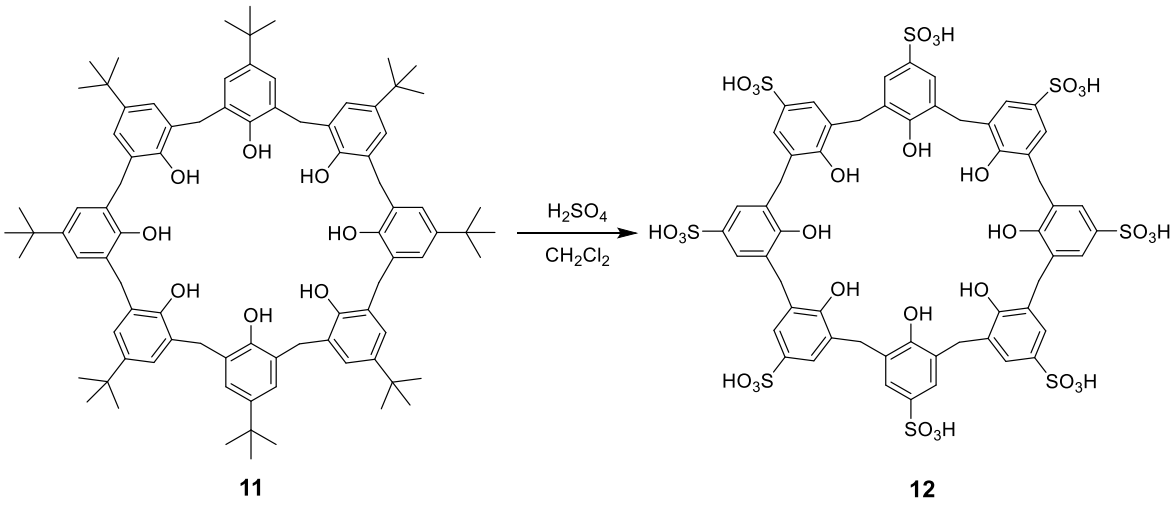

Figure 1.4. Ipso-*sulfonation of calix[8]arene.*

Chlorosulfonation utilizes chlorosulfonic acid instead of sulfuric acid, providing a parallel path from calix[4]arene **10** to 4-sulfocalix[4]arene **3** . The intermediate chlorosulfonyl groups can be readily hydrolyzed to sulfonates upon treatment with water (Figure 1.5).[25,26] This reaction has a tendency to remove lower rim ether groups, which significantly limits its usage.[27]

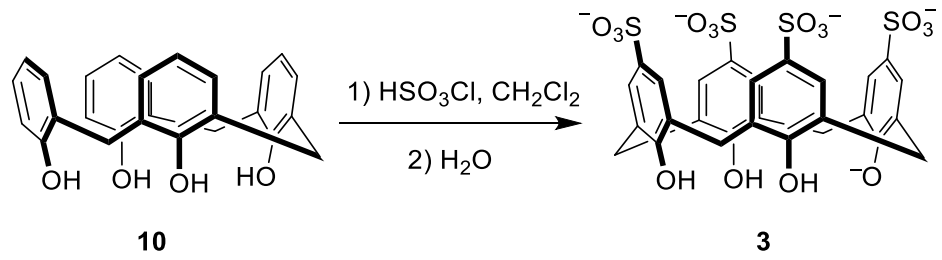

Figure 1.5.The chlorosulfonation route to sulfonated calixarenes.

Finally, lower-rim sulfonation differs from the other three methods, since it is not an electrophilic aromatic substitution, but instead involves an alkylation of **10** with 1,3-propane sultone in tetrahydrofuran (THF).[18] The resulting host **2** is water-soluble, due to the pendant sulfonates, but has the charged groups farther from the concave guest-binding pocket (Figure 1.6).

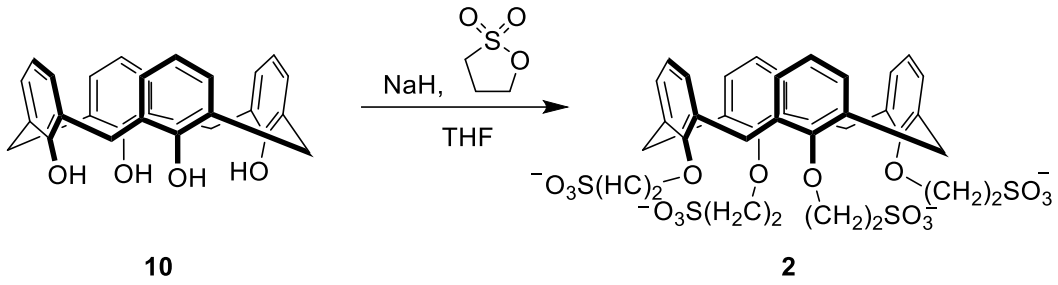

10 **2**

Figure 1.6. An example of lower-rim sulfonation of calixarenes.

1.2.2 Phosphonation and phosphorylation

Just like with sulfonation, phosphonic groups can be installed either in *p*-position of the aromatic ring or on the phenolic hydroxyl. The first historical method was developed by Ungaro et al.[28] The reaction proceeds via chloromethylation of **10** with chloromethyl octyl ether to **13** followed by the Arbuzov reaction and subsequent partial (**15)** or full hydrolysis of the resulting phosphonic esters or McKenna deprotection with bromotrimethylsilane **(14)** (Figure 1.7).

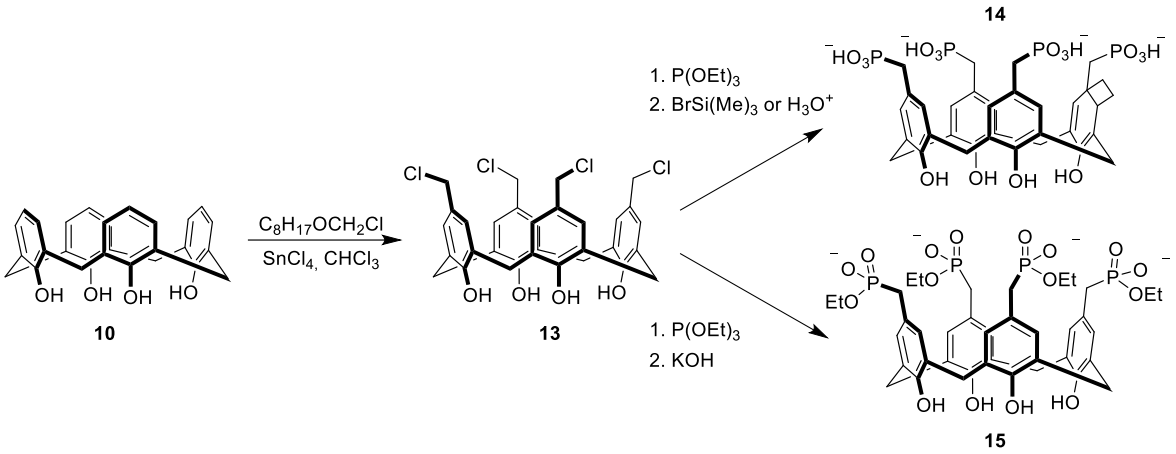

Figure 1.7. Upper-rim phosphonation via chloromethylation.

Direct phosphonation was described by Kalchenko et al.[29] It relies on a similar Arbuzov reaction but is preceded by direct *ipso*-bromination[30] of **1** with *N*-bromosuccinimide (NBS), with subsequent McKenna deprotection or hydrolysis to obtain 4-phosphonatocalix[4]arene **8**.[26] Both of the aforementioned types of macrocyles have solubilities in the mM range (Figure 1.8).

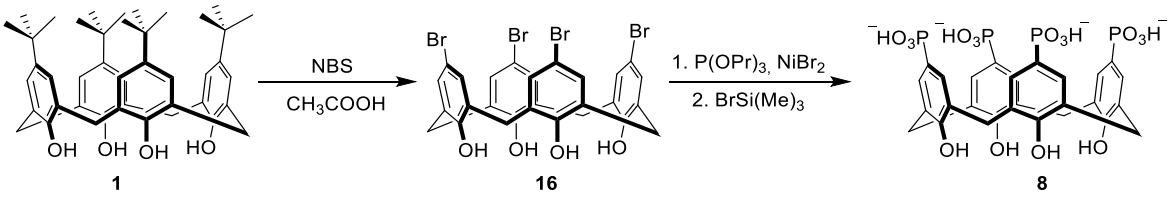

Figure 1.8. Direct upper-rim phosphonation.

Finally, lower-rim phosphorylation can be achieved by reaction of **10** with diethyl chlorophosphate followed by hydrolysis or McKenna conversion of intermediate phosphonate esters into phosphonic acid **9** (Figure 1.9).[31] These

compounds are known to have amphiphilic properties and were shown to enhance solubility of poorly soluble drugs.[32]

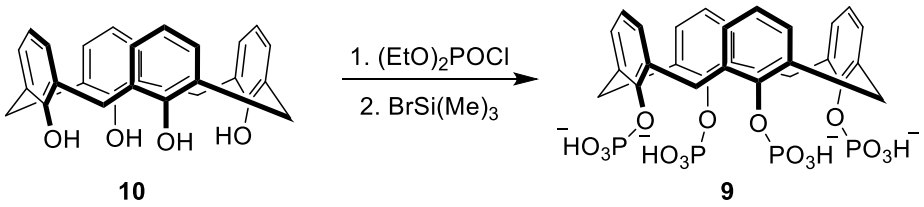

Figure 1.9. Lower-rim phosphorylation.

1.2.3 Carboxylation

Historically the first water-soluble calixarene **7** was created by Ungaro et al. with the help of carboxylic acid functions installed on the lower rim via alkylation of **1** with esters of bromoacetic acid and subsequent hydrolysis (Figure 1.10).[33] While this tetracarboxylic acid did not dissolve on its own, deprotonation to create carboxylate salts with alkali metal counterions provided solubility in the mM range (depending on the metal).

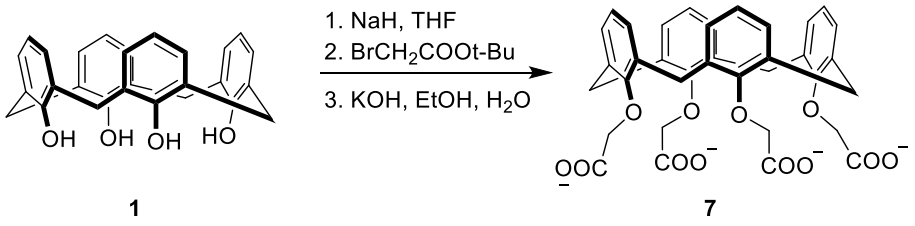

Figure 1.10. Lower-rim carboxylation.

Similarly to previous examples, carboxyl groups can be installed on the *p*-position of the upper rim, although in a more complex procedure designed by

Gutsche et al.[34] Starting from Mannich aminomethylation of **10** (with diallylamine for best results), the resulting amines **17** or are quaternized with methyl iodide. Treatment with sodium diethyl malonate displaces the ammonium leaving group and produces an octaester, which after hydrolysis and decarboxylation gives the desired carboxylic calixarene **5** (Figure 1.11).

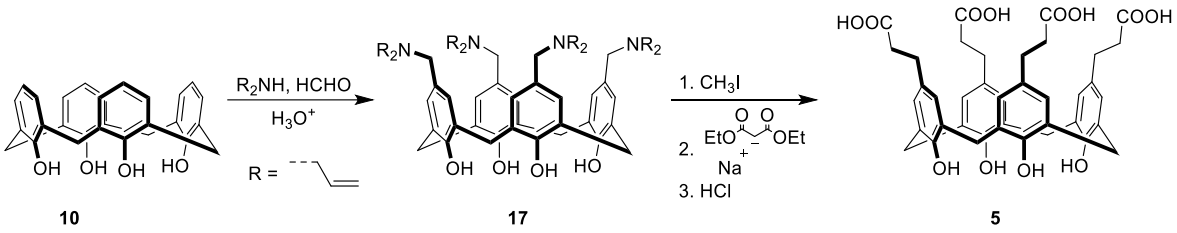

Figure 1.11. Upper-rim carboxylation with ethylene linkage.

Finally, carboxylic acid can be introduced directly on the *para*-position without a linkage, following a procedure similar to previous one (Figure 1.11), but using sodium methoxide as a nucleophile after quaternization. The resulting ether **18**

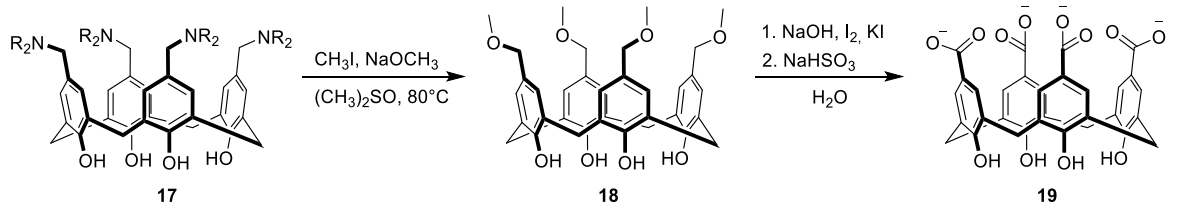

Figure 1.12. Direct upper-rim carboxylation.

is then subjected to oxidation with iodine to produce the desired carboxyl **19** (Figure 1.12).[35,36]

1.2.4 Amination

Aminocalixarenes are somewhat different from the aforementioned calixarenes, due to their positive charge and basic nature, which leads to high affinity towards various anionic guests. DNA and other nucleic acids are of particular interest.[37,38] The first approach suggested by Gutsche utilizes the same Mannich route as mentioned previously to install alkylammonium leaving groups, albeit with an azide as a nucleophile. The resulting azidocalixarene **19** then gets reduced[35] to reveal the primary amine functional groups **4** (Figure 1.13).[31]

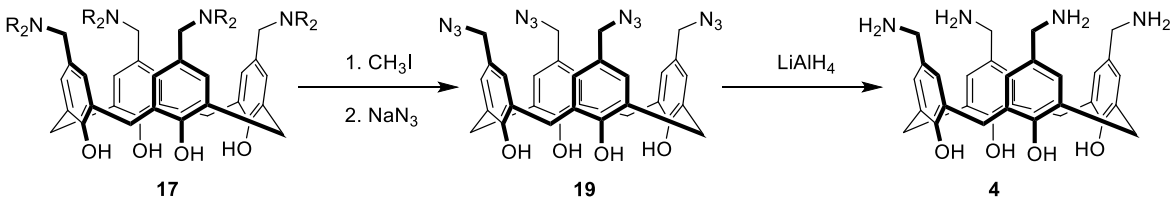

Figure 1.13. Amino-methylation.

An even simpler approach exists to install amines in the *p*-position of the benzene ring. It relies upon *ipso*-nitration of *t*-butyl calixarene with nitric acid to get 4-nitrocalix[4]arene **20**, followed by catalytic reduction to form 4-aminocalix[4]arene **6** (Figure 1.14).[39] These *p*-aminophenol functional groups are not as basic as the primary amines described above and therefore, require more acidic conditions for protonation in water.

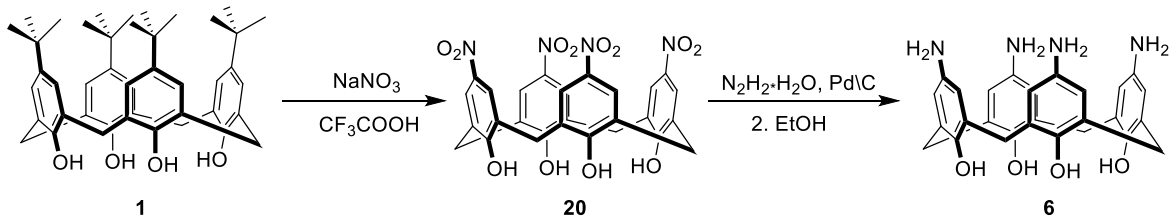

Figure 1.14. Amination via nitration.

An alternative path exists, which relies on reaction of **10** with *p*-substituted anilines**.** Resulting azocalixarenes **21a-c** are subsequently reduced with zinc to obtain **6** (Figure 1.15)**.**

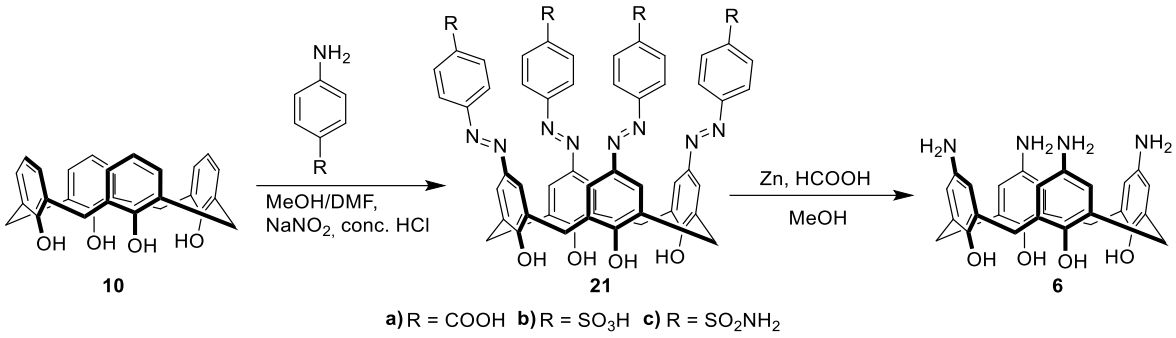

Figure 1.15. Aminocalixrene synthesis via azo path. Azocalixarene is also water-soluble.

It has an added advantage that the same approach can be utilized to introduce water-solubility indirectly by installing a solubilizing group bound to the calixarene via a diazo linkage. Such compounds have promising uses as dyes due to their extended conjugated elements.[40,41]

1.3 Fine tuning

While simple symmetric modifications of all available calixarene rings (such as the aforementioned) can result in biomedical utility, finer tuning is often

required to impart the desired property. The examples of interest for this thesis are those that introduce mixtures of functional groups on the upper rim, which is also the edge of the binding surface of the calixarene pocket. Most synthetic routes usually involve a "building-up" of functionality from a rather limited number of simple functional group handles that lend themselves well to further, late-stage synthetic modifications. The most common are aldehydes, halides, and amines that must first be installed in the *para*-position of the aromatic ring. It is possible to classify existing designs either from the perspective of functional groups present on the final products, or by looking at chemical transformations that introduced said functional groups. To keep the focus of this Chapter on synthetic routes and approaches, I will instead present them by dividing them into categories based on the choice of synthetic *handle* used as a jumping-off point at the initial stage of the synthesis. Such handles do not necessarily provide water-solubility, so often some sort of solubilizing group as described previously must also be installed, which adds further synthetic complications. Phenolic protons on the lower rim, in turn, can also be viewed as handle-like, albeit limited almost exclusively to alkylations and esterifications (Figure 1.16).

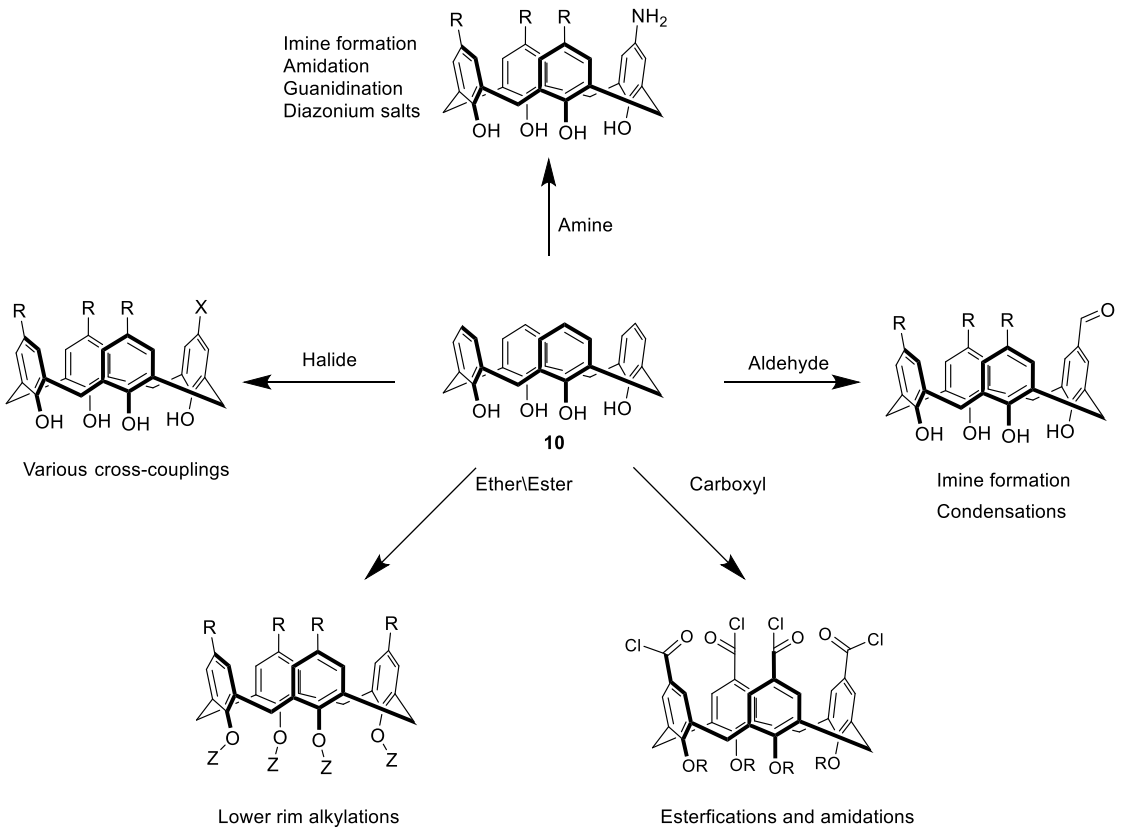

Figure 1.16. Functionalization of water-soluble calixarenes.

1.3.1 Aldehyde handle

One such handle is an aldehyde group. It can be relatively easily installed on the upper rim, yielding mono- (**35)** or di-substituted (**36**, **37**) products for calix[4]arenes and mono-substituted for calix[5]arene (**38**).[15,42,43] First, esterification of calix[4]arene **10** or calix[5]arene **22** with benzoyl chloride is carried out to deactivate the corresponding rings, with varying conditions allowing for regioselectivity with regard to disubstituted products (**23-26**) . Duff formylation follows,[15] installing the desired aldehyde on remaining activated sites, providing **27-30.** Removal of ester groups from the lower rim follows to

obtain **31-34** with subsequent sulfonation to provide desired water-solubility in the presence of one or two aldehyde handles (**35-38**) (Figure 1.17).

While sulfonated aldehydes themselves were shown to be potent binders of cationic guests,[15] they are more important as intermediates on the road towards a rather sizeable array of various upper-rim modifications. Hypothetically, the scope of such modifications is limited only by the chemistry of benzaldehydes, yet only two distinct routes have as-yet been given significant attention – Knoevenagel-type condensation with methyl pyridinium salts, like **39**[22] and formation of hydrazones, such as **40** (Figure 1.18).[21]

The Knoevenagel reaction has proven to be a viable tool for installation of fluorescent chromophores on the upper rim. Combined with an inherent ability of sulfonated calixarenes to form dimers in aqueous solutions, it allowed for creation of a family of supramolecular sensors that exhibit turn-on response towards various biologically relevant targets, such as drugs and proteins.[4,44]

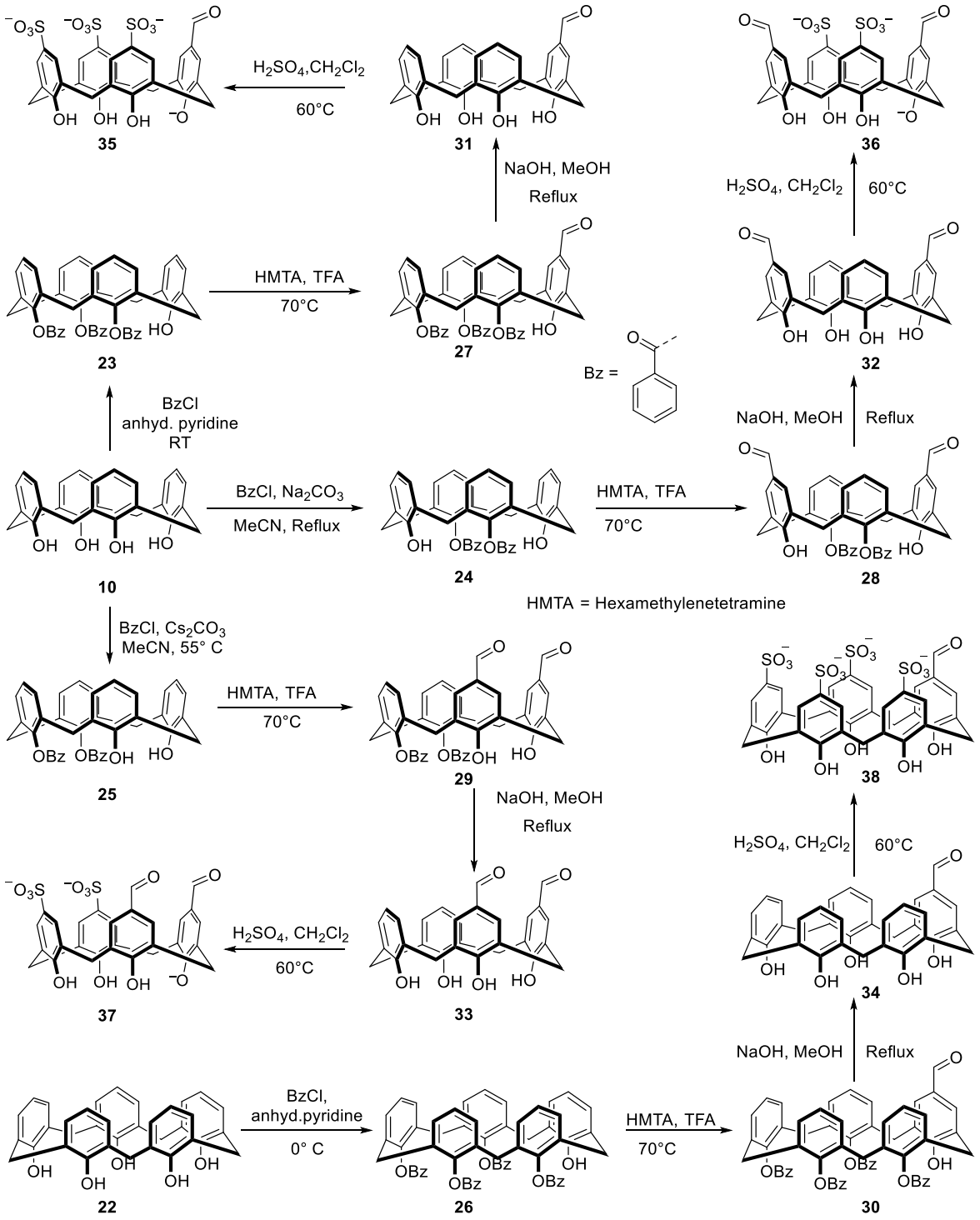

Figure 1.17. Synthetic route towards sulfocalix[4] and [5]arenes with one or two aldehyde handles.

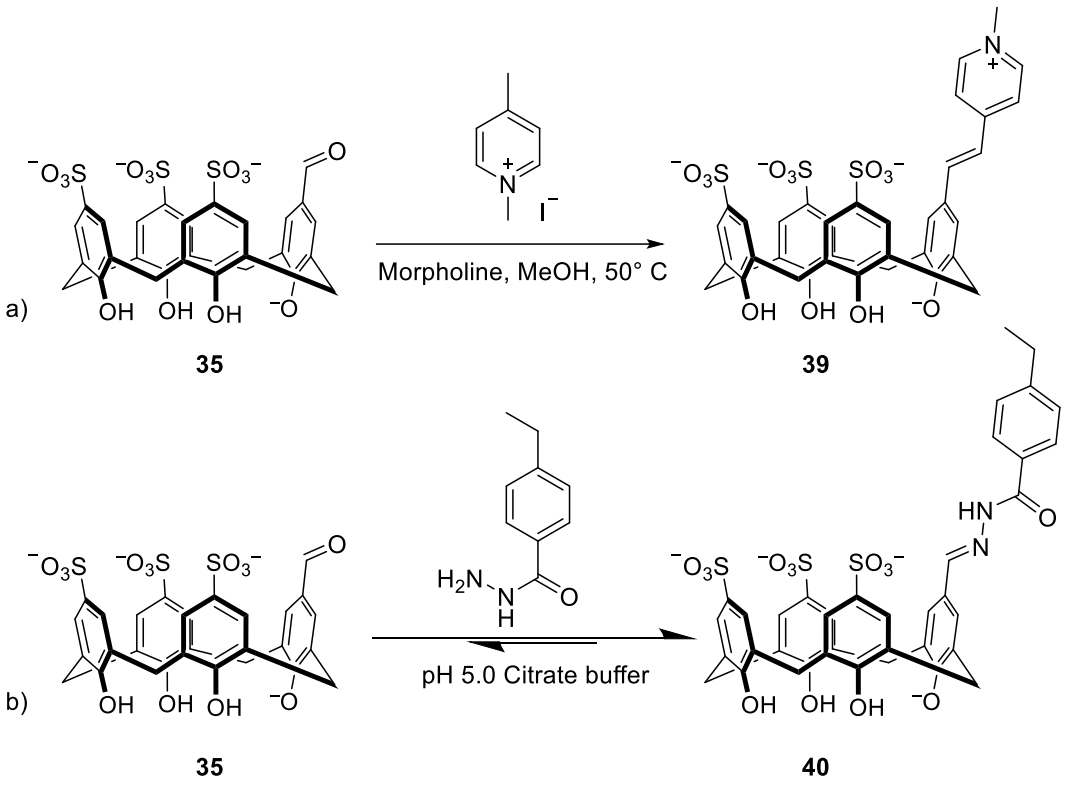

Figure 1.18. a) Example of base-catalyzed methyl pyridinium condensation; b) Example of reversible formation of a hydrazone.

Hydrazone formation is another way to utilize aldehyde moieties as a handle for upper-rim modifications. This happens spontaneously in aqueous solution upon mixing reagents, with the equilibrium position depending on the pH of solution. Despite being essentially a reversible reaction, this exchange results in a surprisingly stable compounds, able to exist and even self-assemble under harsh salty conditions.[21]

1.3.2 Bromide handle

Halides offer another possible handle for functionalization in the *para*-position of the upper rim. There are existing procedures for calixarene chlorination[45] and

iodination,[46] yet only bromide was studied so far with regard to the downstream creation of water-soluble compounds. The synthetic routes towards mono- and disubstituted[47,48] bromides **45** and **46 (**Figure 1.19***)*** generally follow the same scheme for aldehydes from previous paragraphs, starting from lower-rim protected calixarenes **23-24**, with the only exception being an electrophilic bromination of the activated phenolic ring with molecular bromine, to obtain **41-42**. Subsequent deprotection to **43-44** and sulfonation to get **45-46** virtually repeat the same procedure for aldehydes.

Once the handle is established, it paves the road to various possible cross-couplings that rely on aryl halides. However, only Suzuki couplings have been described in the literature thus far, with monosubstituted products **47a-e** being more abundant, then disubstituted (Figure 1.19b).[49,50]

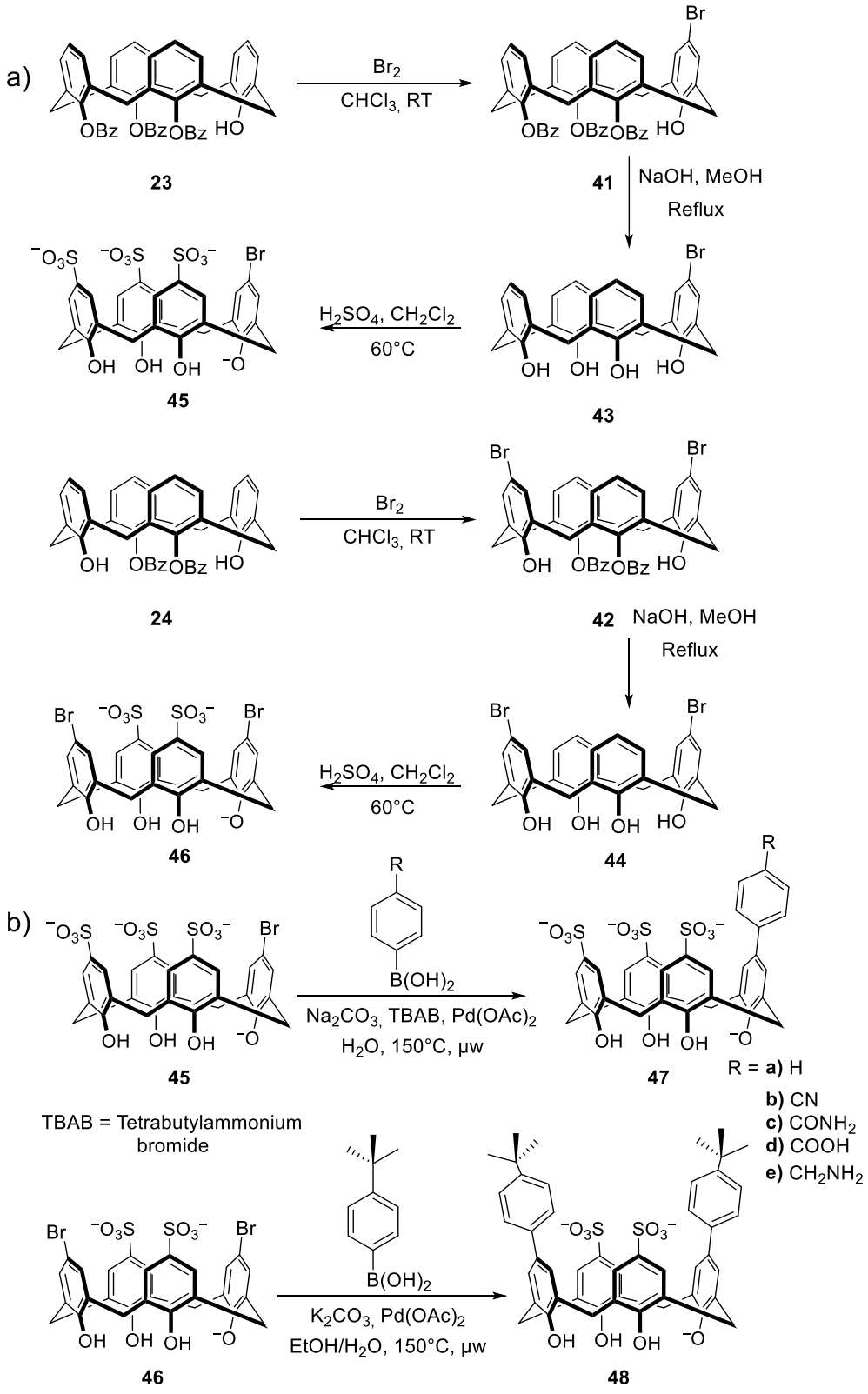

Figure 1.19. a) Synthesis of brominated sulfocalix[4]arenes b) Suzuki couplings of brominated sulfocalix[4]arenes.

1.3.3 Amine handles

In addition to being an important solubilizing substituent, the amine group also has the advantage of being an easily modifiable handle. If the cationic nature of fully substituted aminocalixarenes is undesirable, it can be selectively installed on one or two rings to be used as a handle, while all the others are functionalized, for example, with sulfonates. Similarly to aldehyde and bromide handles, the synthetic scheme (Figure 1.20a) starts from lower-rim protected **23-24**. Nitration and deprotection follows to obtain mono- (**49**) or dintrated (**50**) products, with subsequent sulfonation to **51** and **52** respectively. The nitro group is then reduced with Raney nickel to get sulfonated mono- (**53**) or diamines (**54**). Subsequent amide formation (Figure 1.20b) happens upon reaction with corresponding sulfonyl or acyl chloride in controlled pH, giving way to variety of mono- (**55**) and diamides (**56**).[20,51,52] Fully substituted aminocalixarenes are also able to go through modifications with the aim of enhancing their binding towards relevant targets. Substitution with guanidinium is easily achieved via reaction of lower-rim substituted aminocalixarenes **57a-b** with Boc-protected thiourea in presence of mercury salts, providing guanidiniumcalixarenes **58a-b (**Figure 1.21a).[53]

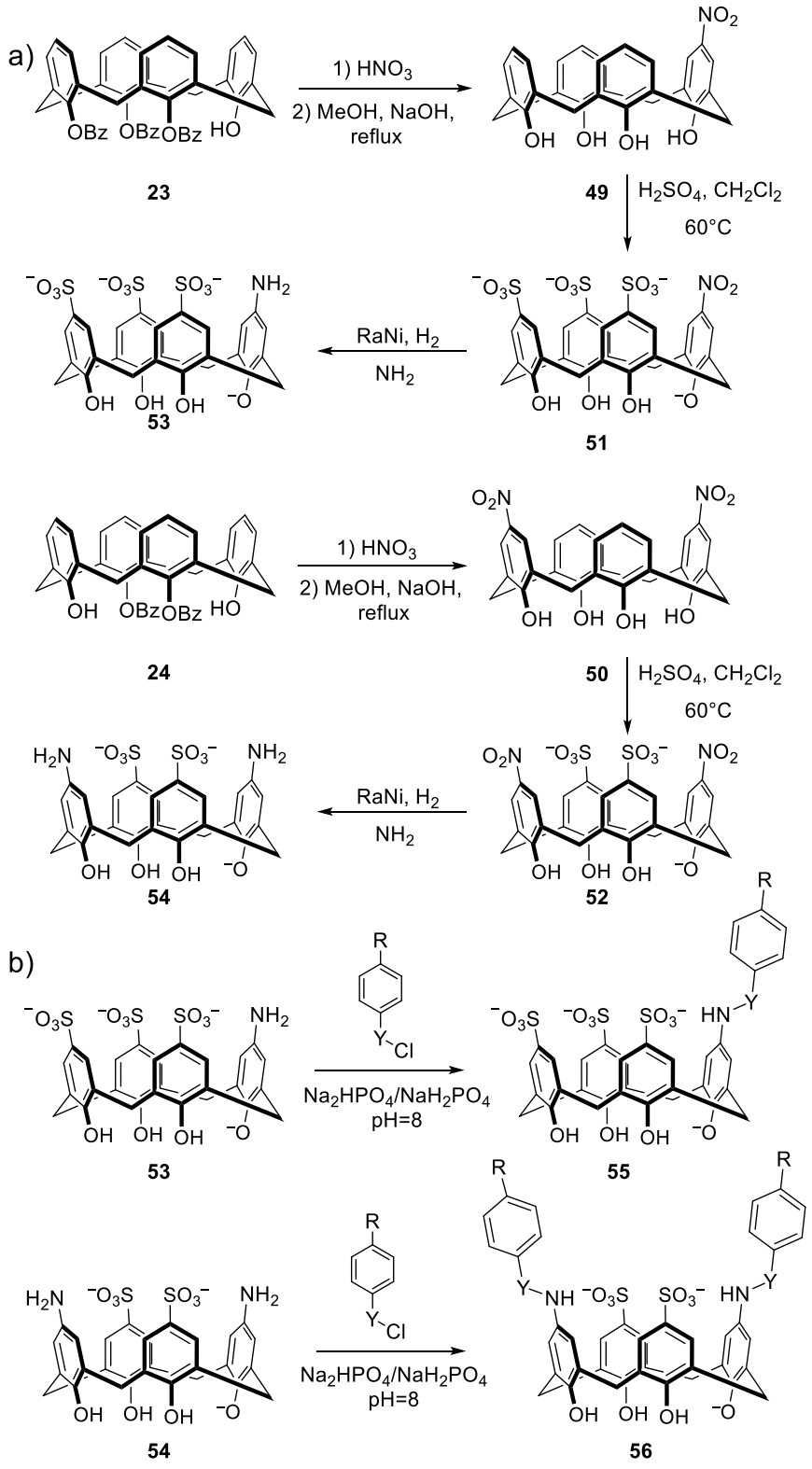

Figure 1.20. a) Selective monoamination and diamination of sulfocalix[4]arene; b) amidation of mono- and diamintaed sulfocalix[4]arenes.

The previously described (Figure 1.13) aminomethyl calixarenes can also be derivatized, with one example using *N*-triflate thioureas to turn lower-rim substituted aminomethylcalixarene **59** into its guanidinium analog **60** (Figure 1.21b).[54]

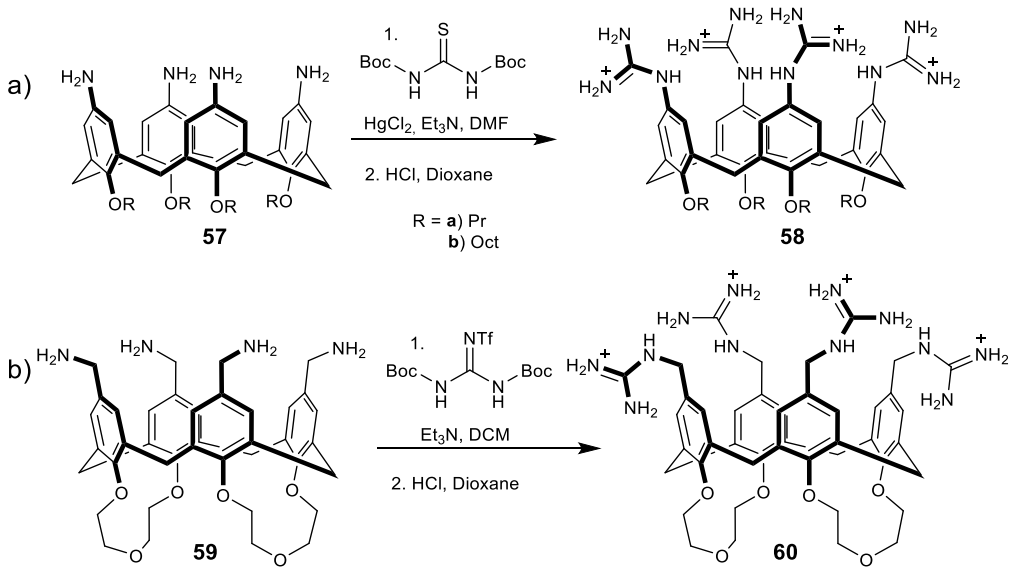

Figure 1.21. Preparation of guanidinium-substituted calixarenes a) from aminocalixarenes; b) from aminomethylcalixarenes.

Amine groups on the upper rim also can be used to form imines, like **61** upon reaction of **6** with aldehydes, providing an alternative to the previously described aldehyde handle. Water-solubility can then be reintroduced via lower-rim carboxylation, followed by deprotection (Figure 1.22). The resulting host **62** has high binding affinity towards cationic species and was shown to possess promising antifungal activity.[55,56]

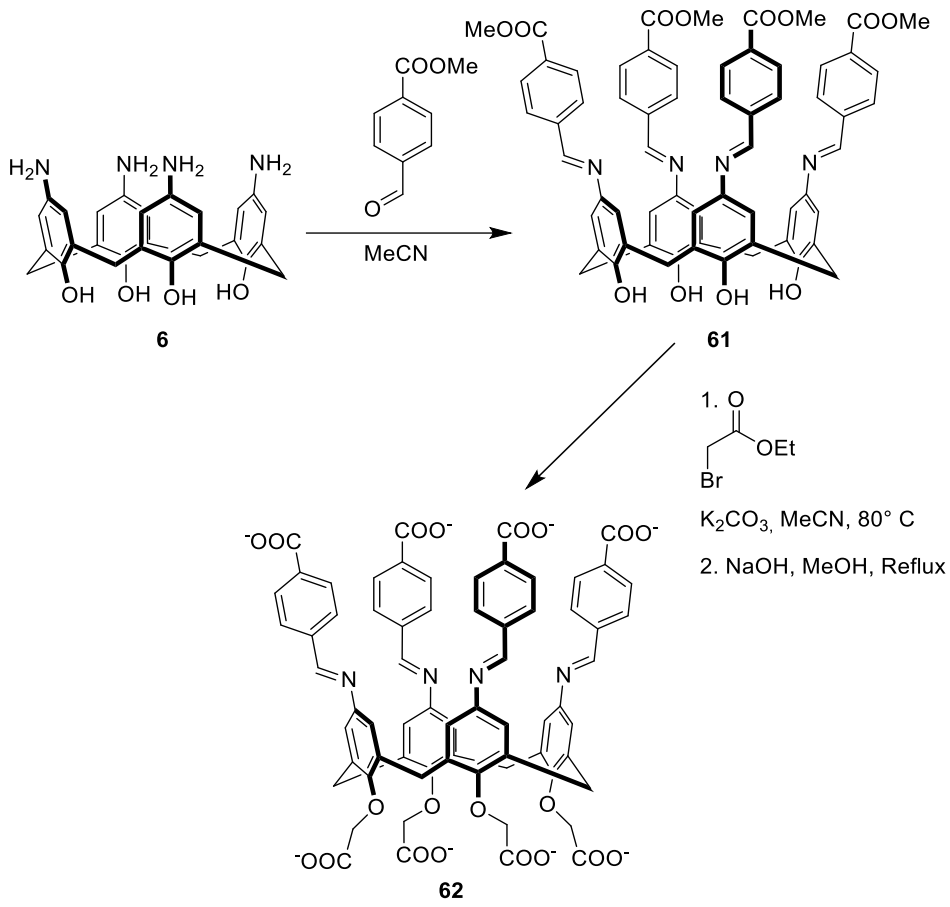

Figure 1.22. Water-soluble iminecalix[4]arenes.

Finally, aminocalixarenes serve as a starting point in recent study which introduces a modified triazole group via a click-reaction. The required aryl azide **63** is synthesized via *in situ* formation of a diazonium salt from the starting amine **6**, followed by nucleophilic substitution with an azide ion under acidic conditions (Figure 1.23). The resulting structure **64** has significant affinity towards DNA and promotes its aggregation into compact nanoparticles, which has promising potential in the development of nucleic acid delivery systems.[57]

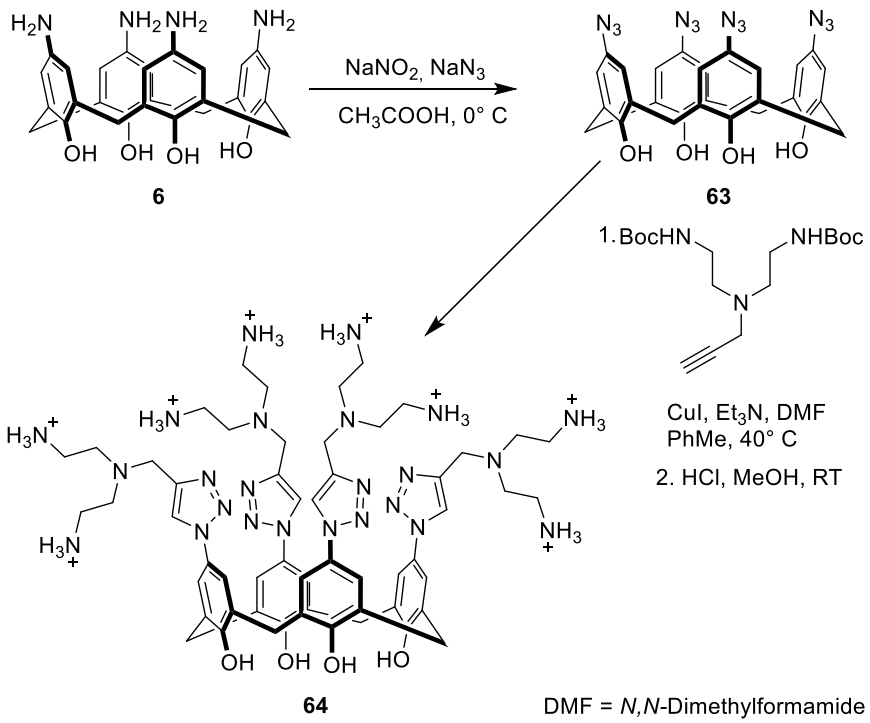

Figure 1.23. Click-synthesis of calix[4]arene triazole via azide intermediate.

1.3.4 Carboxyl handle

The carboxyl group can also be used as a convenient handle, mostly due to its ability to form acyl chlorides, like **65** which can then participate in esterifications (**66a**) and amidations (**66b**). This approach usually requires a certain protecting group to be installed on the lower rim. Benzyl ethers are a common choice, as they can be removed afterwards by hydrogenolysis.[58] Extra solubilizing groups are often required in this case, such as guanidiniums (**67**) or carboxylates (**68**) (Figure 1.24).[59,60]

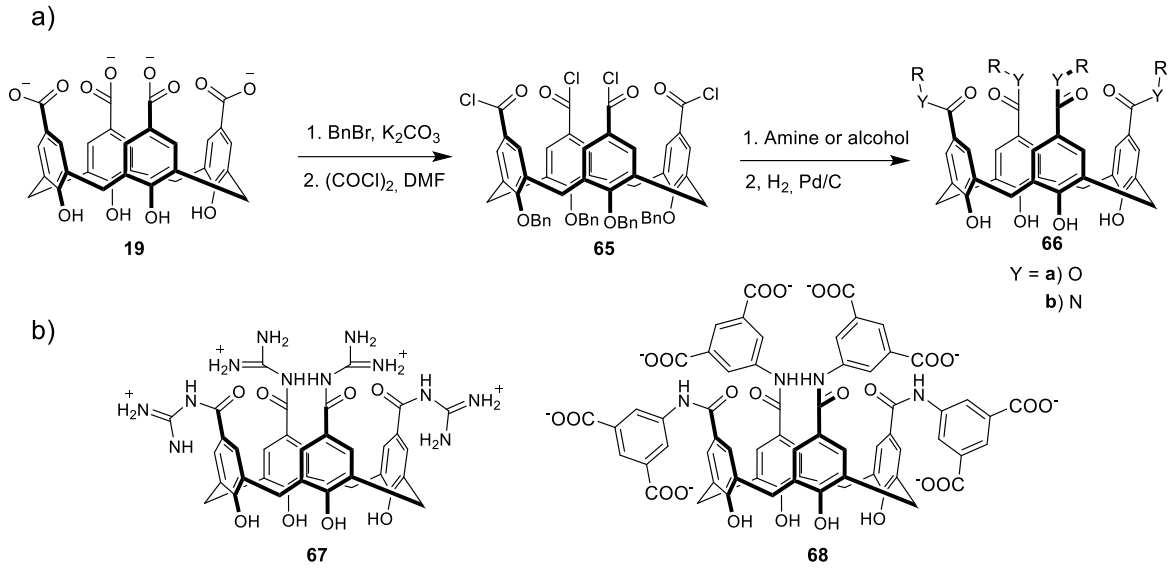

Figure 1.24. a) Functionalization of carboxylatocalix[4]arenes and b) examples of water-soluble products.

1.4 Lower-rim modifications

Modifications on phenolic hydroxyls of the lower rim constitute the largest group of modified calixarenes. However, the chemistry of such transformations is usually limited to either etherification with various alkylation agents or esterification with acyl chlorides (Figure 1.25a). One of the most common strategies is the use of ethyl bromoacetate (Figure 1.25b). In these reactions, the phenolic oxygen atoms will displace bromine in an S_N2-type mechanism. The resulting ethylcarboxymethyl ester groups can be converted into the respective acyl chlorides, which then can be used for further modifications.

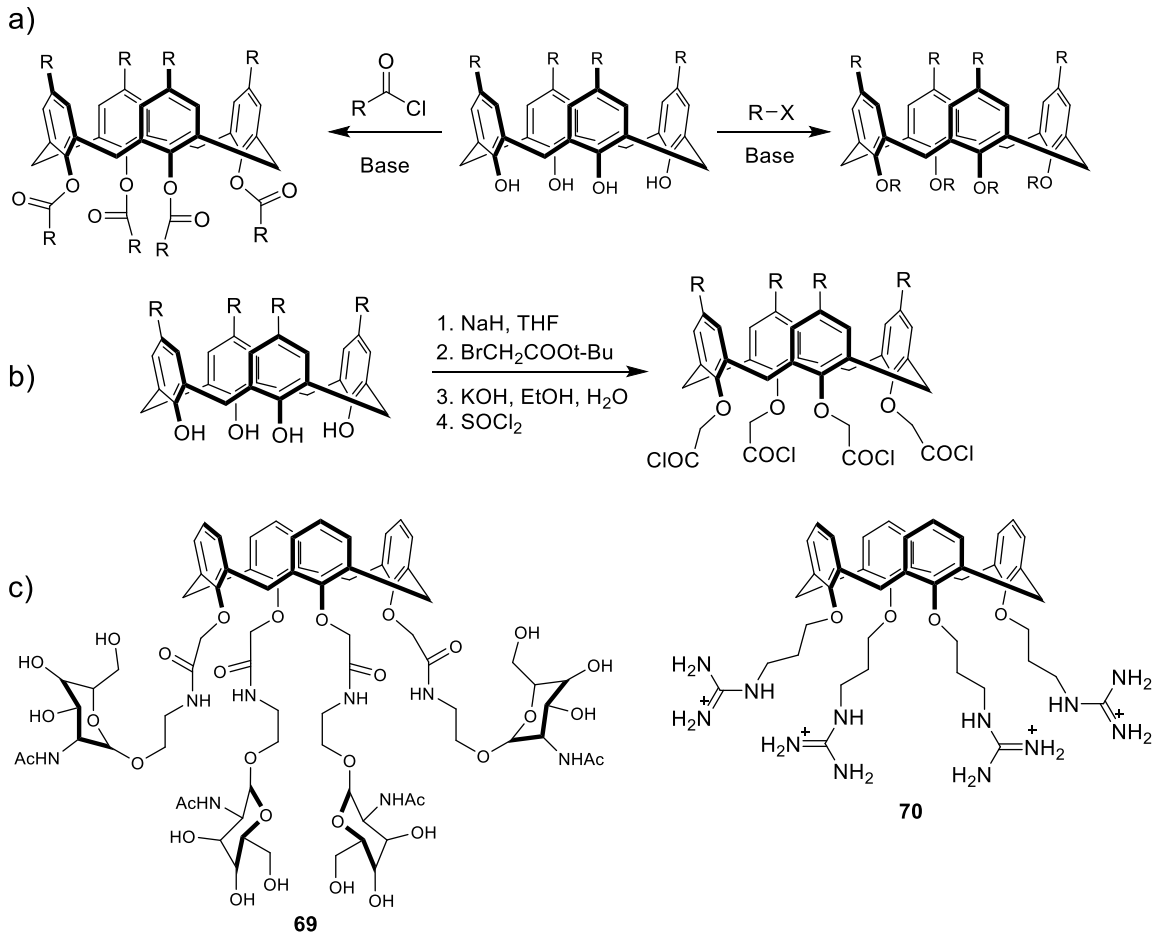

Figure 1.25. a) Typical approaches to lower substitution; b) strategy with ethylbromoacetate; c) some examples of water-soluble products of lower-rim substitution.

As before, extra modifications are required to enable water-solubility because substitution of acidic phenolic protons tend to decrease solubility even in organic solvents. An example of such modifications could be the use of carbohydrates (**69**)[61] or guanidines (**70**)[62] as lower-rim substituents (Figure 1.25c).

1.5 Aims of this thesis

This thesis will attempt to take advantage of high modification potential of calixarenes in order to generate a water-soluble supramolecular host able of reversibly changing its configuration upon irradiation with different wavelengths of light. Such property is usually labelled as photoswitching.

The aims of this thesis are:

1. Development of a synthetic procedure towards such host with a photoisomerizable chromophore
2. Expanding our understanding of its properties and behavior.

This Chapter provided an overview of various existing synthetic routes towards solubilizing of calixarene scaffold as well as methods of their fine modification.

Chapter 2 will revolve around designing photoswitchable supramolecular host based on a sulfocalixarene scaffold and incorporating a hemiindigo chromophore directly on the upper rim.

Finally, Chapter 3 will attempt to unravel the supramolecular properties of the synthesized photoswitchable calixarenes and take a closer look at their behavior in solution and aggregation properties.

Chapter 2. Synthesis of hemiindigo calixarenes

2.1 Introduction

Photoswitches, compounds able to reversibly change their geometry or topology upon irradiation with particular wavelengths, are gaining increasing attention. The broad array of their possible uses includes, but is not limited to, molecular machinery,[63] photopharmacology,[64] tunable optical filters[65] and even 3D printing (which, in this case, sometimes called 4D printing).[66] While many structures can in theory exhibit photoswitching, only a limited number of them is viable in practice. It is because a reliable switch should possess a certain set of properties: high photoconversion efficiency (quantum yield), high thermal stability of isomers (bistability), and a broad gap between excitation wavelengths. The use of visible light and high degrees of photoisomerization at a steady state are among other desirable characteristics. Finally, precise tuning is needed to fully embrace any one of aforementioned applications. Therefore, most modern research in the field concentrates either on modification of existing chromophores or on inventing new ones.

Supramolecular chemists are among potential users of photoswitches. Many common macrocycles were used in conjunction with them, including cucurbiturils,[67–69] pillararenes,[70] cyclodextrins,[71,72] and crown ethers.[73] The ability to reversibly change certain properties of macromolecular hosts has

brought forth their applications in functional materials,[71,74] drug delivery systems,[75] and even as a tool for singlet oxygen generation.[76] It worth mentioning that many such cases do not rely on direct installation of photoswitchable chromophores on the host, but rather on switching molecules that are bound by non-covalent interactions into larger assemblies.

Being one of the most important macrocycles, calixarenes were not left aside either. There are examples (Figure 2.1) of these cyclophanes modified with common switches – azobenzenes (**71a-b**, **77)**[77,78] stilbenes (**72**),[79] acridines (**73a-b**),[80,81] and anthracenes (**74a-b**).[82,83] The most obvious application of such system is an ability to tune binding affinity of the host towards its guests, which in case of calixarenes are often alkaline metal cations.[77] Yet, some more unexpected cases are reported, such as ionic liquid crystals for proton transfer.[84]

A constant search for new selective hosts for drug recognition, especially those active in aqueous media, has already encouraged installation of various chromophores on water-soluble calixarenes. Sulfonated analogs are of particular interest due to their combination of an aromatic binding cavity with negative charges that facilitate binding with cationic drugs which constitute the major part of illicit recreational substances.[4,85]

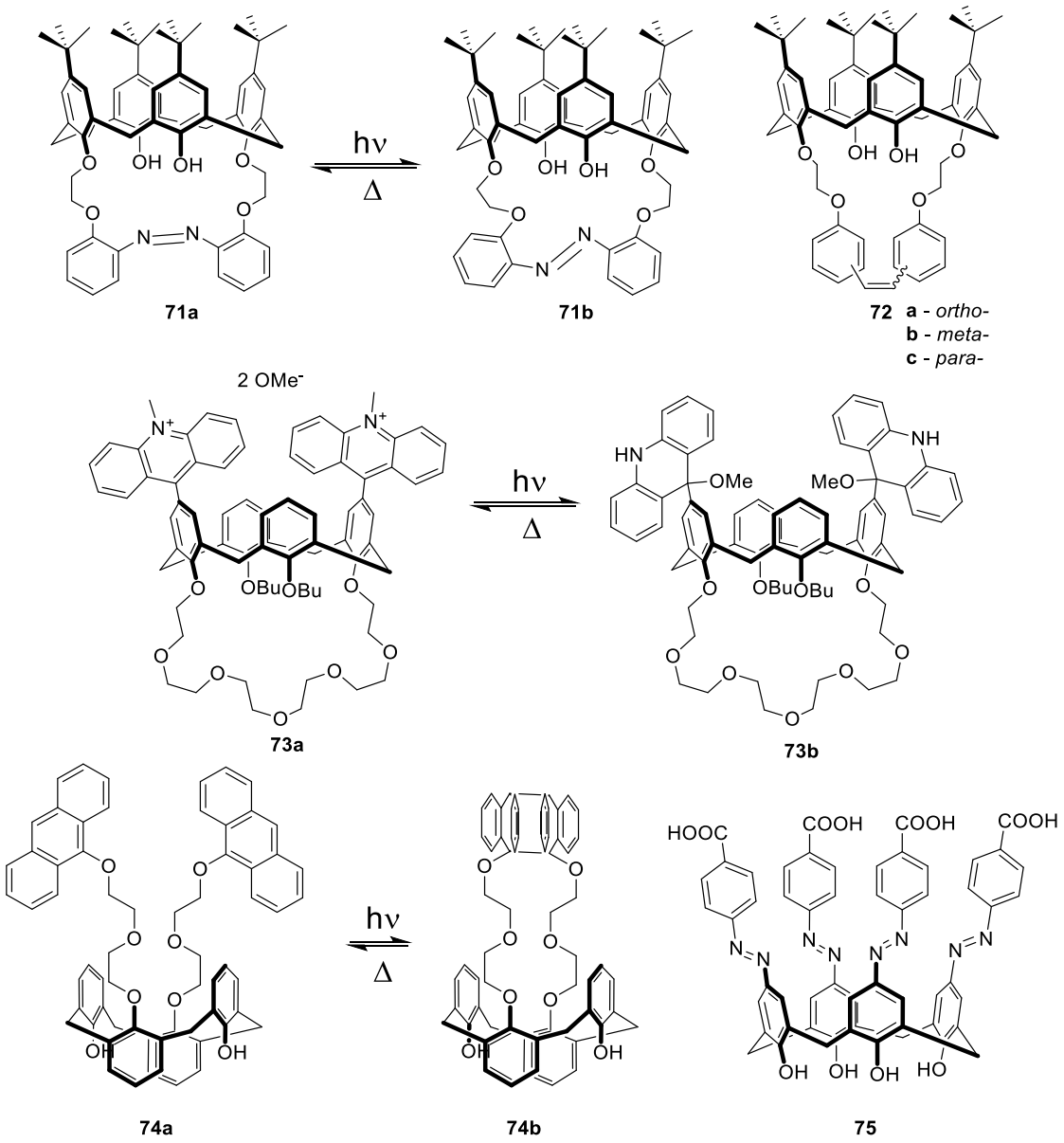

Figure 2.1. Examples of previously synthesized photoswitchable calixarenes and their modes of isomerization.

Yet examples of water-soluble photoswitchable calixarenes remain incredibly scarce.[86] To the best of our knowledge only one such calixarene was made, **75 (**Figure 2.1), that possessed this combination of desired properties. It relies on carboxylic acid to gain water-solubility and was shown to be an effective binder

of neutral molecules, yet its "switchable" side was not explored in depth, probably due to low energy barrier of interconversion.

Hemiindigos belong to a broader class of indigoid chromophores,[87] along with aurones and hemithioindigos, which in recent years have shown significant development and proven themselves useful in a variety of areas.[88–90] They also happen to satisfy requirements such as very good thermal stability, fast conversion and high isomeric yields, and wavelengths of excitation in the visible range. The structural change introduced by light to these structures is rather simple – rotation around C=C bond (E-Z conversion). However, poor water solubility limits their uses in aqueous supramolecular chemistry and in biological applications.

This work attempts to combine the favorable properties of sulfocalixarene hosts with the excellent switching properties of hemiindigos. We aim to do that by introducing a hemiindigo substituent on the upper rim of sulfonated calix[4]arenes and calix[5]arenes. The conceptual design is depicted in Figure 2.2. That would allow the oxygen atoms on the lower rim to serve as electron-donating group to enhance photophysical properties of the chromophore, while aromatic cavity inherent to all calixarenes will provide non-covalent interactions, central to all supramolecular sensors. Sulfonate groups, in turn, will address hemiindigo's general lack of water-solubility. This is a

fundamental study aimed at learning about how such photoswitches might operate while installed in this structural context. But it also considers potential long-term applications of such system that might include localized drug release, controllable reversal agents or water-soluble binders of biomolecules.[91]

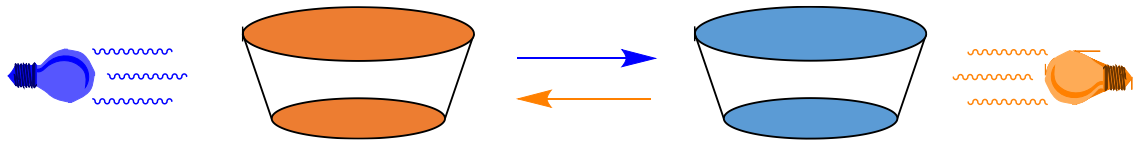

Figure 2.2 Photoswithable calixarene.

2.2 Synthesis of first generation of hemiindigo calixarenes

A recent paper[92] demonstrated that electron donor-substituted hemiindigos possess a number of properties which make them promising photoswitches: long half-lives of pure isomeric states, high isomeric yields of photoconversion, and little to no side reactions that could hamper efficient switching. They also use visible light. *Hemiindigos* are called as such because they essentially consist of two parts: an indole-type moiety, which if combined with another copy of itself would produce the iconic blue dye indigo, and a stilbene-type part which is basically a phenyl group substituted with an ethylene moiety. Stilbene is on its own a well-studied photoswitch.[93] Synthesis of hemiindigos is a relatively simple two-stage one-pot process, starting with basic hydrolysis of indoxyl acetate precursor followed by condensation of the resulting enol with a

benzaldehyde under inert atmosphere and in deoxygenated solvents (Figure 2.3).

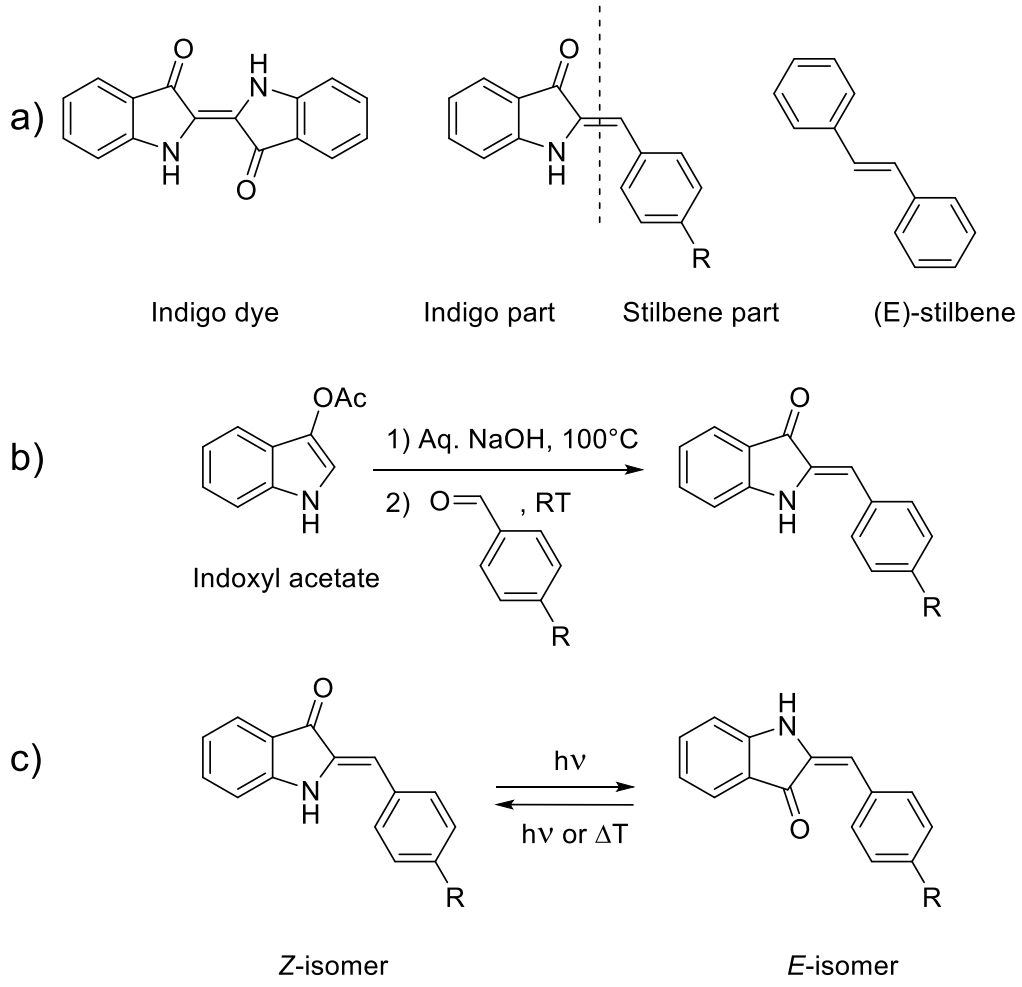

Figure 2.3 a) Constituent parts of hemiindigo dyes; b) Hemiindigo condensation reaction: c) Hemiindigo photoswitching.

Our initial goal was to install hemiindigo chromophore on the upper rim of water-soluble sulfonated calixarene. In this case the stilbene part could be "borrowed" from calixarene skeleton itself. Luckily, an electron-donating phenol is already present on the lower rim, satisfying the requirement and leaving us with chromophore closely resembling the previously described one

integrated directly into the calixarene's macrocyclic structure (Figure 2.4).[94] Both *E* and *Z* isomers are planar in this case, with *Z* being more stable and forming as the only isomer during synthesis due to less steric tension.

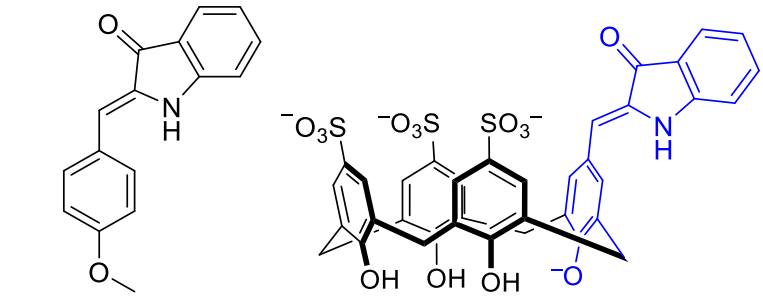

76

Previously described
O-methoxy hemiindigo

77

Initial target

*Figure 2.4 Structures of initial target molecule **77** along with structure of its closest published hemiindigo model compound **76**.*[94]

The synthetic pathway towards sulfonated monoaldehyde calix[4]- and [5]arene intermediates was followed as previously described,[15] starting from de-*tert*-butylation of 4-*tert*-butylcalix[4]arene **1** or 5-*tert*-butylcalix[5]arene **78**, followed by tri- or tetrabenzoylation to get **23** and **26** respectively. Subsequent Duff formylation of the remaining activated unprotected ring allowed for the high-yieleding installation of a single aldehyde group, granting **27** and **30**. Deprotection of the phenols to get **31** and **34** and was followed by sulfonation leading to **35** and **38**. Slightly adjusted conditions[94] were used for the final condensation with indoxyl acetate to produce both sulfonated hemiindigo calix[4]arene **77** (Figure 2.5) and calix[5]arene **79 (**Figure 2.6**)** as brown

powders. Last step is extremely sensitive to oxygen due to formation of indigo dye upon indoxyl oxidation and requires careful deoxygenation. The products also start to decompose, if held for too long in reaction conditions.

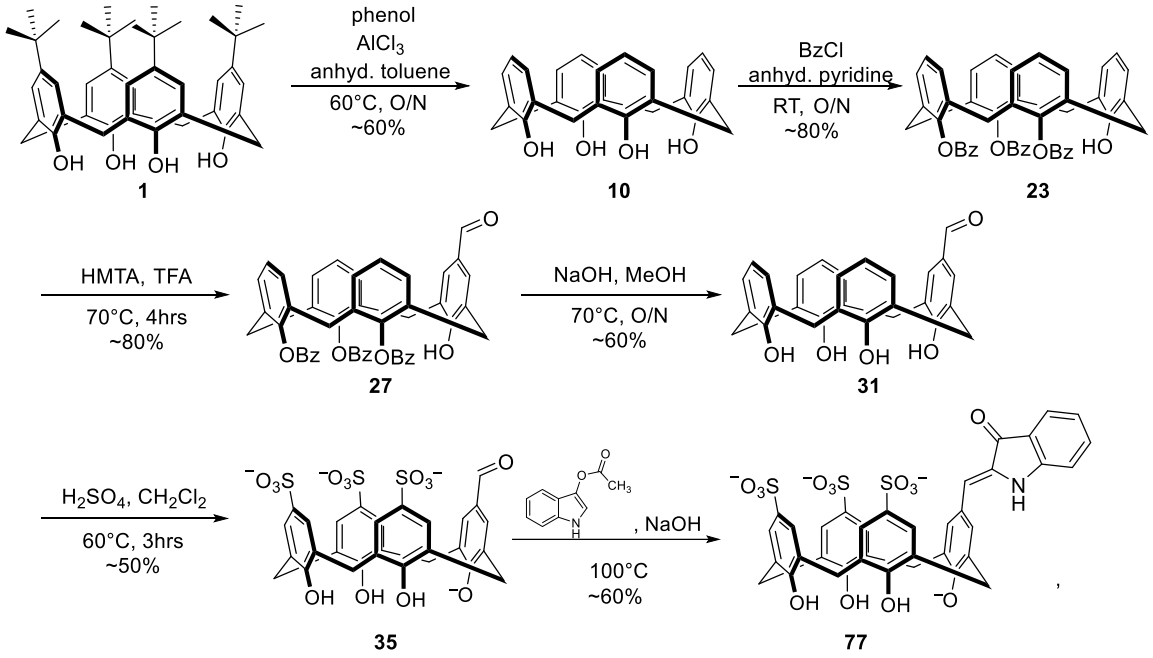

Figure 2.5 Synthesis of hemiindigo calix[4]arene 77.

However, upon being synthesized, both compounds did not show any observable photoswitching properties in water, methanol, and DMSO, despite having virtually identical absorption spectra with previously described *O*-methoxy hemiindigo (Figure 2.8). The exploration of more different solvents was hampered by poor solubility in any solvents less polar than the three that were tested.

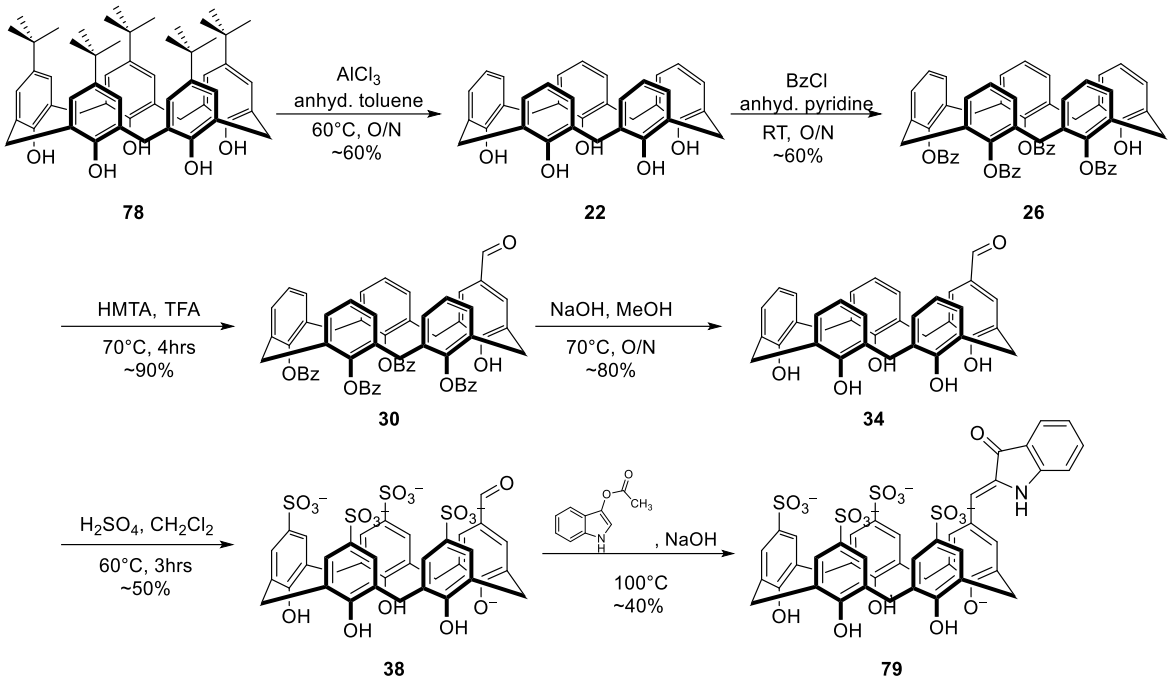

*Figure 2.6 Synthesis of hemiindigo calix[5]arene **79**.*

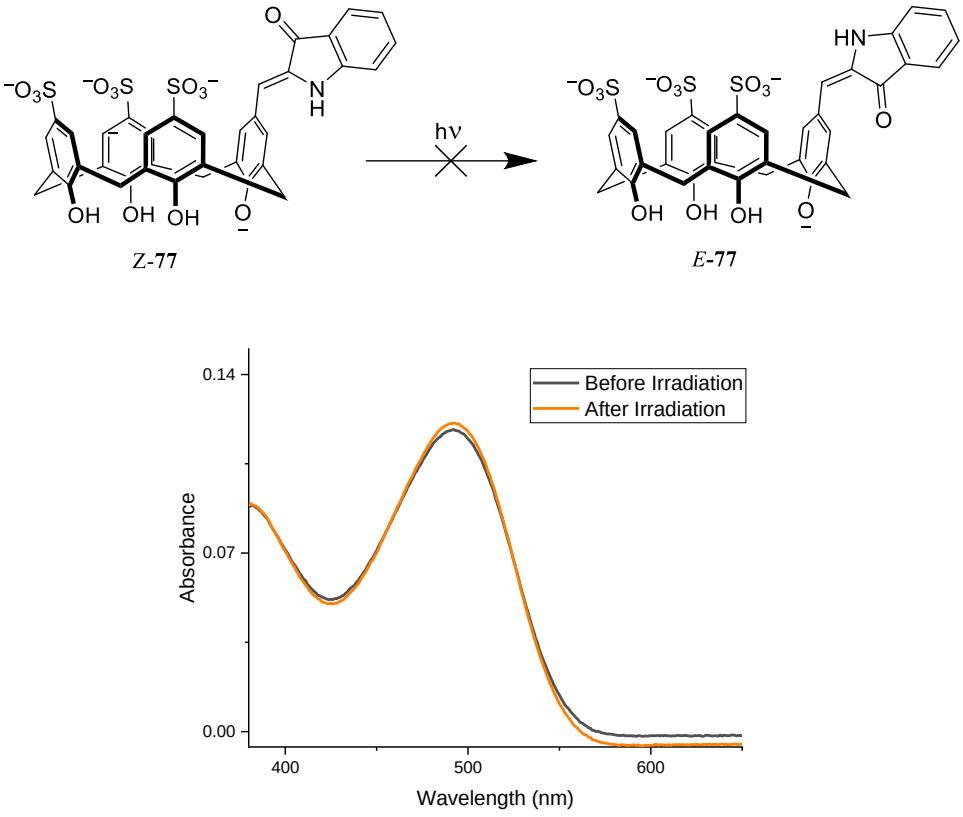

*Figure 2.7 Lack of switching for first generation of hemiindigo calix[4]arene (**77**).*

2.3 Synthesis of second generation of hemiindigo calixarenes

Such disappointing behavior can be possibly explained by relaxation via deprotonation, as opposed to breaking and reforming the double bond, which is reinforced by the fact that previously described hemiindigo photoswitches do not have acidic protons in the chromophore system. That means that they don't have this relaxation pathway available and have no other choice then to release the energy by breaking the double bond.

Thus our next step was to attempt to solve the issue by converting the lower rim hydroxyl to an ether group. In order not to deviate too much from initial target and retain desired properties of calixarene scaffold, we decided that the smallest possible change that could be made to shut down the proton transfer pathway and achieve photoswitching is methylation. So we had to modify our initial synthetic strategy to include it. The best stage to do it – right after the Duff formylation, starting from lower-rim protected aldehydes **27** and **30** for calix[4] and calix[5] respectively. Electron-withdrawing properties of an aldehyde substituent make lower-rim phenol more acidic, allowing for milder conditions, while small size of methyl prevents too much repulsion from bulky benzoyl group on the lower rim, that generally make last remaining phenol less available. Once benzoyl groups are removed, it gets harder to direct the regiochemistry of reaction towards desired monosubstituton, while trying to do

it before formylation might require stronger base, which in turn might put the benzoyl protecting groups at risk.

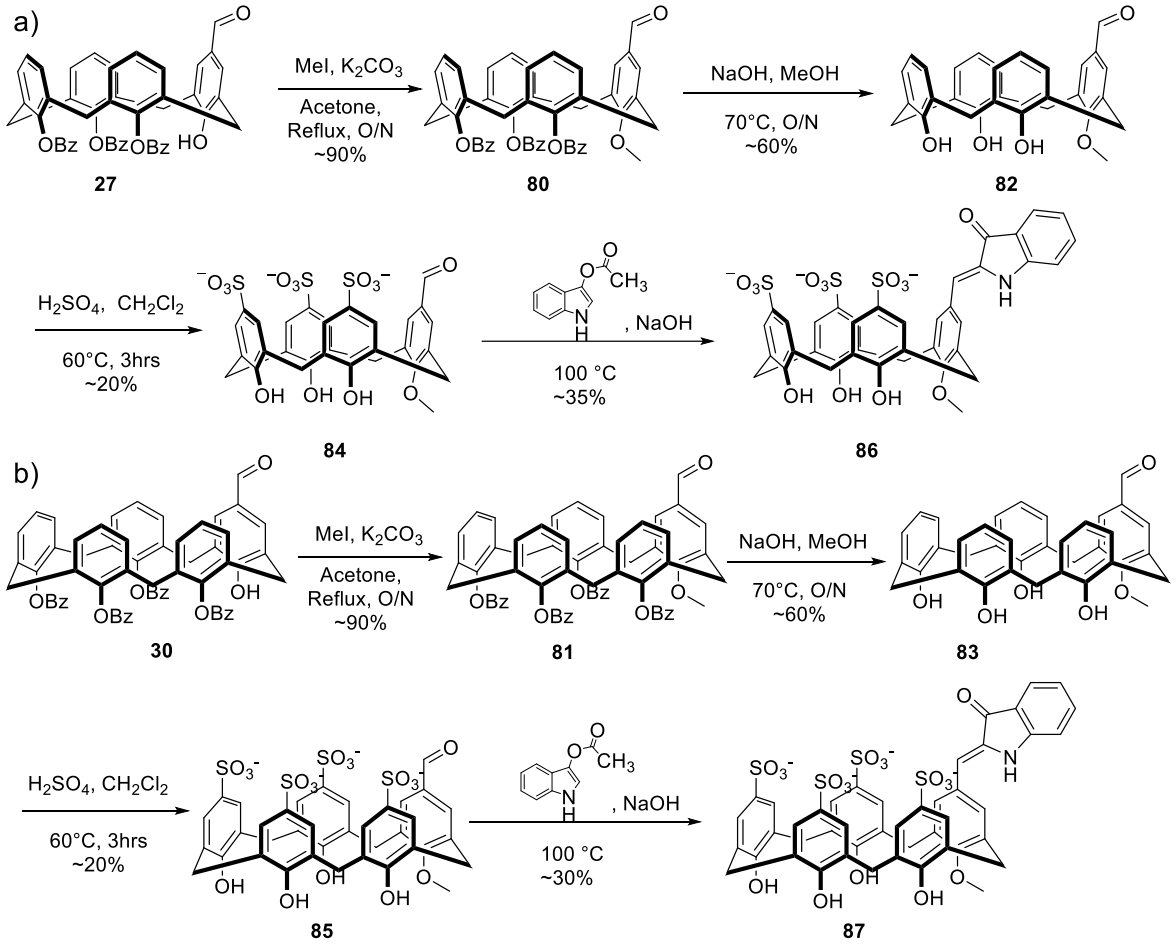

*Figure 2.8 Synthetic scheme of methylated hemiindigo calixarenes: a) Calix[4]arene **86**; b) Calix[5]arene **87**.*

After several unsuccessful attempts, we have arrived at conditions that allowed for essentially quantitative conversion to monomethylated protected aldehydes **80** and **81** (Figure 2.8), using potassium carbonate as a base and methyl iodide as methylating agent. Deprotection step to obtain methylated aldehydes **82** and **83** also went smoothly, mirroring the same procedure for non-methylated

analogue. However the sulfonation step turned out to be troublesome, and yields dropped significantly, in part due to demethylation happening under the strongly acidic conditions needed for sulfonation. Sulfonated monomethylated aldehydes **84** and **85** were eventually obtained, albeit in poor yields, rendering this step as essentially a bottleneck of the whole synthesis. Monomethylated hemiindigo calix[4]- (**86**) and [5]arenes (**87**) were also obtained at modest yields following the same procedure, as for their parent compounds.

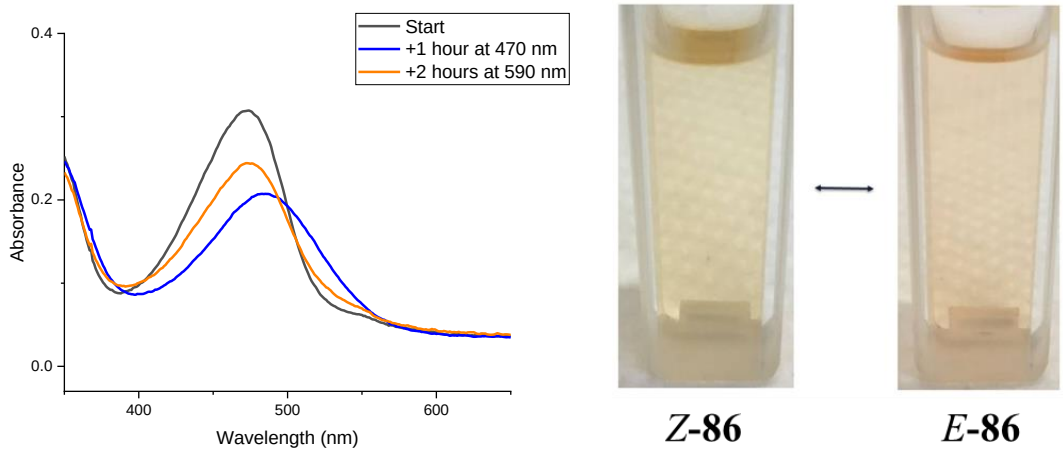

*Figure 2.9. Photoswitching of hemiindigo calix[4]arene **86**.*

The resulting second-generation hemiindigo calixaxarenes were shown to photoisomerize in conditions closely resembling those used for previously described hemiindigos – upon irradiation with blue (470 nm) and amber (590 nm) light. With that said, they did demonstrate some noticeable photobleaching (Figure 2.9 and Figure S2.25), as evidenced by the decrease in absorbance

intensity. This behaviour was also noticed for hemiindigos in the earlier literature, and will be discussed in more detail in Chapter 3.

2.4 Conclusions

Our task was to synthesize water-soluble sulfocalixarene hosts, with photoswitchable hemiindigo moiety on the upper rim. While being successful in our initial synthesis, the resulting molecules did not possess the desired ability to photoswitch. While still being brightly colored dyes, with absorption profile virtually copying that of previously synthesized photoswitch, they lacked certain structural features. We correctly assumed that the source of the problem was the presence easily deprotonatable phenol group embedded in the hemiindgo chromophore. Therefore, our next step was to overcome that challenge without changing supramolecular properties of parent calixarene scaffolds too much. Selective monomethylation of the aforementioned phenol fixed the issued and we were able to detect photoisomerisation of our novel compounds **86** and **87** at micromolar concentrations, albeit with some photobleaching. In process, we have also developed a synthetic procedure towards sulfonated calix[4]- and [5]arene aldehydes **84** and **85**, methylated at the lower rim. It might be useful for future calixarene-based dyes, fluorescent or photoswitchable, because, for example, it might be able to remove the undesirable influence of pH on photophyiscal properties of the chromophore.

2.5 Experimental procedure

2.5.1 Photoswitching studies

Photoswitching studies were done using a 75 W PTI xenon-arc lamp equipped with a PTI 101 0.2 monochromator with a 1200 gr / mm, 300 nm blazed grating for selection of the irradiation wavelength. 470 and 590 nm were used for irradiation. Concentration of hemiindigo calixarenes were set at 20 μM in Milli-Q deionized water.

2.5.2 Synthetic procedures

Compound 80

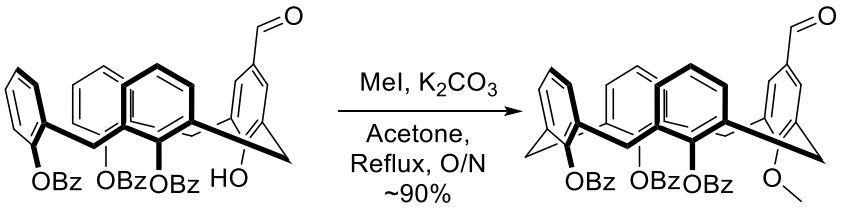

Compound 27 (400 mg, 0.39 mmol) was dissolved in minimal amount (20 ml) of acetone. Potassium carbonate (144.5 mg, 1.05 mmol, 2 eq.) and methyl iodide (593 mg, 260 μl, 4.18 mmol, 8 eq.) were added and reaction was set to reflux overnight. Acetone and unreacted methyl iodide were removed in vacuo, resulting solids were redissolved in CH_2Cl_2 and filtered from salts. CH_2Cl_2 was evaporated in vacuo yielding Compound **80** as white or off-white solid (390 mg, 92%) which was used without purification.

Compound 81

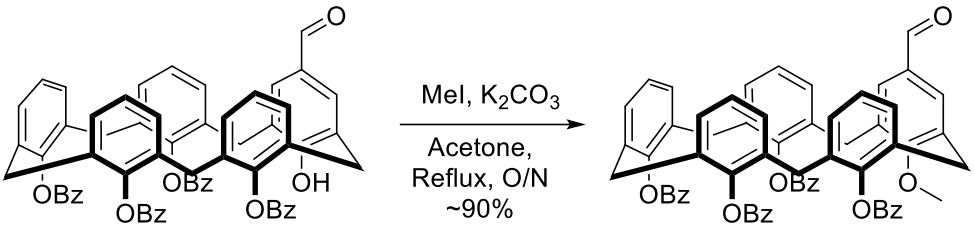

Compound 30 (400 mg, 0.42 mmol) was dissolved in minimal amount (20 ml) of acetone. Potassium carbonate (112 mg, 0.84 mmol, 2 eq.) and methyl iodide (282 mg, 204 µl, 3.28 mmol, 8 eq.) were added and reaction was set to reflux overnight. Acetone and unreacted methyl iodide were removed in vacuo, resulting solids were redissolved in CH_2Cl_2 and washed once with water to dissolve residual potassium carbonate. CH_2Cl_2 was evaporated in vacuo yielding Compound **81** as white or off-white solid (380 mg, 94%) which was used without purification.

Compound 82

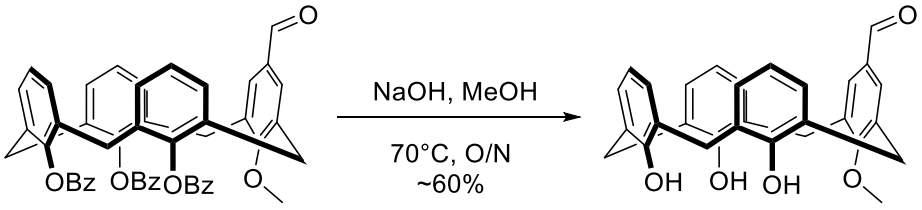

Compound 80 (0.390 g, 0.5 mmol) was added to methanol (15 mL). Sodium hydroxide (0.4 g, 10 mmol, 20 eq.) was added to the suspension. The solution was heated at 70° C for 4 hours. The reaction was quenched with hydro-chloric acid (1 M) and the precipitate was collected by vacuum filtration. The crude

product was triturated in hot hexanes to remove the benzoic acid and then purified by flash column chromatography (eluent CH_2Cl_2) to yield compound **82** as white solid (0.15 g, 64%). **^{1}H NMR** (500 MHz, $CDCl_3$): δ 9.78 (s, 1H), δ 9.48 (s, 1H), δ 9.13 (s, 2H), δ 7.64 (s, 2H), δ 7.15 (dd, J_1 = 7.55 Hz, J_2 = 1.55 Hz, 2H), δ 7.09 (dd, J_1 = 7.68 Hz, J_2 = 1.48 Hz, 2H), δ 7.02 (d, J = 7.58 Hz, 2H), δ 6.72 (m, 3H), δ 4.44 (d, J = 13.2 Hz, 2H), δ 4.29 (d, J = 13.9 Hz, 2H), δ 4.20 (s, 3H), δ 3.60 (d, J = 13.2 Hz, 2H), δ 3.51 (d, J = 13.9 Hz, 2H). **^{13}C NMR** (126 MHz, $CDCl_3$): δ 191.1, 157.8, 150.9, 149.0, 135.3, 134.1, 131.3, 129.3, 128.9, 128.7, 128.6, 127.49, 122.3, 121.3, 77.2, 64.0, 31.9, 31.4. Melting point = 231-233°C. FT-IR (cm^{-1}): 3177 (br), 1691 (s), 1593 (w), 1465 (s), 1279 (m), 1117 (s), 984 (m), 757 (s). **HRMS:** found 465.17051 (Calculated for **$C_{30}H_{26}O_5$ [M-H]$^{1-}$** = 465.17074)

Compound 83

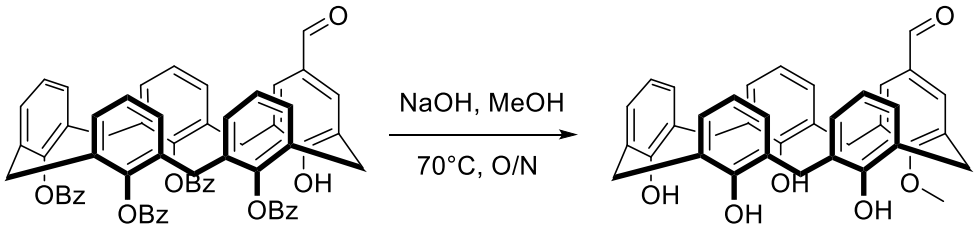

Compound 81 (0.380 g, 0.5 mmol) was added to methanol (15 mL). Sodium hydroxide (0.316 g, 7.91 mmol, 20 eq.) was added to the suspension. The solution was heated at 70° C for 4 hours. The reaction was quenched with hydrochloric acid (1 M) and the precipitate was collected by vacuum filtration. The

crude product was triturated in hot hexanes to remove the benzoic acid and then purified by flash column chromatography (eluent CH_2Cl_2) to yield compound **83** as yellow solid (0.115 g, 51%). **^{1}H NMR** (500 MHz, $CDCl_3$): δ 9.75 (s, 1H), δ 7.90 (s, 4H), δ 7.61 (s, 2H), δ 7.24 (m, 4H), δ 7.15 (m, 4H), δ 6.87 (t, J = 7.45 Hz, 2H), δ 6.82 (t, J = 7.53 Hz, 2H), δ 3.99 (s, 4H), δ 3.85 (s, 7H), δ 3.80 (s, 2H). **^{13}C-NMR** (126 MHz, $CDCl_3$): δ 191.5, 158.7, 151.9, 150.2, 134.4, 133.61, 130.9, 129.8, 129.8, 129.5, 129.3, 127.2, 127.1, 126.1, 121.7, 120.7, 63.0., 31.8, 31.1, 30.8. Melting point >230°C. FT-IR (cm^{-1}): 3341 (br), 1684 (s), 1594 (w), 1465 (s), 1372(w), 1273 (m), 1202 (w), 1120 (m), 987 (w), 754 (s). **HRMS:** found 571.21111 (Calculated for **$C_{37}H_{32}O_6$ [M-H]$^{1-}$** = 571.21261)

Compound 84

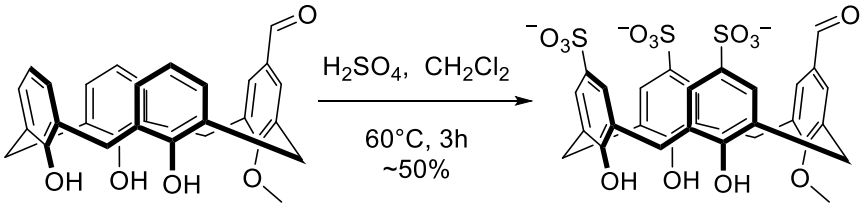

Compound 82 (50 mg, 0.11 mmol) was dissolved in minimal amount of CH_2Cl_2 (3 ml) in a microwave vial. While stirring, sulphuric acid (0.709 g, mmol) was added, vial sealed and the solution was heated to 60°C for 3 hours. The CH_2Cl_2 was decanted and a minimum amount of ethyl acetate was added to the precipitate after which a slurry was formed by sonication. The crude product was suspended by pouring the slurry into a 50 mL Falcon tube containing ice-

cold ether (35 mL). The suspension was settled by centrifugation and the supernatant was discarded. The pellet was air dried and purified by high pressure liquid chromatography. The fractions were collected and lyophilised, yielding compound **84** as a light pink solid (20 mg, 27%). **^{1}H NMR** (500 MHz, D_2O): δ 9.59 (s, 1H), δ 7.74 (s, 2H), δ 7.70 (s, 2H) δ 7.66 (s, 2H), δ 7.42 (s, 2H) δ 4.3 (t, J = 14.3 Hz, 4H), δ 4.03 (s, 3H), δ 3.82 (d, J = 14.3, 2H), δ 3.71 (d, J = 14.3 Hz, 2H). **^{13}C NMR** (126 MHz, DMSO-*d6*): δ 191.5, 158.9, 152.9, 150.0, 139.5, 138.4, 138.4, 134.5, 133.2, 130.9, 127.5, 127.5, 127.1, 126.6, 126.4, 126.4, 63.3, 39.5, 31.1, 30.7. **Melting point** >230°C. **FT-IR** (cm^{-1}): 3185 (br), 1681 (m), 1594 (w), 1450 (m), 1122 (s), 1034 (s), 886 (w), 787 (w), 723 (w), 623 (s), 558 (s). **HRMS:** found 707.05562 (Calculated for **$C_{30}H_{26}O_{14}S_3$ $[M+H]^{+1}$** = 707.05575)

Compound 85

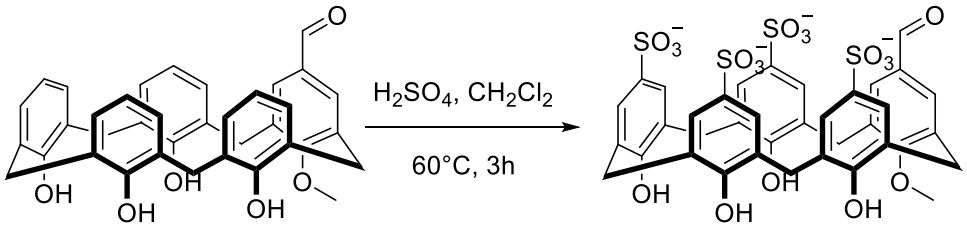

Compound 83 (50 mg, 0.09 mmol) was dissolved in minimal amount of CH_2Cl_2 (3 ml) in a microwave vial. While stirring, sulphuric acid (0.709 g, mmol) was added, vial sealed and the solution was heated to 60°C for 3 hours. The CH_2Cl_2 was decanted and a minimum amount of ethyl acetate was added to the

precipitate after which a slurry was formed by sonication. The crude product was suspended by pouring the slurry into a 50 mL Falcon tube containing ice-cold ether (35 mL). The suspension was settled by centrifugation and the supernatant was discarded. The pellet was air dried and purified by high pressure liquid chromatography. The fractions were collected and lyophilised, yielding compound **85** as a light brown solid (18 mg, 23%). **^{1}H NMR** (500 MHz, D_2O):): δ 9.69 (s, 1H), δ 7.70 (s, 2H),), δ 7.65 (d, J = 2.3 Hz, 2H), δ 7.60 (d, J = 2.3 Hz, 2H), δ 7.41 (d, J = 2.3 Hz, 2H), δ 7.27 (d, J = 2.3 Hz, 2H), δ 3.88 (s, 6H), δ 3.78 (s, 4H), δ 2.62 (s, 3H**). ^{13}C NMR** (126 MHz, D_2O): δ 195.3, 161.2, 153.6, 153.1, 135.5, 134.8, 132.01, 129.4, 128.9, 128.6, 127.9, 127.0, 126.4, 126.3, 125.8, 60.2, 32.4, 30.5, 30.1. **Melting point** > 230°C. **FT-IR** (cm^{-1}): 3320 (br), 1694 (m), 1591 (w), 1471 (m), 1109 (s), 1036 (s), 885 (w), 738 (w), 623 (m), 558 (m). **HRMS:** found 893.05395 (Calculated for **$C_{37}H_{32}O_{18}S_4$ $[M+H]^{+1}$** = 893.05443)

General Procedure for preparation of hemiindigo calixarenes

Adapted from existing procedure.[94] 1.5 M solution of NaOH in deionized water was used as a solvent for reactions. Under argon gas atmosphere, a solution of indoxyl-3-acetate (2 equivalents) in aqueous NaOH (1.5 M, 2 mL, freeze-thaw degassed) was heated at 100 °C for ca. 15 min. Then, the mixture was cooled to 0 °C and a solution of a sulfonated aldehyde calixarene (100 mg) in aq. NaOH (1.5 M, 2 ml, freeze-thaw degassed) was added upon vigorous stirring. After

the addition of the aldehyde, the mixture was warmed to ambient temperature and stirred for 4 hours. Then the mixture was neutralized with 1 M aq. HCl, filtered from insoluble indigo side-product, purified on HPLC (see SI for details) and lyophilized.

Compound 77

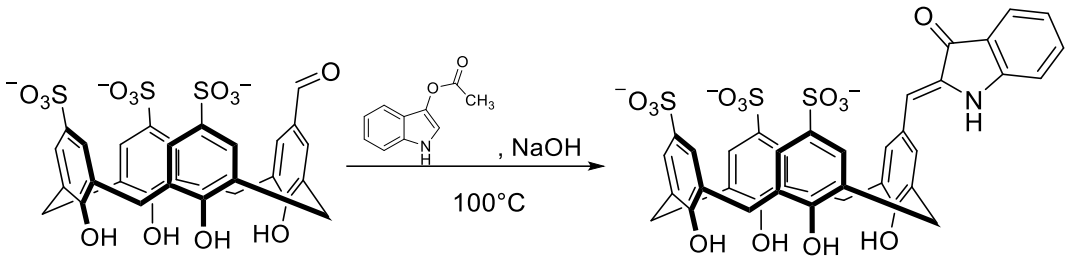

Reagents used: sulfonated aldehyde **35** (100 mg, 0.14 mmol), indoxyl acetate (51mg, 0.029 mmol), NaOH (1.5 M, 2 ml+2 ml). Brown powder. Yield: 75 mg (64%). **^{1}H NMR** (500 MHz, D_2O): δ 8.38 (s, 1H), δ 7.84 (s, 2H), δ 7.65 (s, 1H), δ 7.46 (d, J = 13.7 Hz, 2H), δ 7.32 (s, 1H), δ 6.70 (d, J = 7.1 Hz, 1H), δ 6.59 (s, 1H), δ 5.67 (s, 1H), δ 4.43 (s, 3H), δ 4.24 (d, J = 12.3 Hz, 1H), δ 4.13 (m, 3H), δ 3.80 (d, J = 13.4 Hz, 2H), δ 3.50 (d, J = 7.54 Hz, 3H), δ 3.23 (s, 1H)**. ^{13}C NMR** (126 MHz, D_2O): δ 187.3, 153.1, 152.9, 150.2, 148.8, 137.1, 136.3, 135.7, 135.0, 134.3, 132.5, 129.6, 128.8, 128.1, 127.3, 126.9, 126.3, 122.3, 119.1, 118.0, 114.7, 110.5, 30.4, 30.1, 29.1. **Melting point** > 230°C. **FT-IR** (cm^{-1}): 3251 (br), 1634 (m), 1590 (m), 1519 (w), 1454 (w), 1388 (w), 1278 (w), 1205 (m), 1165 (s), 1136 (s), 1111 (s), 1038 (s), 884 (w), 810 (w), 785 (w), 749 (w),

655 (m), 624 (s), 554 (s). **HRMS:** found 808. 4708192 (Calculated for **$C_{37}H_{29}NO_{14}S_3$ [M+H]$^{+1}$** = 808.08230)

Compound 79

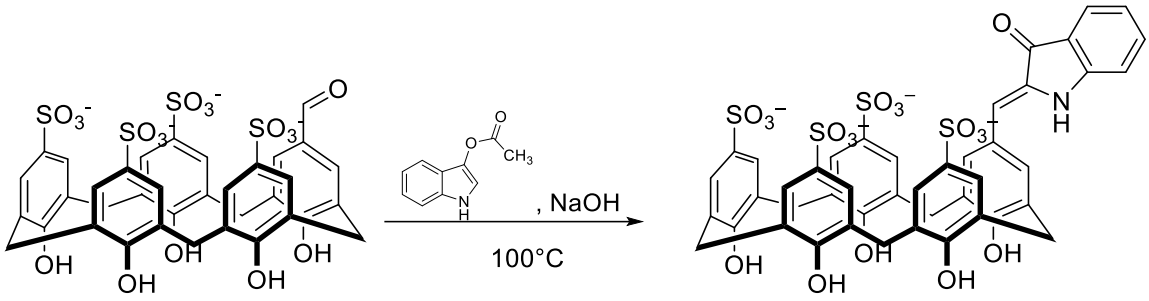

Reagents used: sulfonated aldehyde **38** (100 mg, 0.11 mmol), indoxyl acetate (40 mg, 0.023 mmol), NaOH (1.5 M, 2 ml+2 ml). Bright orange powder. Yield: 42 mg (46%). **^{1}H NMR** (500 MHz, D_2O):): δ 7.78 (s, 2H), δ 7.70 (s, 2H), δ 7.62 (s, 2H), δ 7.29 (s, 3H), δ 7.05 (s, 2H), δ 6.68 (s, 1H), δ 6.53 (s, 1H), δ 6.42 (s, 1H), δ 6.14 (s, 1H), δ 3.91(s, 4H), δ 3.89 (d, J = 5.2 Hz, 4H), δ 3.41 (s, 2H)**.** **^{13}C NMR** (126 MHz, D_2O): δ 188.0, 153.5, 153.1, 153.1, 152.0, 137.2, 135.6, 135.0, 133.7, 130.8, 130.2, 128.9, 128.6, 128.4, 128.3, 126.9, 126.6, 126.6, 126.3, 123.5, 120.1, 119.5, 116.0, 112.4, 31.0, 30.4, 30.1. **Melting point** > 230°C. **FT-IR** (cm^{-1}): 3375 (br), 2384 (br), 1622 (m), 1476 (m), 1376 (w), 1272 (w), 1161 (s), 1112 (s), 1042 (s), 939 (s), 793 (w), 730 (w), 657 (m), 624 (m), 558 (m), 495 (s). **HRMS:** found 247.26181 (Calculated for **$C_{44}H_{35}NO_{18}S_4$ [M-4H]$^{-4}$** = 247.26115)

Compound 86

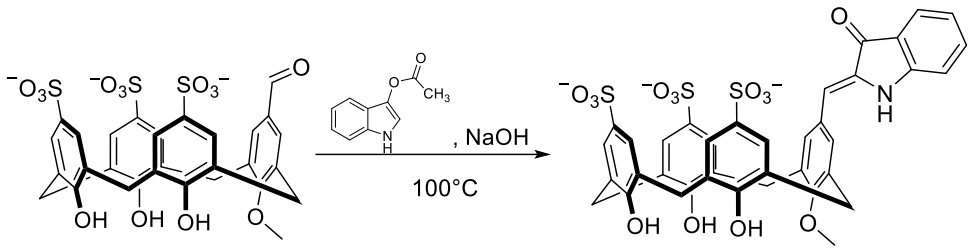

Reagents used: sulfonated aldehyde **84** (100 mg, 0.14 mmol), indoxyl acetate (50 mg, 0.028 mmol), NaOH (1.5 M, 2 ml+2 ml). Reddish brown powder. Yield = 38 mg (33%) **^{1}H NMR** (500 MHz, D_2O):): δ 8.47 (s, 1H), δ 7.88 (s, 2H), δ 7.22 (s, 1H), δ 7.40 (s, 2H), δ 7.34 (s, 1H), δ 6.80 (d, J = 7.4 Hz, 1H), δ 6.70 (s, 1H), δ 5.64 (s, 1H), δ 4.53 (s, 3H), δ 4.26 (s, 2H) δ 4.14 (s, 3H), δ 4.06 (s, 1H), δ 3.79 (d, J = 13.9 Hz, 2H), δ 3.62 (d, J = 11.2, 1H), δ 3.44 (s, 1H), δ 3.20 (s, 1H)**. ^{13}C NMR** (126 MHz, D_2O): δ 188.3, 154.2, 152.9, 152.7, 150.6, 136.8, 135.7, 134.7, 133.2, 132.4, 131.5, 130.9, 129.0, 128.6, 127.4, 126.7, 126.5, 122.4, 119.3, 118.1, 112.7, 110.6, 64.4, 30.5, 30.0, 29.0. **Melting point** > 230°C. **FT-IR** (cm^{-1}): 3311 (br), 1687 (w), 1622 (m), 1636 (m), 1591 (w), 1476 (m), 1385 (w), 1280 (w), 1205 (s), 1134 (s), 1114 (s), 1038 (s), 995 (m), 887 (w), 784 (w), 751 (w), 657(s), 625 (s), 560 (s), 521 (w), 489 (w), 471 (w). . **HRMS:** found 822.09777 (Calculated for **$C_{38}H_{31}NO_{14}S_3$ $[M+H]^{+1}$** = 822.09795)

Compound 87

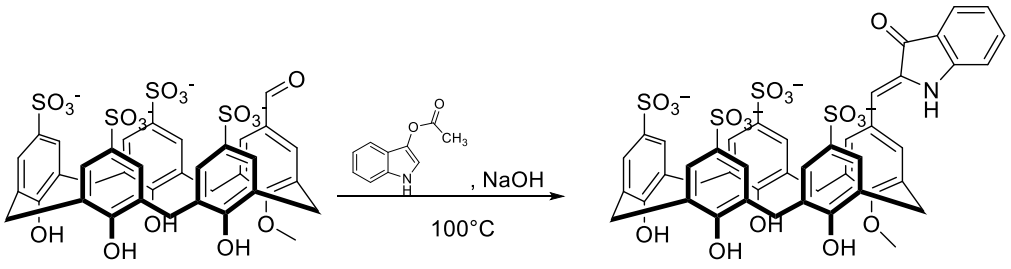

Reagents used: sulfonated aldehyde **85** (100 mg, 0.11 mmol), indoxyl acetate (39 mg, 0.023 mmol), NaOH (1.5 M, 2 ml+2 ml). Reddish brown powder. Yield = 30 mg (32%). **^{1}H NMR** (500 MHz, D_2O): δ 7.65 (d, J = 1.7 Hz, 2H), δ 7.53 (m, 4H), δ 7.43(d, J = 7.52 Hz, 1H), δ 7.34 (s, 2H), δ 7.09 (t, J = 7.7 Hz, 1H), δ 6.72 (t, J = 7.48, 2H), δ 6.49 (s, 1H), δ 6.19 (d, J = 8.3 Hz, 1H), δ 3.92 (s, 4H), δ 3.87 (s, 4H), δ 3.34 (s, 2H), δ 3.21 (s, 3H)**. ^{13}C NMR** (126 MHz, D_2O): δ 188.4, 155.9, 153.7, 153.2, 153.1, 152.8, 152.5, 137.7, 135.3, 134.9, 134.8, 134.7, 130.7, 129.8, 128.9, 128.4, 126.7, 126.5, 126.4, 126.3, 123.8, 120.5, 119.6, 114.7, 112.3, 61.0, 30.8, 30.2. **Melting point** > 230°C. **FT-IR** (cm^{-1}): 3347 (br), 1637 (w), 1591 (w), 1473 (w), 1276 (w), 1201 (m), 1134 (s), 1112 (s), 1038 (s), 891 (w), 752 (w), 734 (w), 661 (m), 624 (s), 561 (s) . **HRMS:** found 1008.09614 (Calculated for **$C_{45}H_{36}NO_{18}S_4$ [M+H]$^{+1}$** = 1008.09663)

2.6 Supporting information

2.6.1 General considerations

Proton ^{1}H and carbon ^{13}C NMR were recorded in a Bruker Avance Neo 500 MHz spectrometer or Bruker AV300 MHz spectrometer and processed with MestReNova 12.0.0 or TopSpin 4.4.0. ^{13}C spectra in D_2O were calibrated using Bruker internal calibration. Infrared (IR) spectra were obtained in a Perkin Elmer Spectrum-2 (ATR-FTIR). Melting points were taken on a Gellenkamp Melting Point Apparatus. Absorption spectra were recorded using Varian Cary 100 UV-Vis Spectrophotometer. High-resolution mass spectra were taken in a Thermo Scientific Ultimate 3000 ESI-Orbitrap Exactive. Reagents for synthesis were purchased from either Sigma-Aldrich or TCI chemicals and used as received. HPLC purification was carried out in Teledyne ACCQPrep HP125 HPLC system on a Phenomenex Luna C18(2) column (21.2 mm x 250 mm) with 5 μm particle and 100 Å pore size. The gradient consisted of water and acetonitrile, both spiked with 0.1% of TFA, and a DAD detector set to 280 nm was used. Samples were dissolved in a 90:10 mixture of H_2O/MeCN (0.1% TFA), centrifuged and pre-filtered using Captiva Premium Syringe filters with a 0.45 μm PES membrane. Gradients started with a 90:10 H_2O/MeCN hold for a minute, and then it switched to a 10:90 H_2O/MeCN over the course of usually 20 minutes (gradient time was adjusted depending on peak retention time).

2.6.2 Characterization data

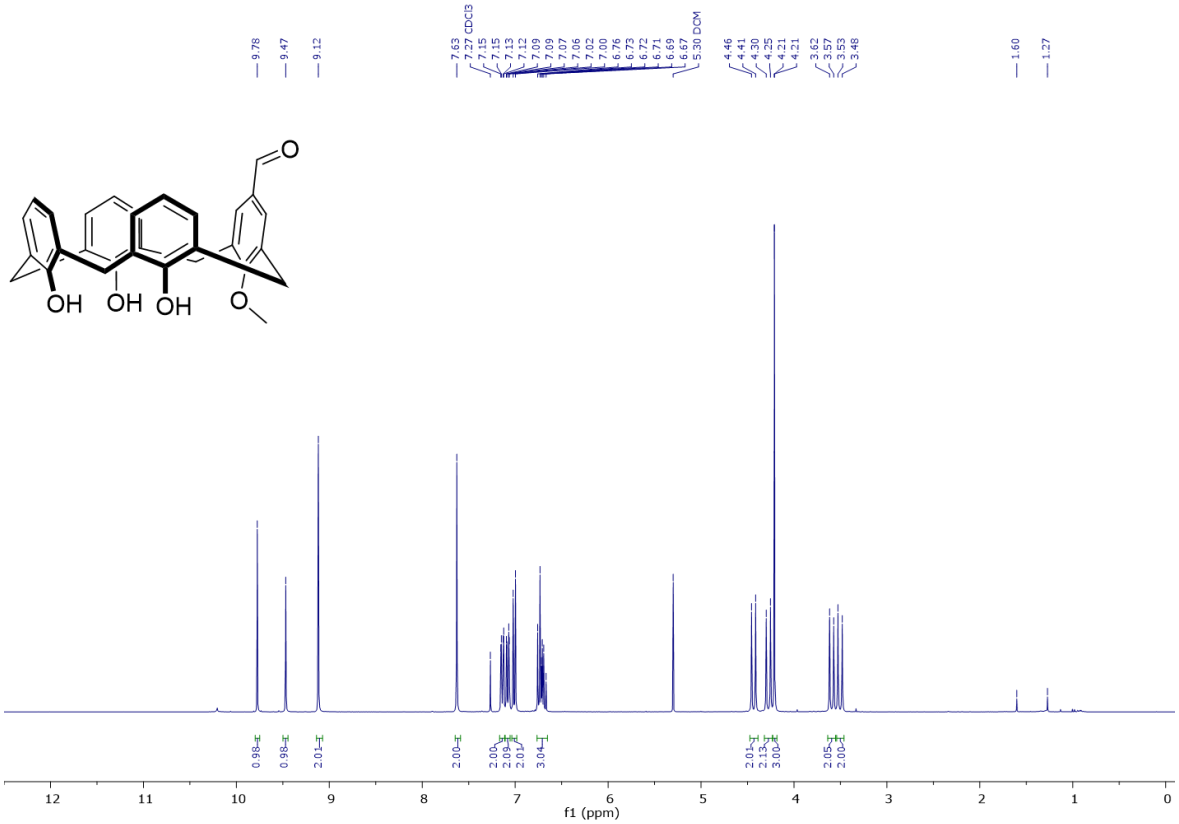

*Figure S2.1. ^{1}H NMR of **82** in $CDCl_3$.*

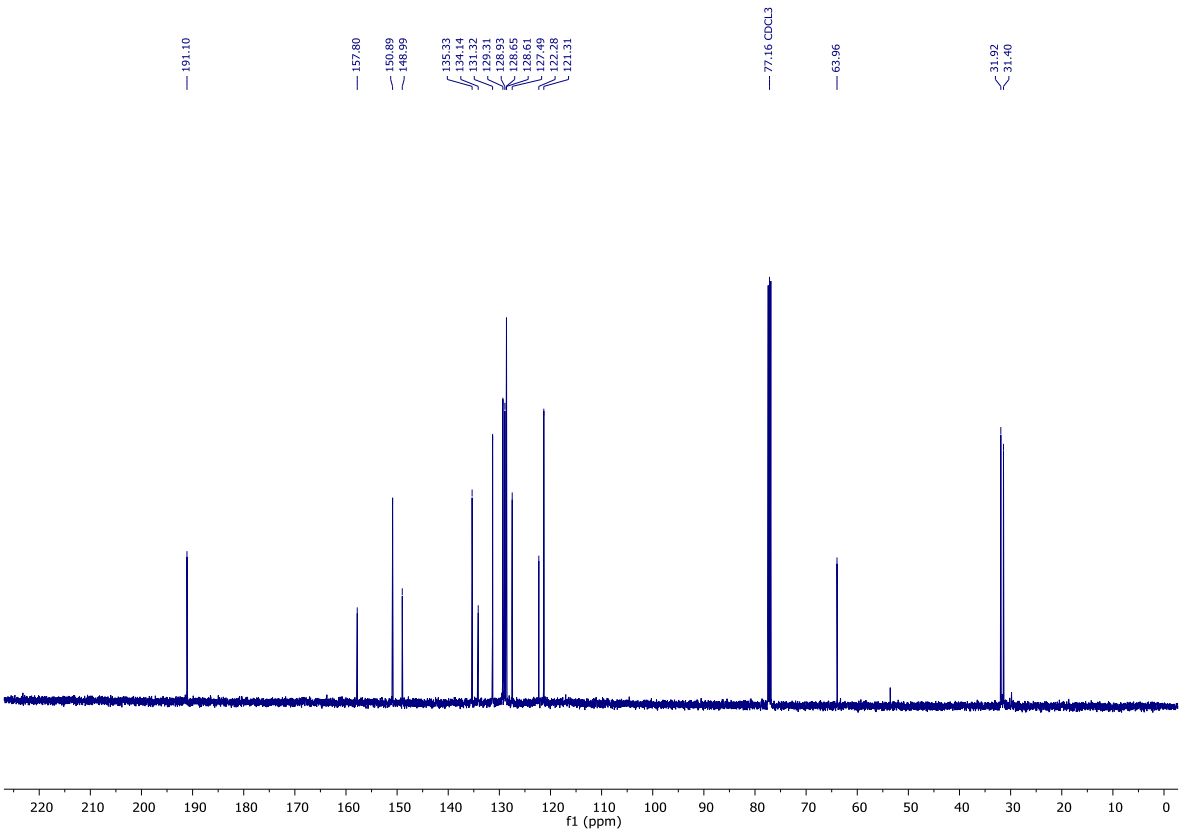

*Figure S2.2. ^{13}C NMR of **82** in $CDCl_3$.*

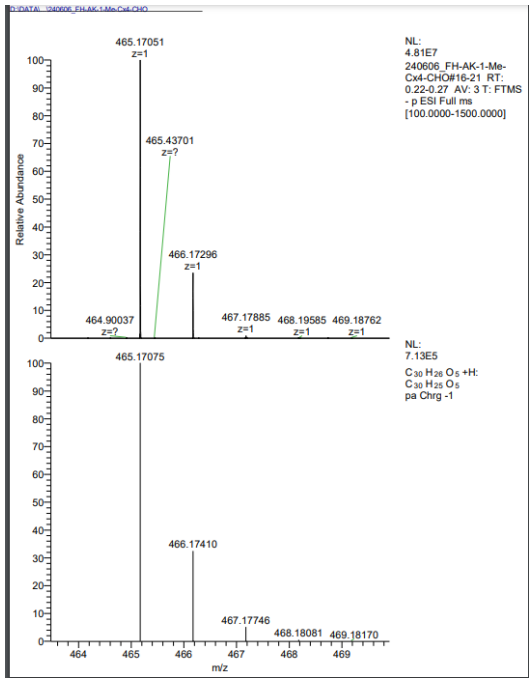

*Figure S2.3. HRMS of **82**.*

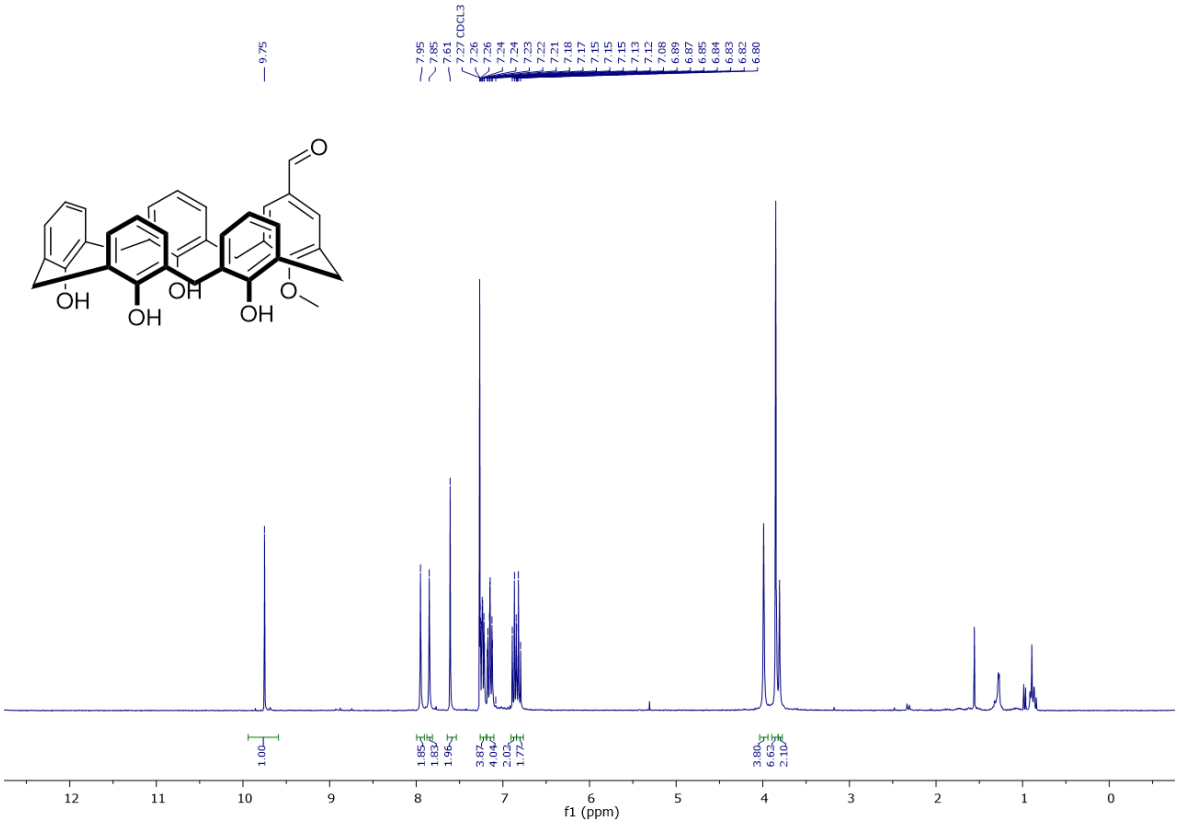

*Figure S2.4. ^{1}H NMR of **83** in $CDCl_3$.*

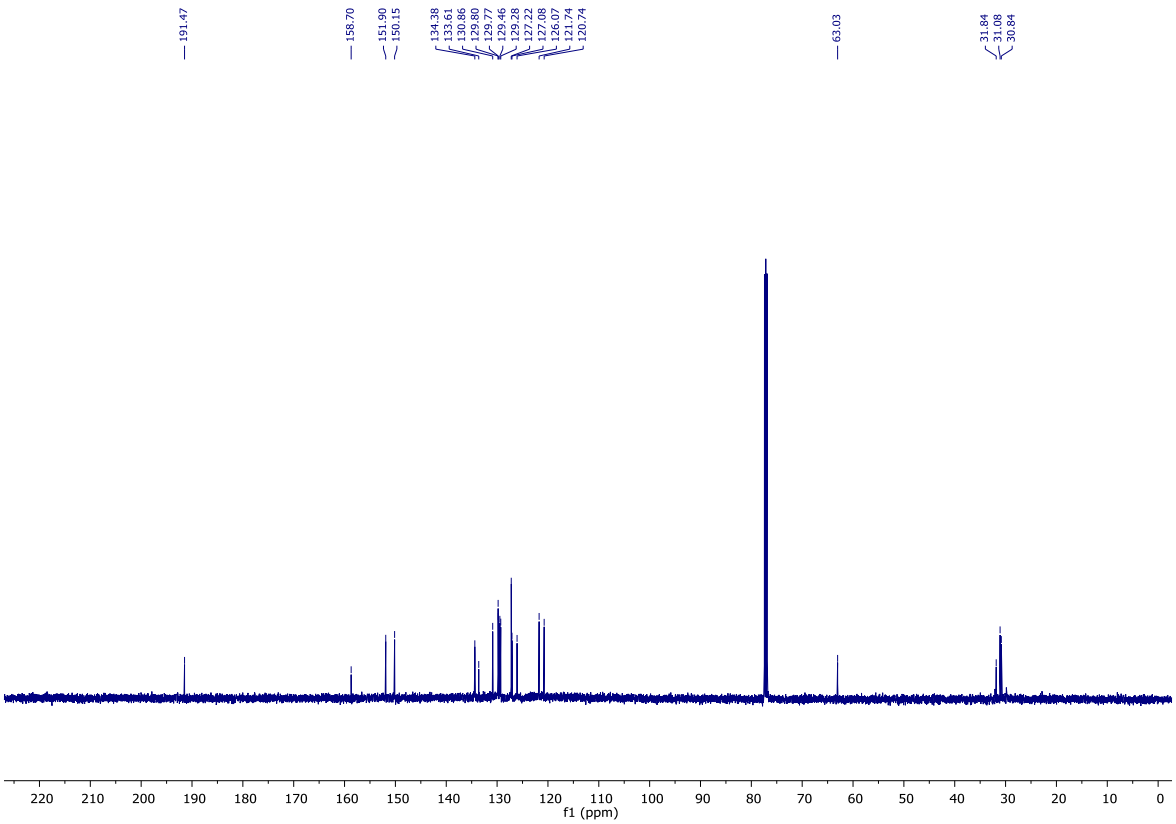

*Figure S2.5. ^{13}C NMR of **83** in $CDCl_3$.*

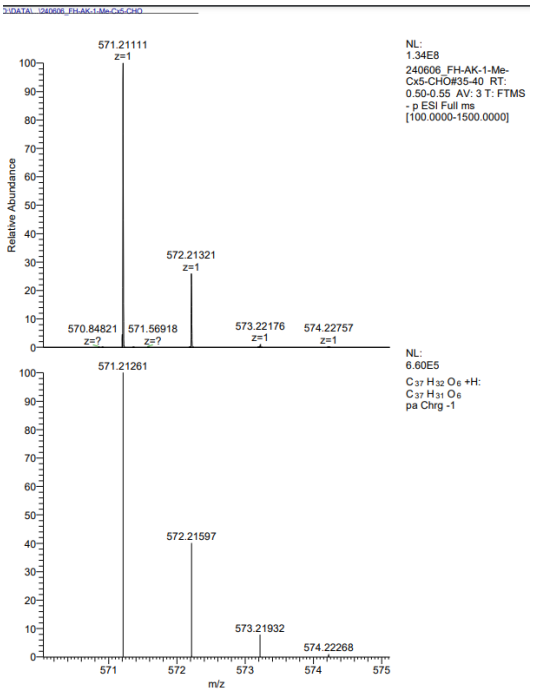

*Figure S2.6. HRMS of **83**.*

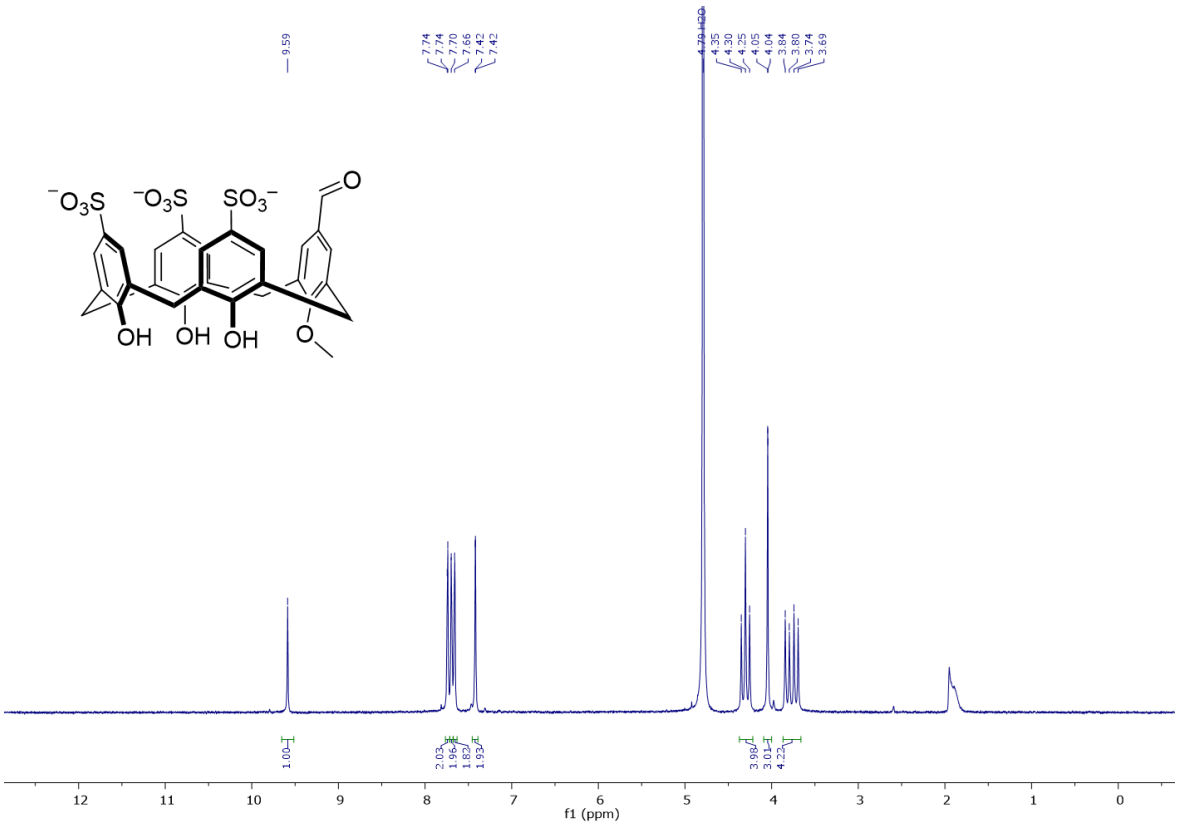

*Figure S2.7. ^{1}H NMR of **84** in D_2O.*

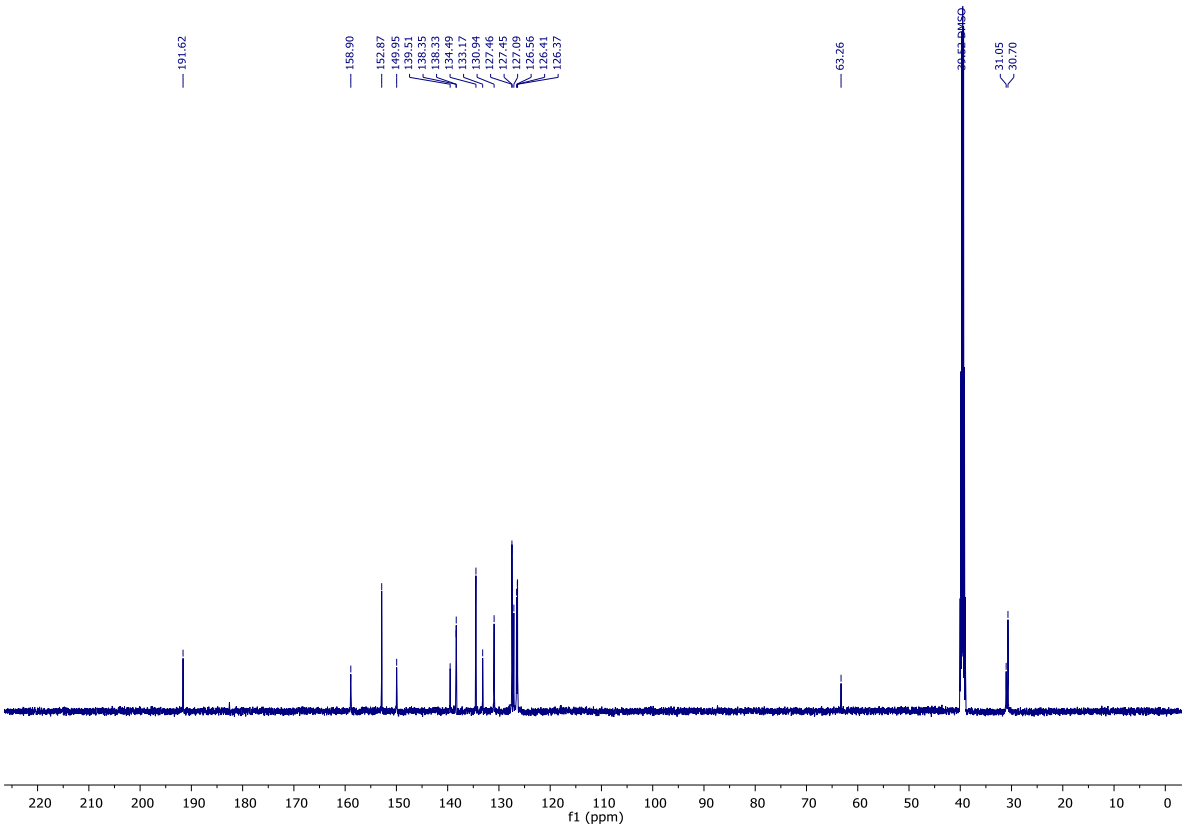

*Figure S2.8. ^{13}C NMR of **84** in DMSO.*

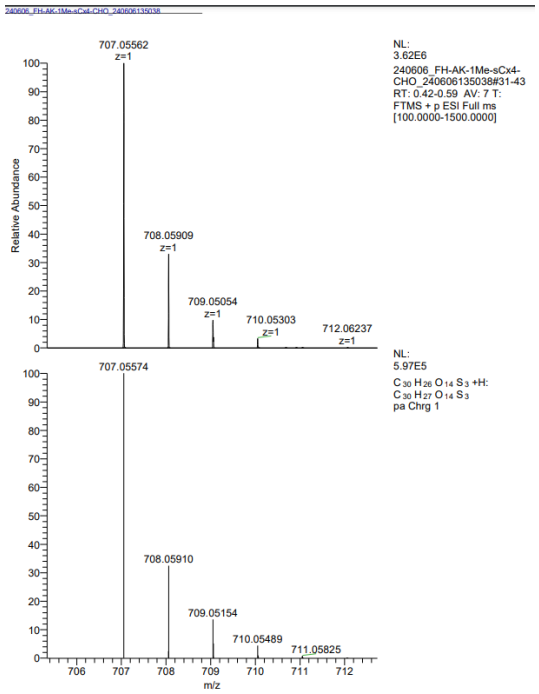

*Figure S2.9. HRMS of **84**.*

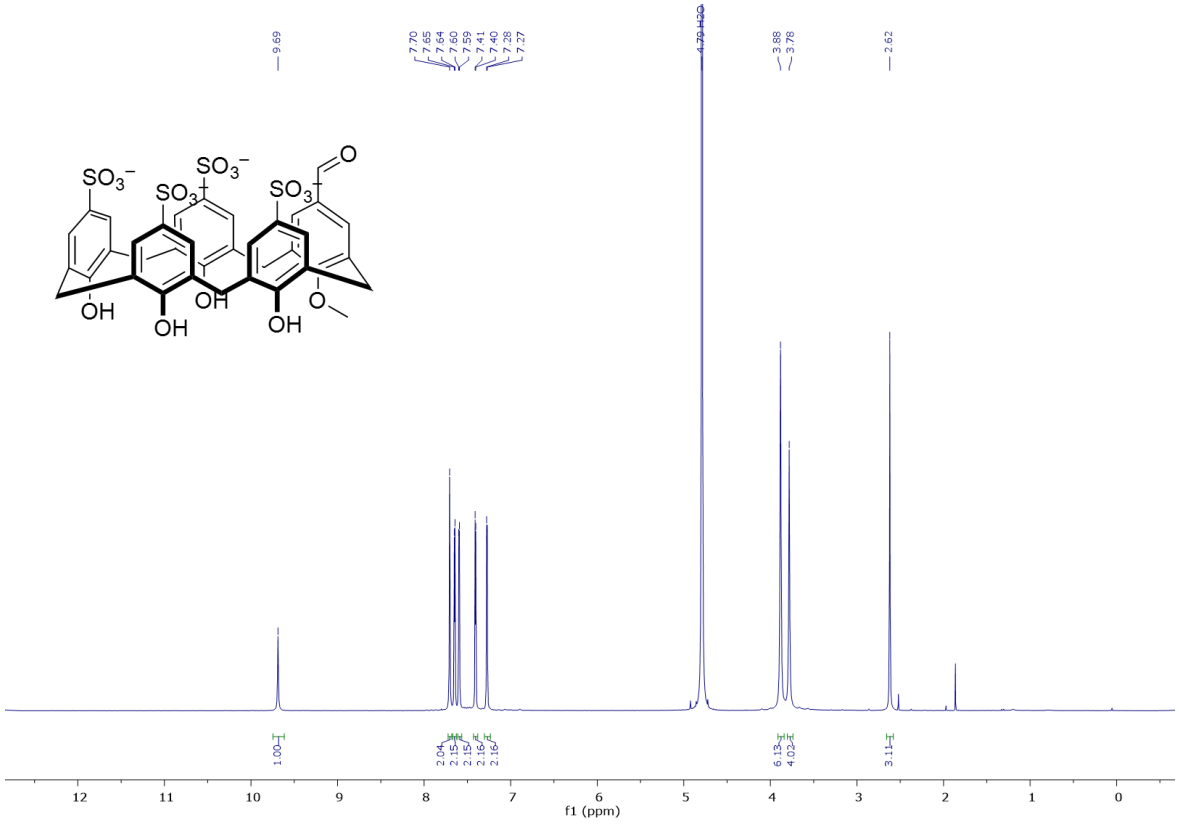

*Figure S2.10. ^{1}H NMR of **85** in D_2O.*

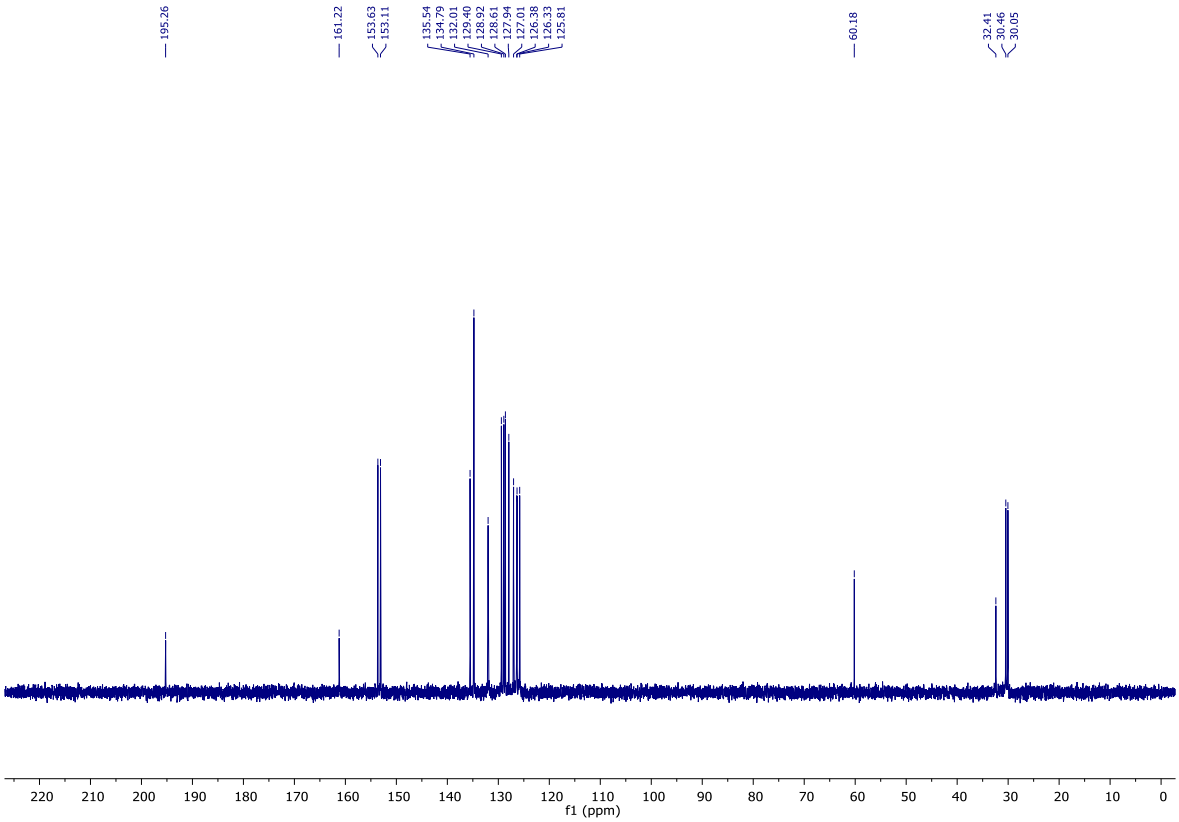

*Figure S2.11. ^{13}C NMR of **85** in D_2O.*

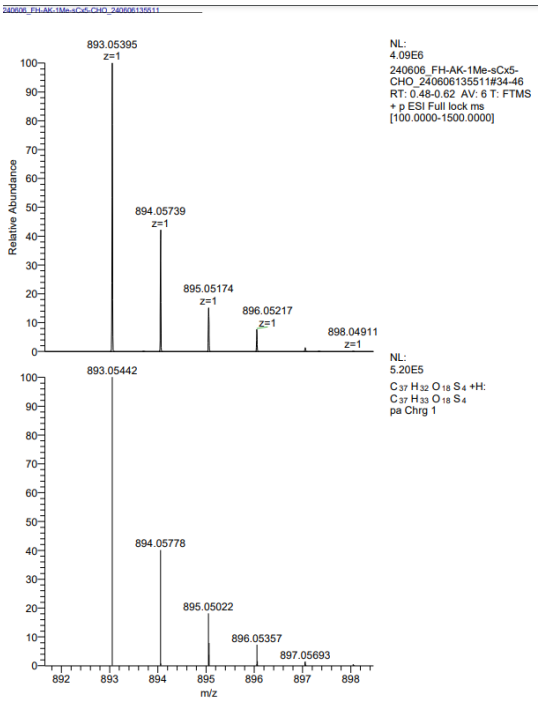

*Figure S2.12. HRMS of **85**.*

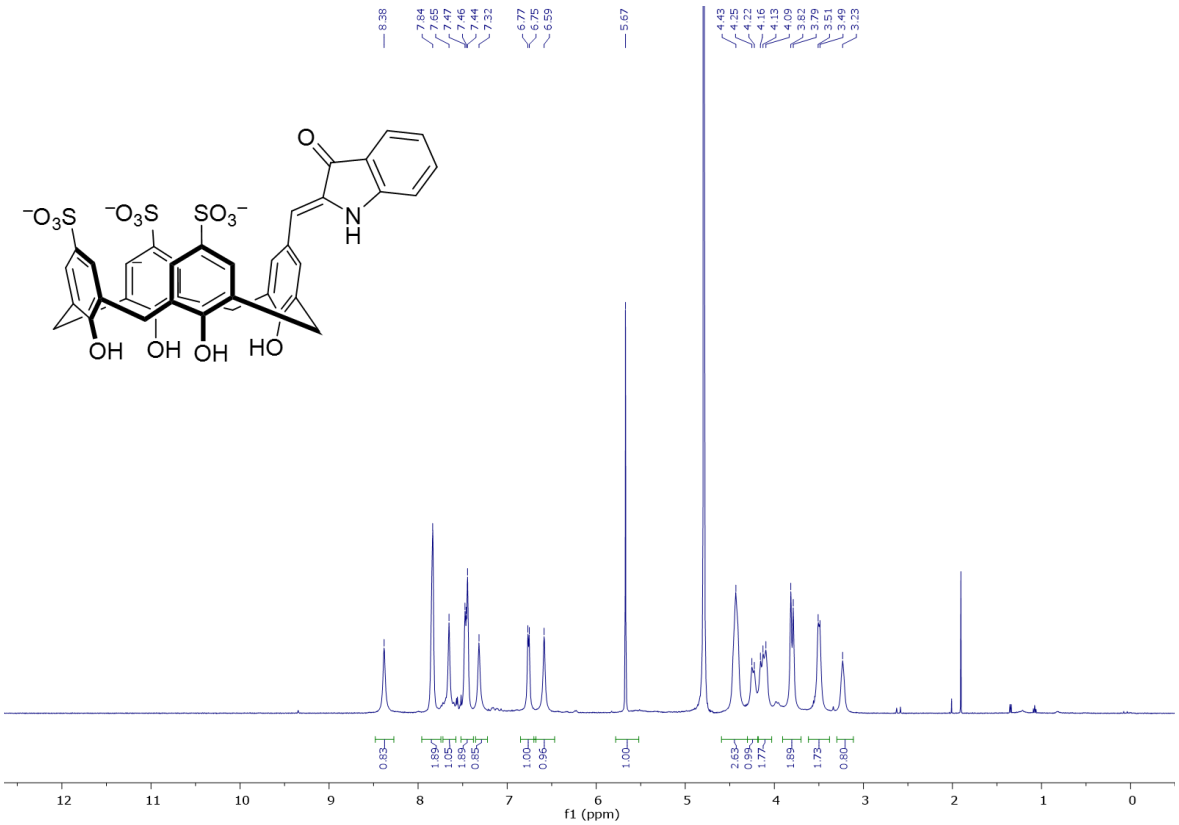

*Figure S2.13. ^{1}H NMR of **77** in D_2O.*

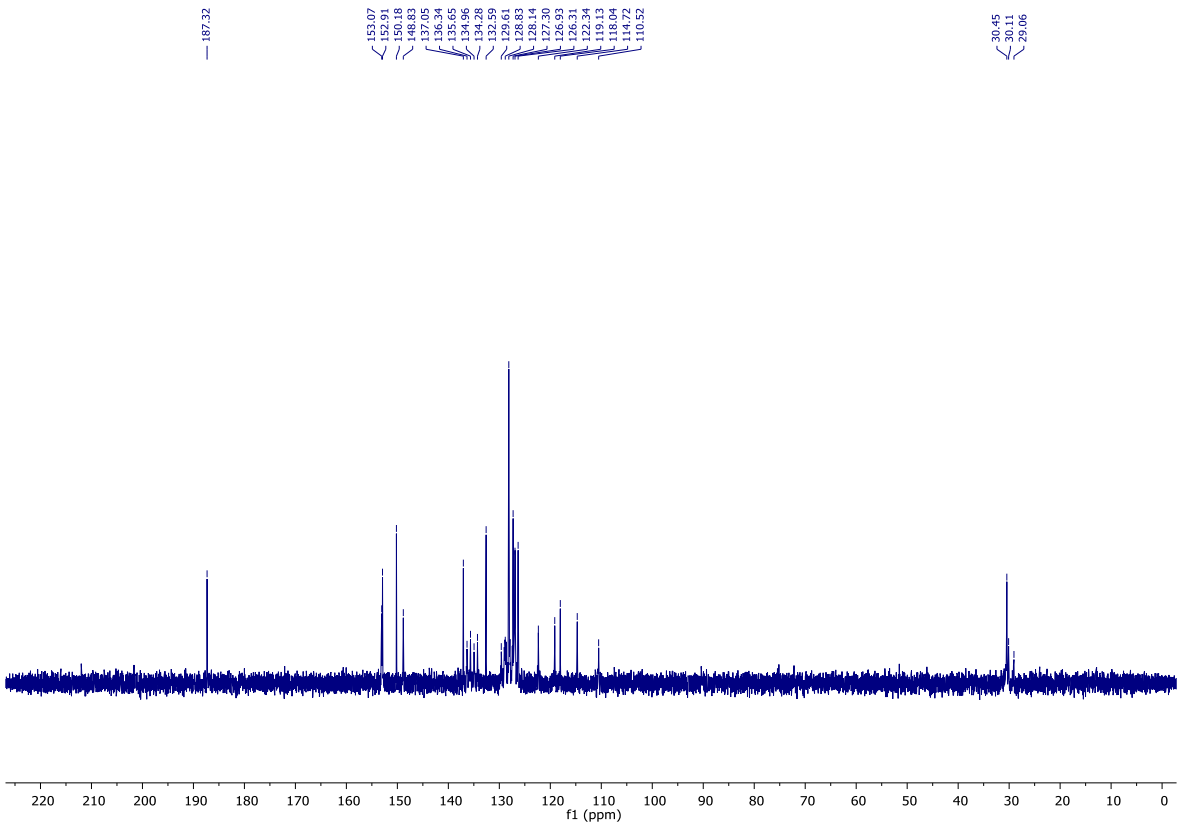

*Figure S2.14. ^{13}C NMR of **77** in D_2O.*

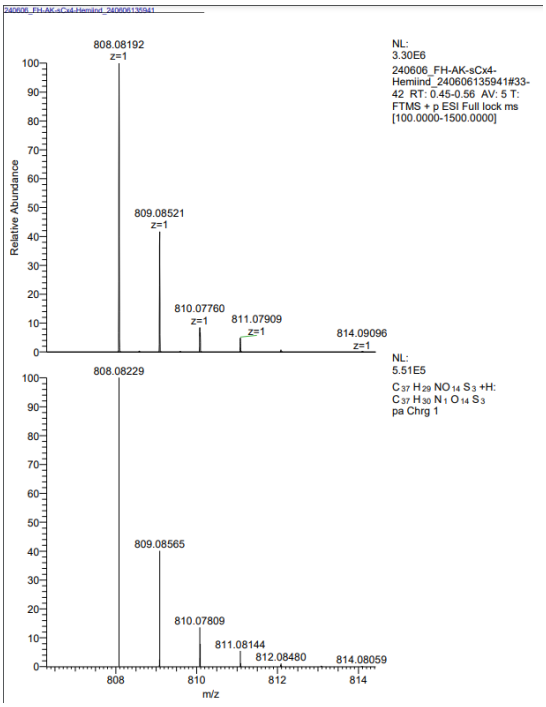

*Figure S2.15. HRMS of **77.***

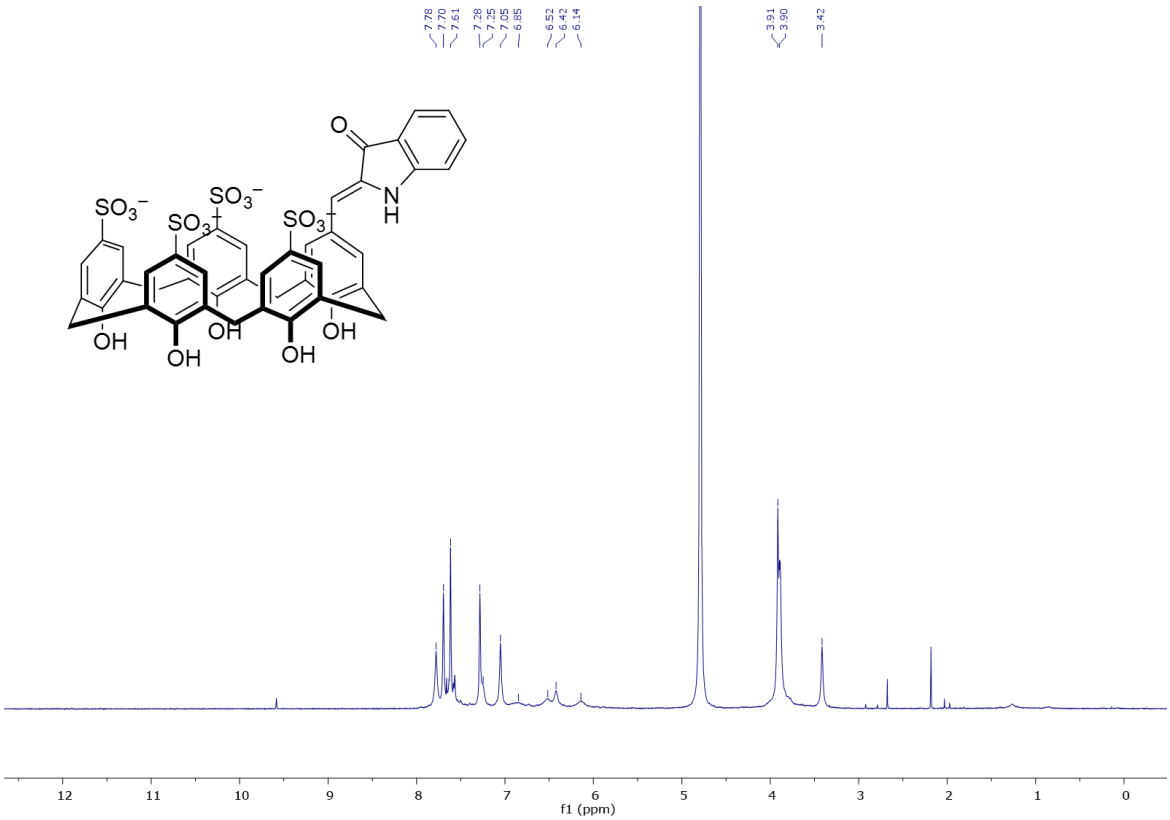

*Figure S2.16. ^{1}H NMR of **79** in D_2O.*

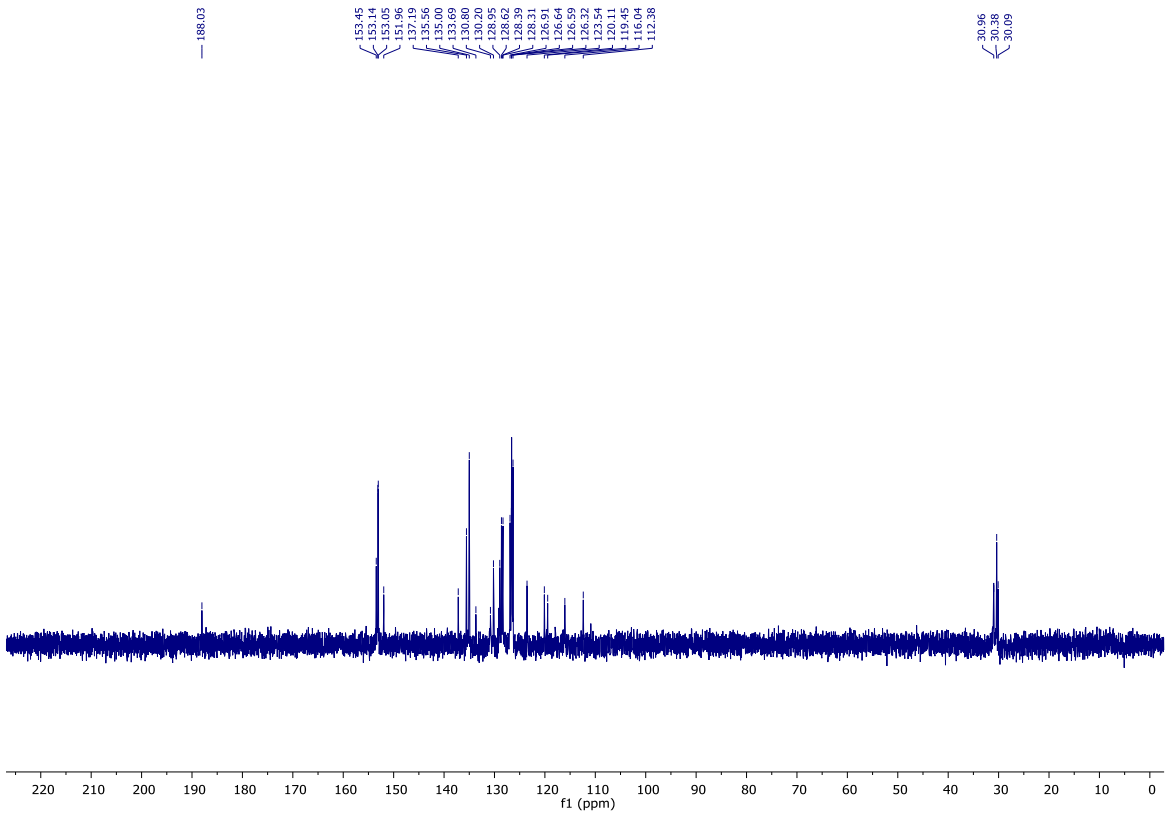

*Figure S2.17. ^{13}C NMR of **79** in D_2O.*

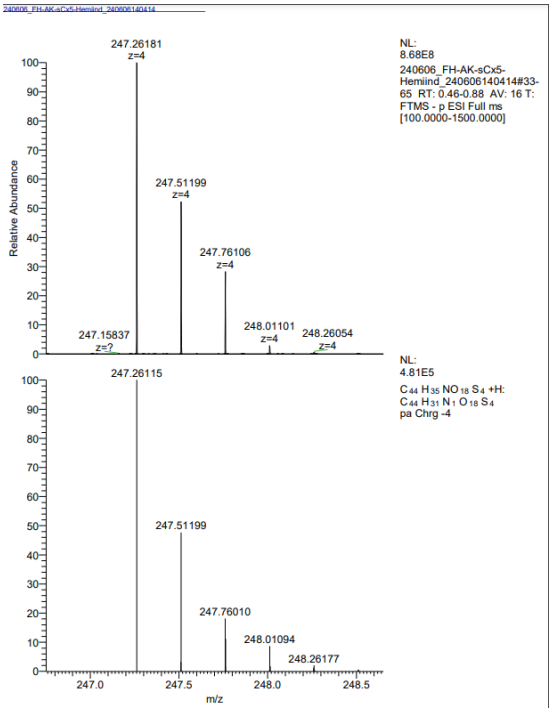

*Figure S2.18. HRMS of **79**.*

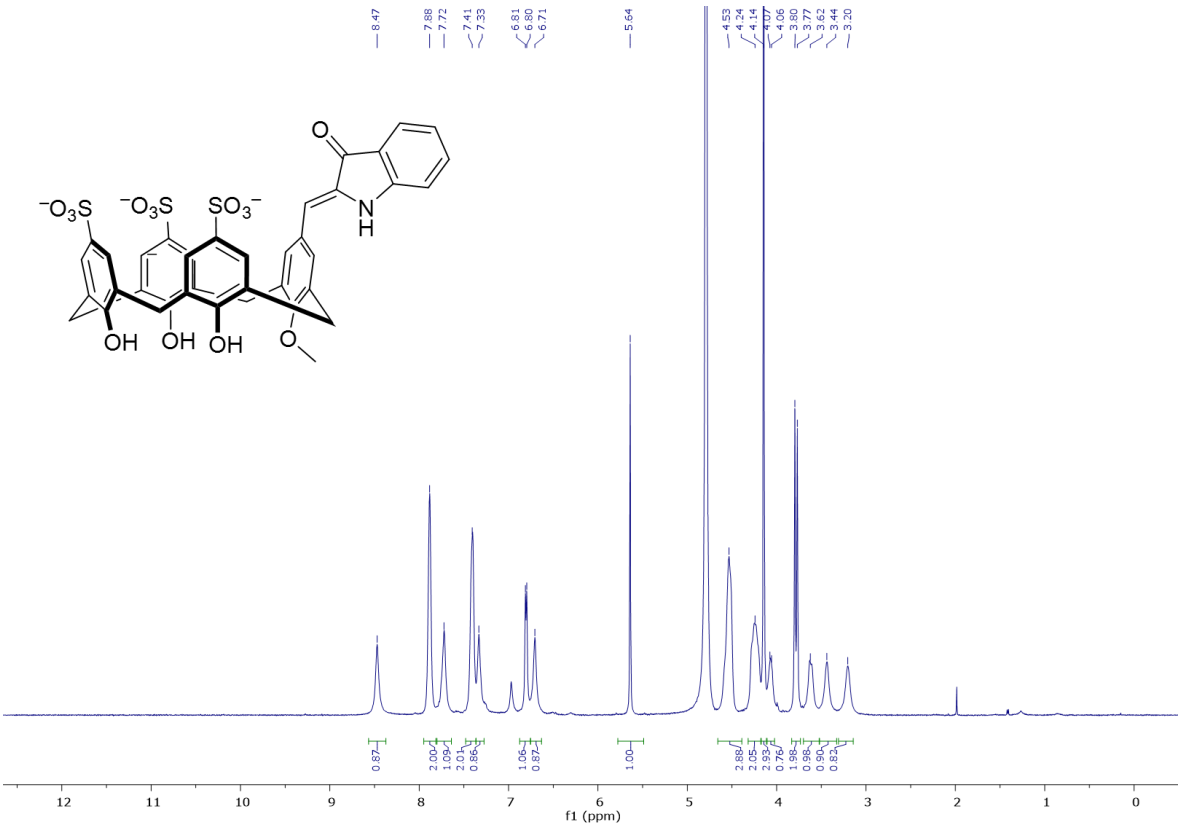

*Figure S2.19. ^{1}H NMR of **86** in D_2O.*

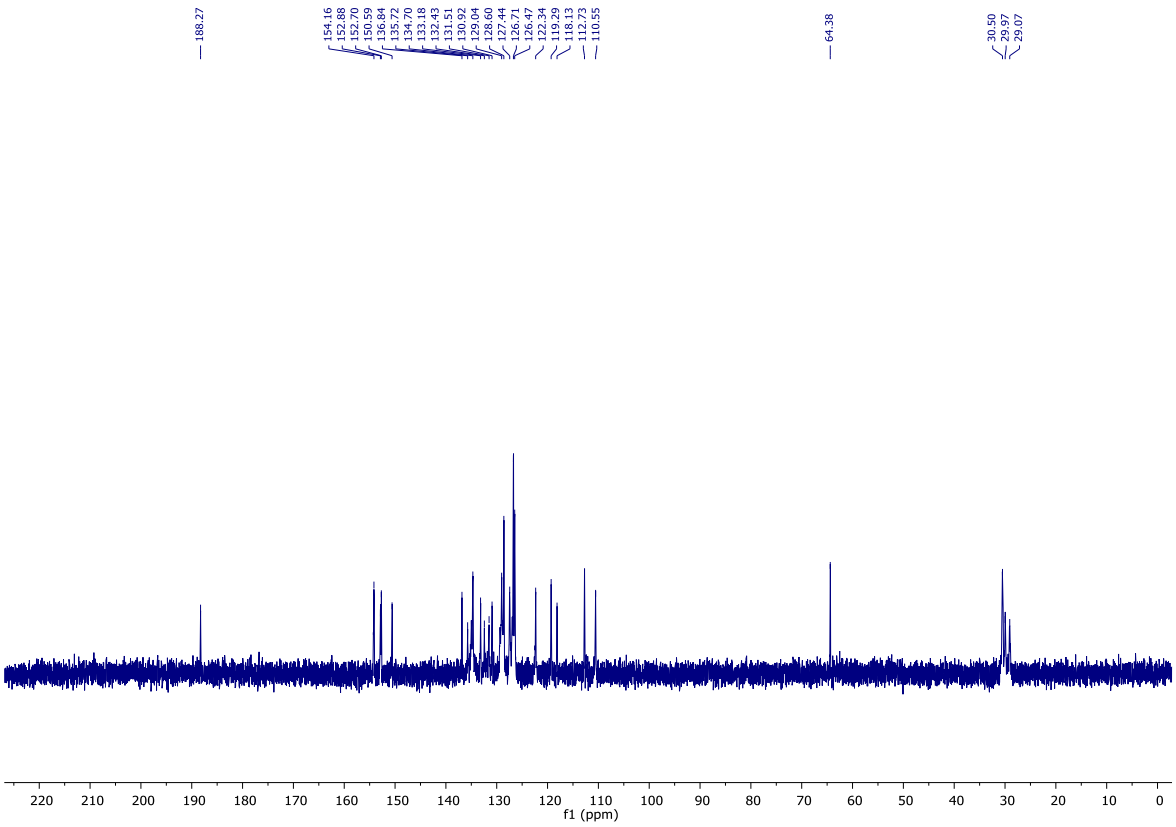

*Figure S2.20. ^{13}C NMR of **86** in D_2O.*

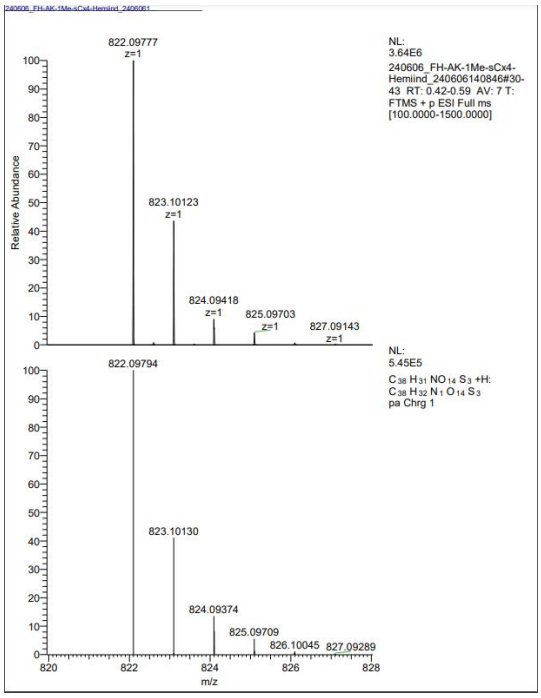

*Figure S2.21. HRMS of **86.***

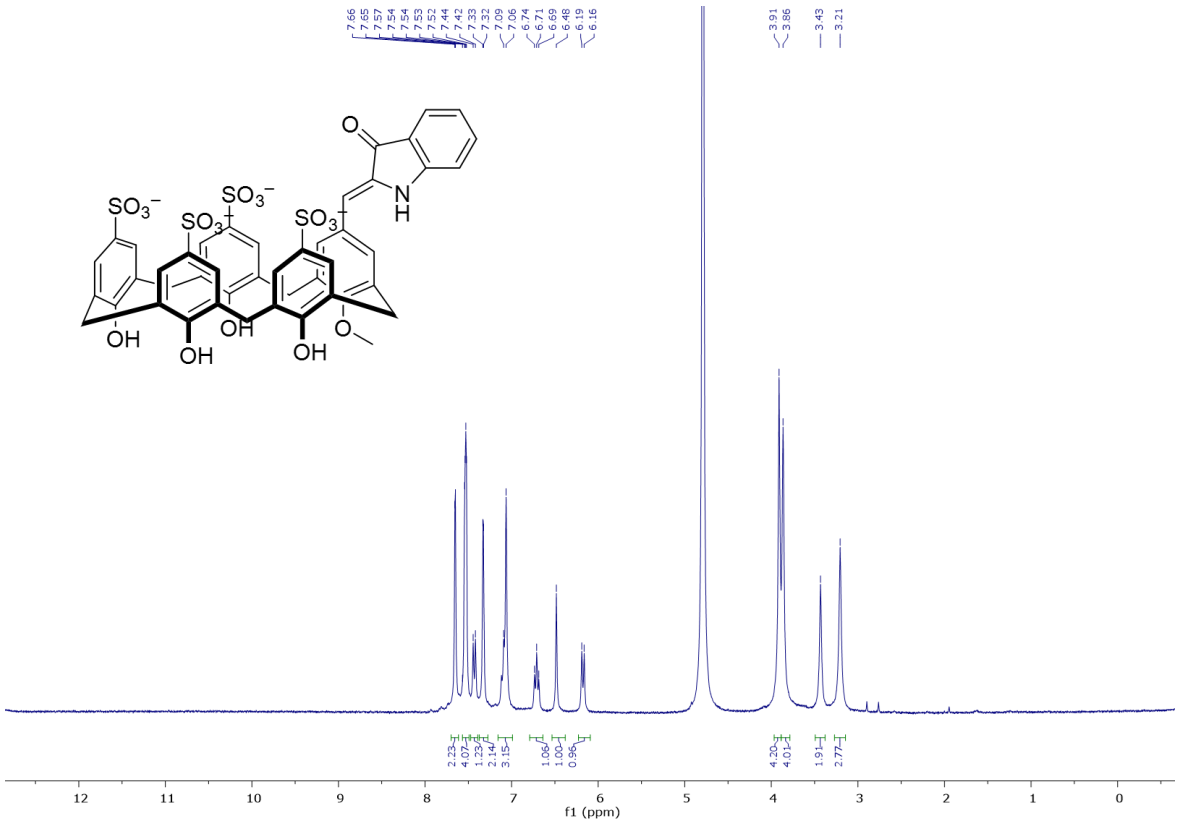

*Figure S2.22. ^{1}H NMR of **87** in D_2O*

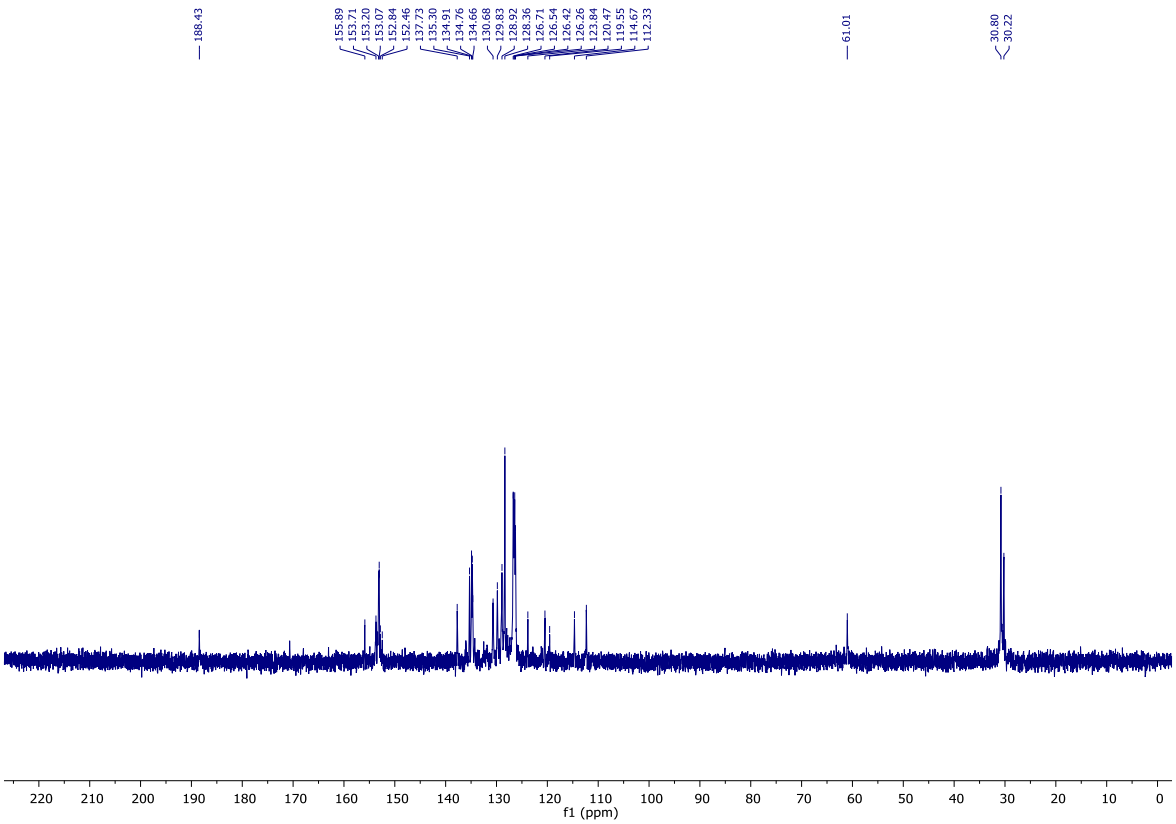

*Figure S2.23. ^{13}C NMR of **87** in D_2O.*

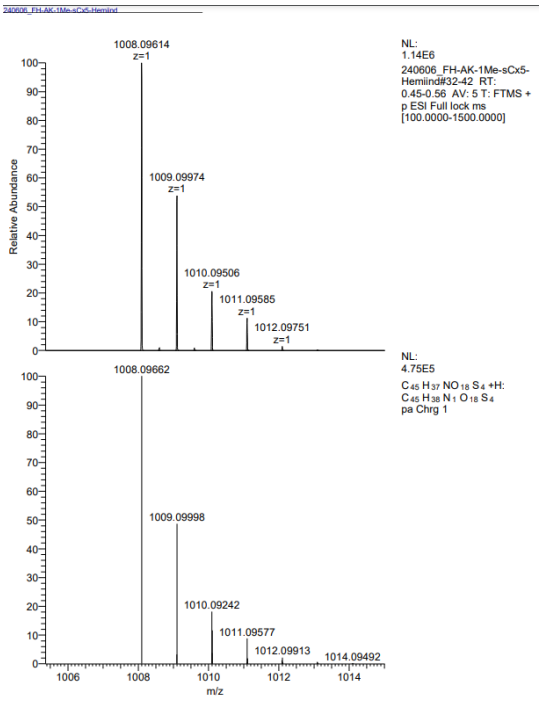

*Figure S2.24. HRMS of **87**.*

2.6.3 Photoswitching data

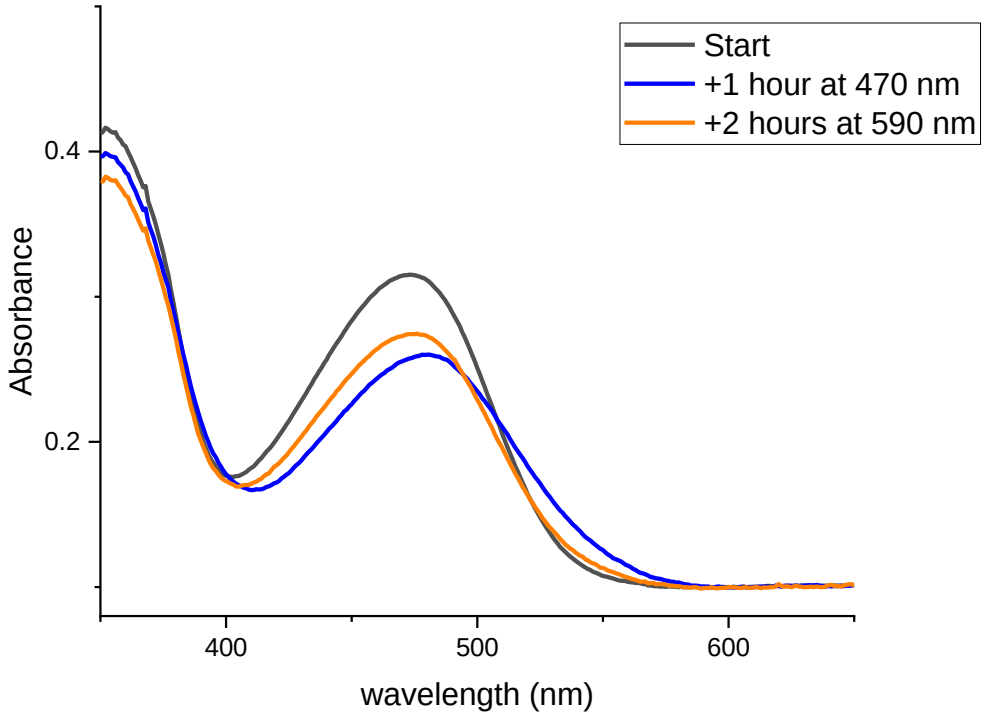

Figure S2.25. Photoswitching of hemiindigo calix[5]arene ***87.***

Chapter 3. Mechanistic studies

3.1 Motivation

In Chapter 2 we have described the synthetic pathway towards hemiindigo calix[4]arene (**86**) and calix[5]arene **(87)** and demonstrated their principal ability to photoisomerize. Our next task was to examine their behavior more thoroughly in order to understand their supramolecular organization and properties.

Previously, sulfonated calixarenes with similar "one-armed" chromophore structures at the upper rim were shown to possess an ability to form dimers in aqueous solutions, which in turn affected their photophysical properties.[4,21,95] The dimers are driven by the pendant arm of one molecule interacting with the binding pocket of the other either by charge attraction to sulfonate groups (for positively charged pendant chromophores) and/or by hydrophobic interactions with the aromatic cavity. So, our first goal was to learn more about underlying "supramolecular" mechanisms which define hemiindigo calixarenes: would they form dimers or other aggregates, what would be their structure, would they be easy to disrupt? We also wanted to confirm if our molecules would be able to bind guests, which might unlock a path to potential applications.

Our next point of interest was to compare hemiindigo calix[4]arene **86** and hemiindigo calix[5]arene **87**. While being chemically similar, the parent

macrocycles themselves are known to have different dynamics in solutions.[96–98] We were interested if similar behaviors would be present in our systems, and what effects they might have on the overall molecules.

Finally, we were interested if photoisomerization would in any way affect (or be affected) by the aforementioned supramolecular behaviors. That would require checking if we would be able to isolate separate isomers first and then comparing them with each other.

3.2 Introduction

In order to analyze behavior and properties of hemiindigo calixarenes an array of techniques was used. Here we will provide a short overview of them, elucidate the main principles, describe the types of data they can provide and explain why they are relevant to our systems.

NMR (nuclear magnetic resonance) spectroscopy is a bread and butter technique for modern synthetic chemistry and is usually used in order to confirm structure of organic molecules and/or to track the changes that happen during reaction. Yet, its scope goes far beyond that. With regards to calixarene chemistry it has been used extensively to provide invaluable information about conformations,[99,100] aggregation[101,102] and guest binding in solutions.[103–105] Since calixarenes are rather flexible molecules, they are prone to conformational changes. Such changes can happen due to interaction with

solvent, self-assembly or guest binding. Since NMR shift depends strongly on electronic surrounding of the target nuclei, with protons being particularly sensitive, it can tell if there are changes taking place. Another important indicator is chemical shifts of interacting guests which are often immediately observable due to strong upfield-shifting effect of the aromatic cavity.[106] This is a basis of NMR titrations. NMR capabilities are even broader, though, and not limited to simple 1D ^{1}H experiments. For example, Nuclear Overhauser Effect Spectroscopy (NOESY) allows to understand molecular geometry while Diffusion Ordered Spectroscopy (DOSY) gives an insight into the aggregation states of our systems.

Correlational Spectroscopy (COSY) is one of the simplest and most commonly used 2D NMR techniques. Like with any 2D NMR experiment, the underlying principle is addition of a second variable time domain, which is time difference between two 90° pulses that happen before "normal" FID collection, which gives rise to second, "artificial" FID, also known as interferogram. For each difference point the "normal" FID is collected and Fourier-transformation of both FID's gives us the desired 2D spectra. In case of COSY, second 90° pulse transfers some polarization from certain nuclei to its spin-coupled partners. Since we have two time domains, a small fraction of said partners will then precess in "normal" time domain with frequency acquired from "artificial" time domain, giving rise to correlations.[107,108]In practice, this method allows for

precise assignment of signals in complex spectra and clarification of molecular topology. It has been extensively utilized for characterization of calixarenes, including chiral ones.[109–111]

Nuclear Overhauser Enhancement Spectroscopy (NOESY) is another NMR technique that looks into correlations between different parts of the molecule. Contrary to COSY, which observes indirect spin-spin correlations transmitted by electrons, NOESY looks at direct spatial magnetic interactions – dipole couplings. It allows to elucidate 3D structures and see which parts of the molecule interacts with each other, since only spins that are close to each other in space are able to experience the NOE. In short, NOE can be defined as a change of intensity of one resonance, when the spin transitions of another are somehow perturbed. In case of simple ^{1}H NOE, it starts with irradiation of the sample on resonance frequency of certain proton, usually denoted as S (source). This perturbation changes the energy level population. If there are any protons in vicinity (usually no more than 5 Å), dipole-dipole coupling occurs. This changes the energy level population of "enhanced" resonance, denoted as I (interesting). Depending on the type of predominant cross-relaxation, we then observe either positive (increase of signal intensity) or negative (decrease) NOE on NMR spectra. By subtracting the resulting spectra from starting one, we can easily figure out the interacting protons. As a general rule, molecules that tumble fast in solution tend to have positive NOE's, those that tumble

slowly usually have negative.[112] This approach was broadly used for characterization of calixarene-like systems, for identifying host-guest interaction,[103,113,114] as well as observation of host aggregation. Interestingly enough, the same pulse-delay-observe style of NMR sequence that works for NOESY can also be used to detect protons that exchange identities with each other, in which case it is called EXSY (exchange spectroscopy).[115,116]

DOSY is an NMR technique that allows one to measure a diffusion coefficient of particles is solution.[117] It relies on rather complicated Pulse Gradient Spin Echo (PGSE) sequences, but what essentially being tracked is the Larmor precession frequency's dependence on the *z*-coordinate within the NMR tube. Angular frequency is given by Equation 3.1,

$$\omega(r) = -\gamma B(r) \tag{3.1}$$

where *B(r)* is a magnitude of the applied magnetic field and γ is a gyromagnetic ratio. If the gradient only applied along *z*-axis, then the acquired phase angle is given by Equation 3.2, where δ is the duration of a gradient.

$$\Phi(z) = -\gamma B(z)\delta \tag{3.2}$$

The experiment starts in external magnetic field, so all spins are oriented along the *z*-axis. Then a 90° radiofrequency pulse is applied, so the magnetization rotates from the *z*-axis to the *xy*-plane. The aforementioned magnetic field pulse gradient along the *z*-axis is then applied at time t_1, so all spins experience a

phase shift during the time period τ. Next step is the application of a 180° pulse, which changes the sign of phase shift. It is followed by application of magnetic field gradient, identical to the previous one, at the time $t_1 + \Delta$. If there is no translational motion (i.e. no diffusion), the phase shift after the first τ period is equal to the phase shift after the second τ period and opposite in sign. Hence, they cancel each other, spins refocus, and maximum echo signal is obtained. If there is some diffusion the phase shifts are different, because the applied magnetic field depends on the *z*-coordinate of the molecules. In this case shifts do not fully cancel each other and a weaker echo signal is obtained. By changing the diffusion time we can then track how fast molecules move in solution and find the diffusion coefficient of species present in the system. According to the Einstein-Smoluchowski Equation 3.3, where D is the diffusion coefficient, T is the absolute temperature and k_b is the Boltzmann constant, we can get f, which is so-called hydrodynamic frictional coefficient.

$$D = \frac{k_b T}{f} \tag{3.3}$$

For spherical particles sliding in a solution with viscosity η, according to the Stokes Equation 3.4, we arrive at the Einstein-Stokes Equation 3.5. It worth mentioning that it only works in case of spherical particles, and that more complicated geometries would require a different approach. Making a simple

transformation we arrive at Equation 3.6 to find the Stokes radius r_s, which is the radius of the particle plus its hydration shell.

$$f = 6\pi\eta r_s \tag{3.4}$$

$$D = \frac{k_b T}{6\pi\eta r_s} \tag{3.5}$$

$$r_s = \frac{k_b T}{6\pi\eta D} \tag{3.6}$$

Knowing r_s (also called hydrodynamic radius), we can estimate the size of aggregates present in solution and subsequently, what type of aggregates, if any, a molecule forms under given conditions.[118,119] With regards to calixarenes, this technique has already become a standard, being used for systems of varying sizes, solubilities and chemical modifications.[116,120–123]

The combination of these NMR methods allow one to establish relatively clean and coherent pictures of a system's supramolecular properties by:

1. Accurately assigning protons to corresponding chemical shifts, and making conclusions from their values
2. Establishing the projected 3D model of molecules by analyzing spatial and spin correlations
3. Elucidating the aggregation state of an assembled system

3.3 Results and discussion

3.3.1 Degradation studies

We began our investigation of properties from an attempt to photoizomerize and isolate hemiindigo calixarenes **86** and **87** on a scale big enough to allow characterization of photoswitched samples by NMR. While we were able to detect switching on much smaller UV-Vis scale (20 μM), NMR-scale photoswitching experiments (1 mM) produced somewhat underwhelming results (Figure 3.1).

We will attempt to interpret and assign ^{1}H NMR spectra of hemiindigo calix[4]arene **86** later in this Chapter due to its complexity. But it has one characteristic and recognizable resonance at 5.5 ppm which belongs to the alkene CH proton. We can see, how after prolonged irradiation it disappears completely, giving place to another highly characteristic resonance around 9.3 ppm.

The resulting spectrum looks strikingly similar to that of the aldehyde starting material, leading us to the conclusion that at higher concentrations the photobleaching process dominates over photoswitching, preventing us from observing the desired isomerization. Not surprisingly, the same behavior is exhibited for the calix[5]arene version **87** (Figure 3.2).

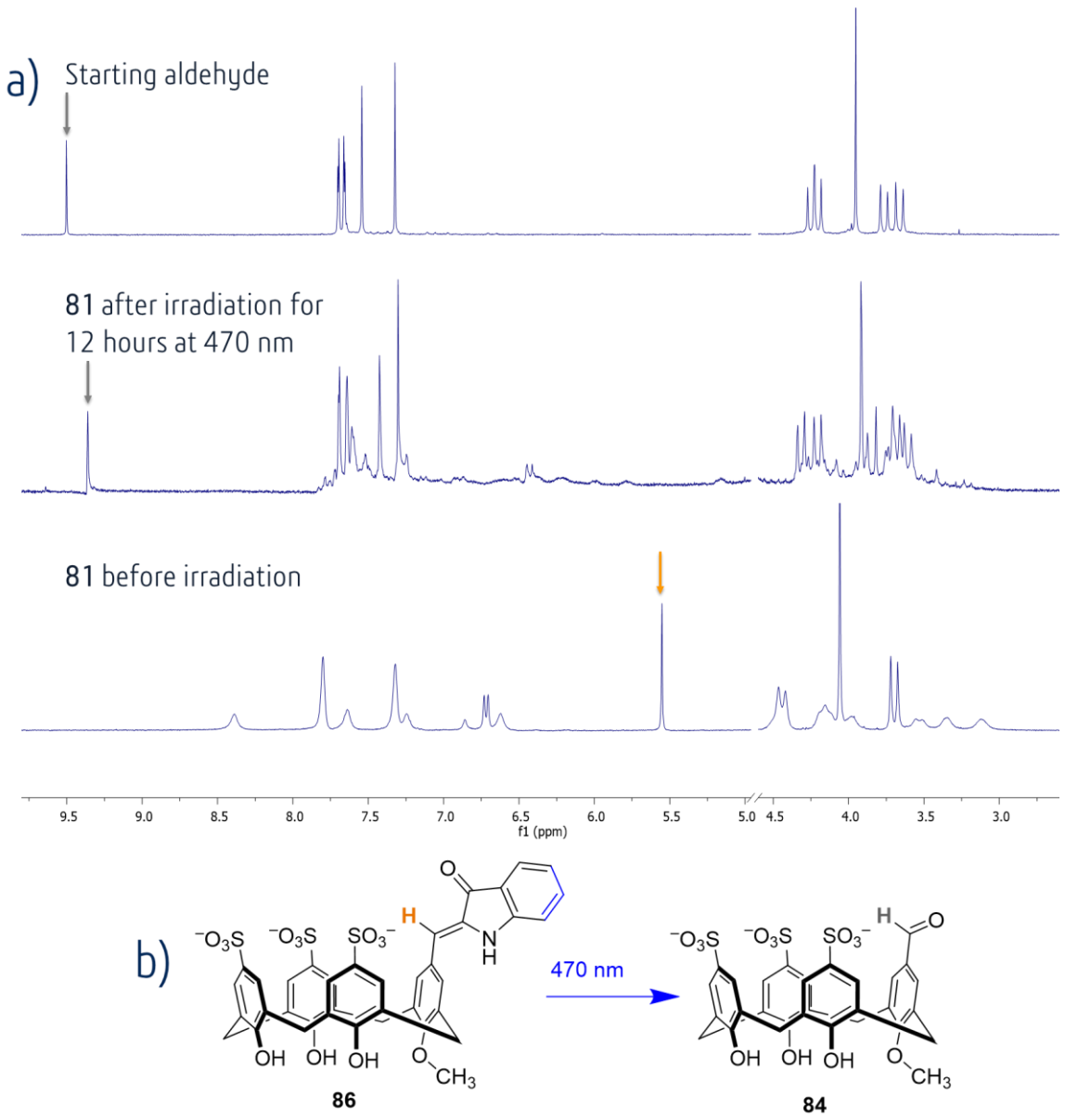

*Figure 3.1. a) [1]H NMR of hemiindigo calix[4]arene **86** in D_2O before and after irradiation at 470 nm and of starting lower-rim methylated aldehyde; b) reaction scheme of photobleaching.*

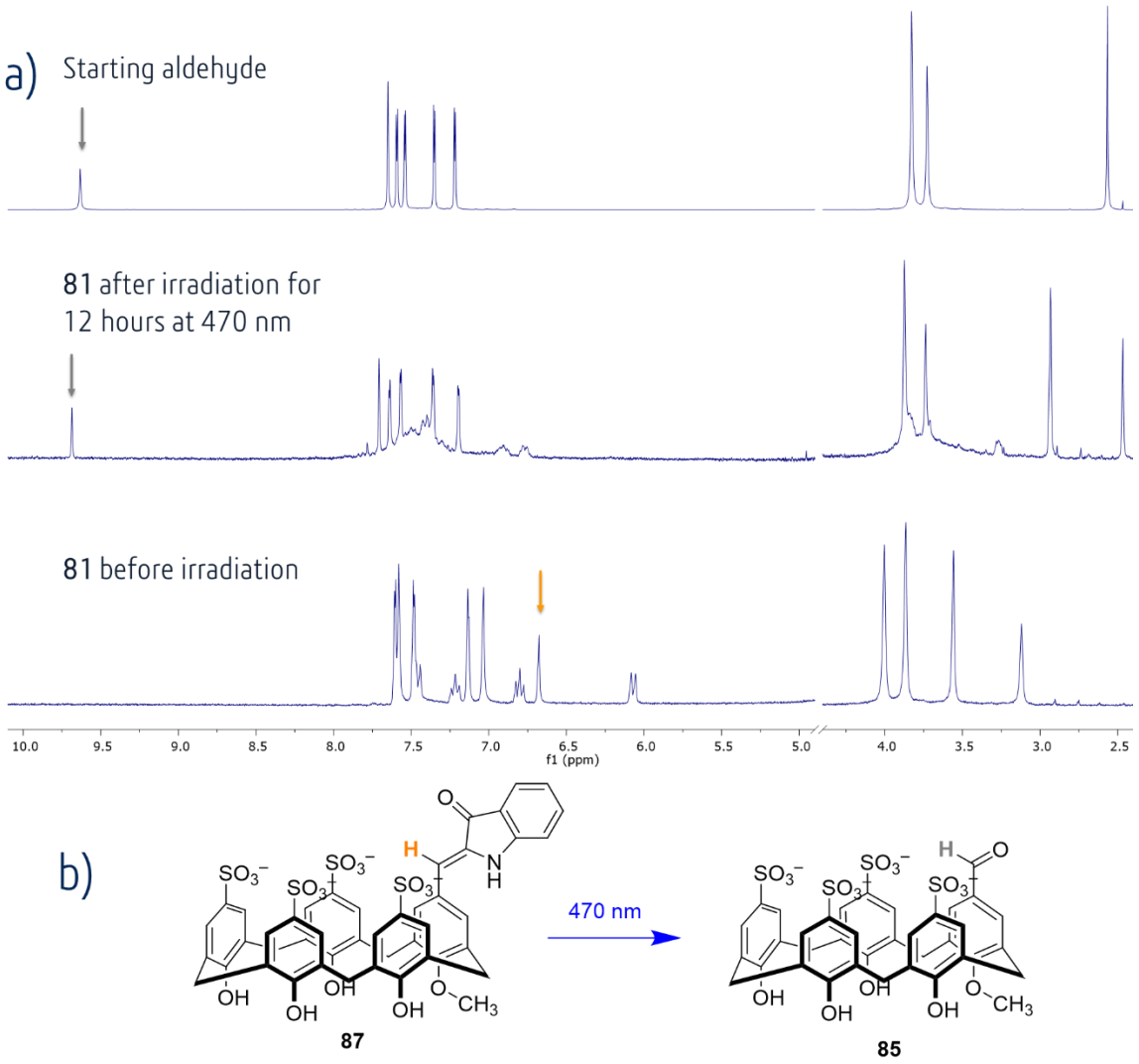

*Figure 3.2. a) ^{1}H NMR of hemiindigo calix[5]arene **87** in D_2O before and after irradiation at 470 nm and of starting lower-rim methylated aldehyde; b) reaction scheme of photobleaching.*

3.3.2 Dimerization study

As we mentioned before, our next goal was to fully assign and understand the ^{1}H NMR spectra of our compounds. We noticed that despite structural similarities, the spectra of **86** and **87** in D_2O looked very different (Figure 3.3).

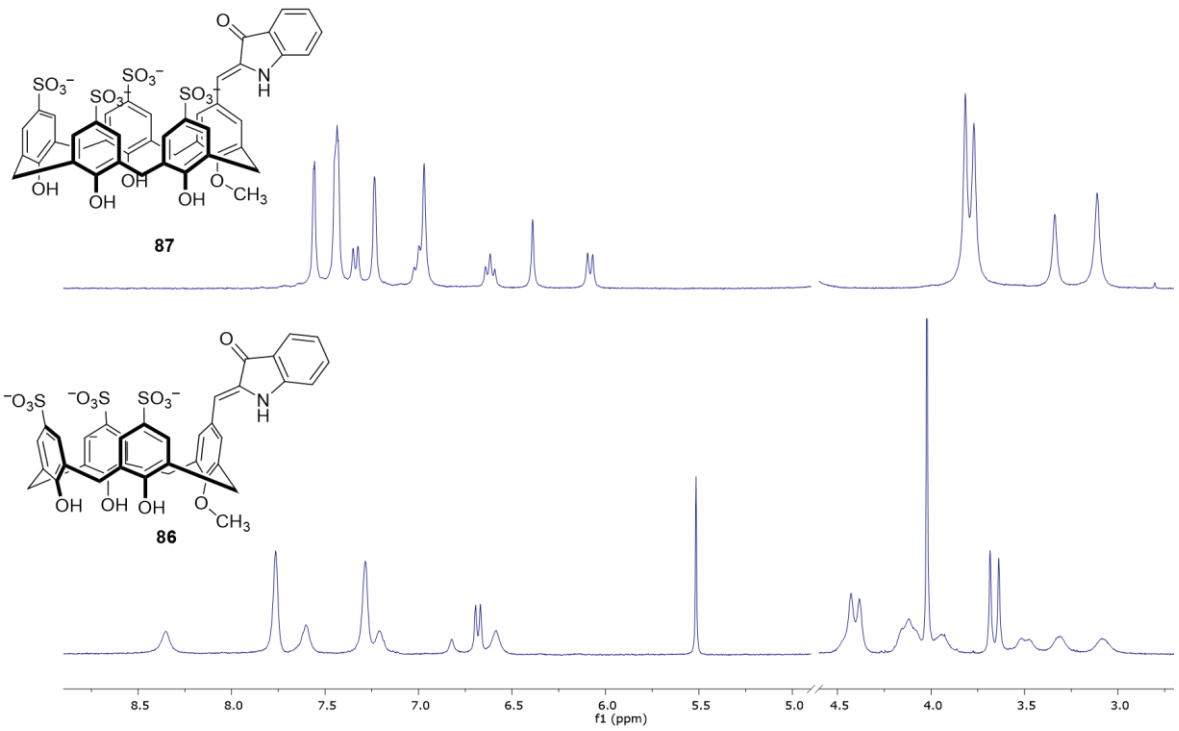

*Figure 3.3. ^{1}H NMR spectra of hemiindigo calixrenes **86** and **87** in D_2O.*

One thing that draws attention is unexpectedly high number of peaks in the upfield region, where normally only the methylene resonances would be present. Normally in this region we would expect to see four doublets, each integrating to two and representing four pairs of diastereotopically unequal axial and equatorial protons on methylene bridges, along with one pronounced *O*-methoxy singlet, integrating to three (Figure S2.7). This pattern arises from the restricted ability of calix[4]arenes to flip through the cavity and was previously observed.[4,21] Yet for **86** we observe 7 signals in the region of 3.0–4.5 ppm, excluding *O*-methoxy, with integration ranging from 1 to 3 and sometimes having unclear multiplicity. In addition to that, the aromatic region

is missing three aromatic multiplets from the hemiindigo pendant arm. Interestingly, **87** does not exhibit this trait. Its aldehyde parent **85** has 3 resonances in methylene region, one being *O*-methoxy, easily identifiable by its integration, and two peaks integrating to 4 and 6, representing methylene bridges (Figure S2.10).

Hemiindigo derivative **87** generally repeats this trend, the only difference being better resolved bridge opposite to the pendant arm. Calix[5]arene can flip easier due to bigger cavity size, which explains the lack of diastereotopically unequal protons and broader signals.

Such anomalous appearance of the hemiindigo calix[4]arene **86** led us to suspect the possibility of dimer formation. We hypothesized that aromatic protons from the pendant arm might have shifted upfield due to shielding effects of the electron-rich cavity. It is geometrically impossible for a pendant arm to "collapse" into the cavity of the same molecule because it is too rigid. As mentioned above, similar homodimerization behavior has been already described for substituted sulfonated calixarenes.[4] It is further reinforced by the fact that in deuterated DMSO, which generally does not favor homodimer formation, the pattern of ^{1}H NMR resonances looks exactly as expected for a monomeric calixarene.

In order to confirm dimer formation we decided to use DOSY technique. Determination of hydrodynamic radii of hemiindigo calixarene aggregates and comparing it with known dimers[4] and monomers drawn from a family of structurally similar calixarenes allows us to draw more reliable conclusions about the nature of aggregation. We have found hydrodynamic radii of **86** to be 10.8 ± 0.1 Å and that of **87** to be 9.8 ± 0.1 Å (Figure 3.4). A full description of the procedure along with the calculation of the diffusion coefficients can be found in SI. While this difference is small, the fact that radius of calix[4]arene turned out to be bigger, allows us with reasonable degree of certainty claim the presence of dimer formation for **86**, and it its absence for calix[5] analogue **87**. This is fully consistent with the 1D ^{1}H NMR spectra, which show upfield-shifted aromatic resonances that are indicative of dimer formation only for the calix[4]arene analog **86**. This conclusion was further supported by comparison to hydrodynamic radii of comparable calixarenes (Table 3.1). Calix[4]arene-based molecule of comparable structure **88**, was previously shown to have a radius of 12.4 ± 0.7 Å in a dimeric state and 8 ± 1 Å upon guest-induced dimer disruption, while for its non-dimerizing aldehyde precursor **35** it was only 7.4 ± 0.3 Å.[4] Similar study was also conducted on calix[5]arenes, albeit for covalently bound dimer **89**, which possess radius of 12.6 ± 0.2 Å, with its precursor **38** being 9.0 ± 0.1 Å.[10] Radius of hemiindigo calix[5]arene **87** is

significantly closer (less than 1 Å) to the monomeric aldehyde **38**, taking the size of the pendant arm into the account.

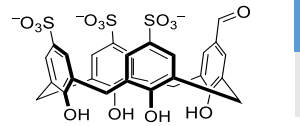

35

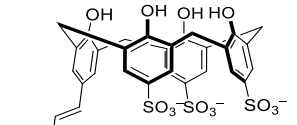

88

Compound	Diffusion coefficient, m^2/s	r_s , Å
Calix[4]arenes		
35	$3.29 \pm 0.02 \times 10^{-10}$	7.4 ± 0.3
88 (dimer)	$1.96 \pm 0.05 \times 10^{-10}$	12.4 ± 0.7
88 (monomer)	$2.7 \pm 0.3 \times 10^{-10}$	8 ± 1
86	$2.26 \pm 0.03 \times 10^{-10}$	10.8 ± 0.1
Calix[5]arenes		
38	$2.79 \pm 0.03 \times 10^{-10}$	9.0 ± 0.1
89	$2.00 \pm 0.03 \times 10^{-10}$	12.6 ± 0.2
87	$2.49 \pm 0.01 \times 10^{-10}$	9.8 ± 0.1

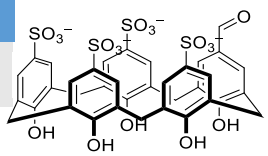

38

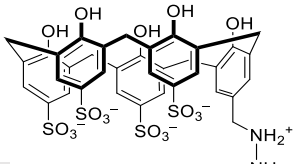

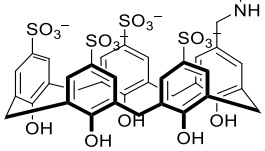

89

*Table 3.1. Comparison of diffusion coefficients and Stokes radii of known monomeric and dimeric calixarenes with hemiidnigo calixarenes **86** and **87**.*

For calix[4]arene **86** situation looks a bit less obvious, although it does lean more towards “dimeric size”, with difference being around 1.5 Å, while the difference from monomer is approximately 3 Å. This can be possibly explained by slightly smaller length of pendant arm and by closer packing compared to **88**.

To finalize the assignment and confirm our assumptions we have conducted COSY experiments (Figure 3. 5). The most prominent feature is the correlation

of the doublet at 6.75 ppm with the broad signal at 3.9 ppm. This signal then correlates with two other signals at 3.15 ppm and 3.35 ppm.

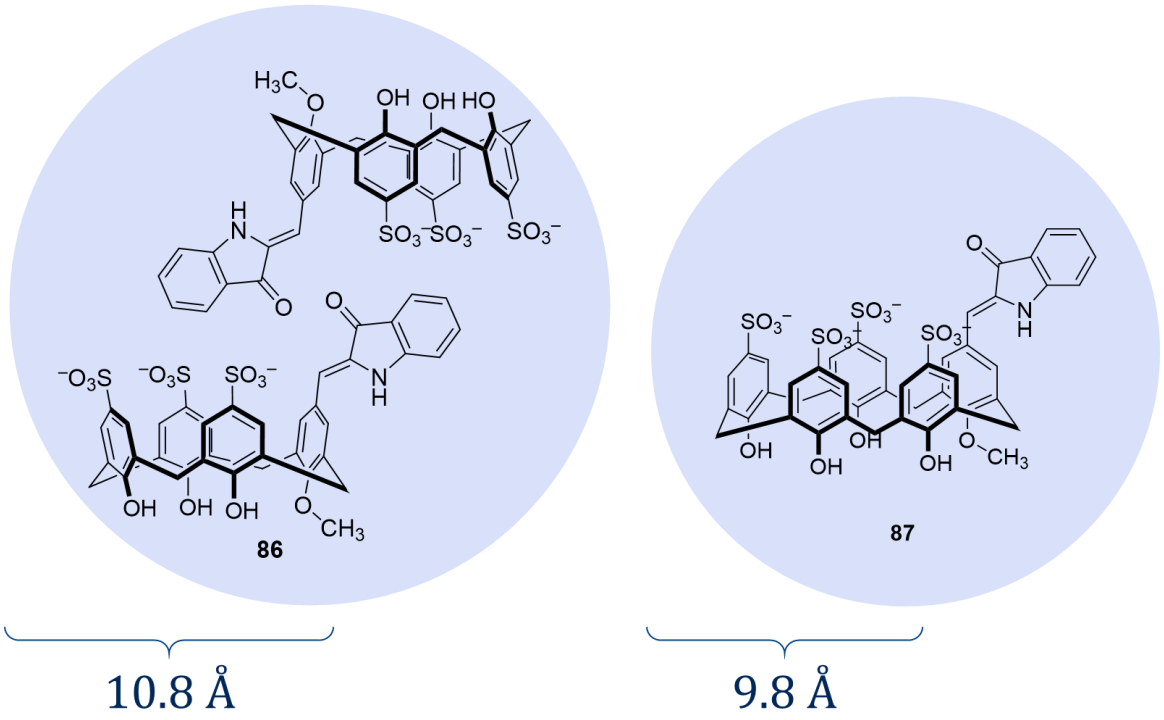

*Figure 3.4. Hydrodynamic radii of hemiindigo calixarenes **86** and **87**.*

Such a chain of correlations among four proton resonances is only possible for aromatic protons on the hemiindigo pendant arm. This led us to a conclusion that larger part of the pendant arm stays inside the cavity of its dimer partner. Another noteworthy observation is the fine structure of the broad peak at 4.4 ppm. It is clearly visible from the 2D spectra, that it is in fact two peaks, one that integrates to 2, another to 1. The molecular symmetry of hemiindigo calix[4]arene **86** implies that methylene bridges would show 4 resonances with integration of 2 each. Presence of two methylene signals that integrate to 1 hints

to a possibility of unsymmetrical structure of dimer partners. One possible homodimeric structure was determined by molecular modeling using molecular mechanics by manual docking followed by energy optimization in the software package called Avogadro[124] (Figure 3.6). This is a relatively low level of theory, which means that it can allow us to rationalize and understand structures that are confirmed by other experimental data, but can't allow us to draw *a priori* conclusions about whether monomer or dimer are formed for any given system.

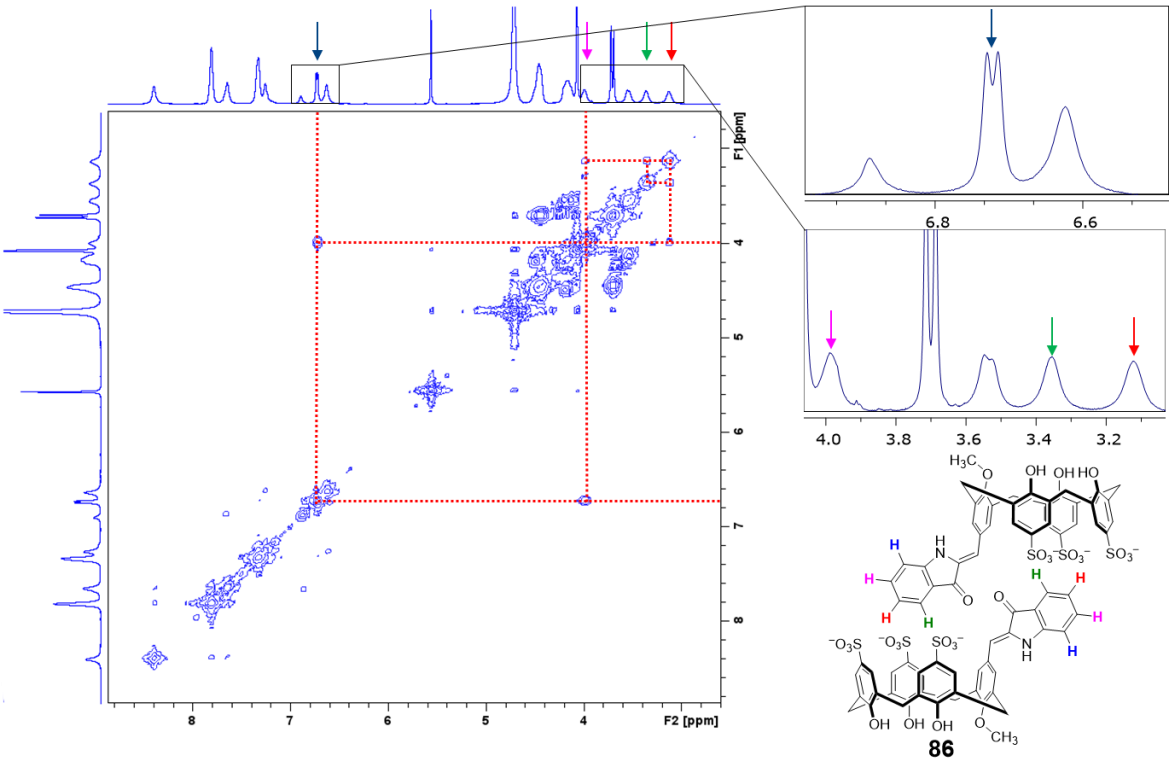

*Figure 3. 5. ^{1}H COSY NMR of **86**.*

It is visible in the modeled structure how 3 out of the 4 indigo aromatic hydrogens are staying inside the cavity, which agrees with the observation that

three of those four aromatic resonances appear shifted far upfield in the ^{1}H NMR (Figure 3.6). The modeled structure also lacks a plane of symmetry, explaining that there are so many distinct methylene signals in the NMR.

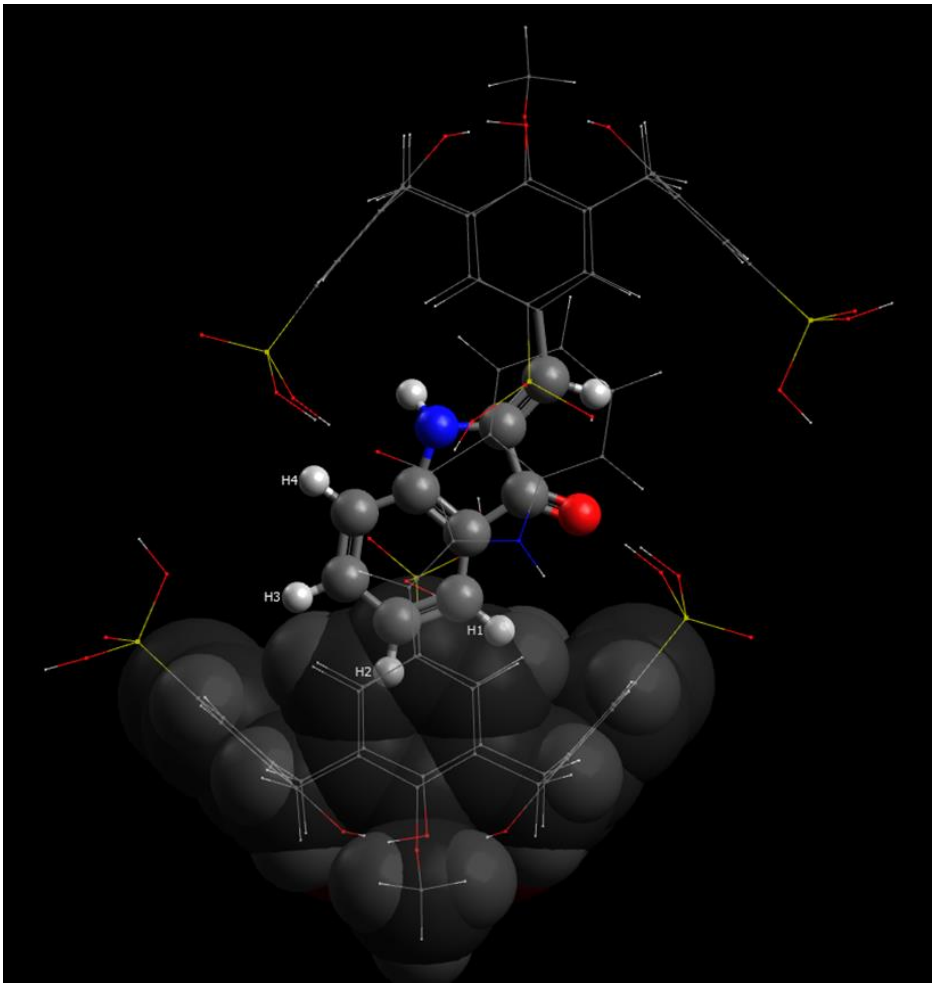

*Figure 3.6. Possible dimer structure of **86**. Only important parts are rendered for better visibility.*

We conducted the same set of NMR experiments for hemiindigo calix[5]arene **87**, to explore our initial conclusion that it does not dimerize (Figure 3.7). As can be seen in the COSY, it has the same pattern of a 4 proton correlated spin

system among the aromatic indigo protons. But unlike the calix[4]arene analog, those resonances are present at the chemical shifts that would normally be expected for aromatic protons (6.0–7.5 ppm) and are not shifted upfield by binding within an aromatic binding pocket.

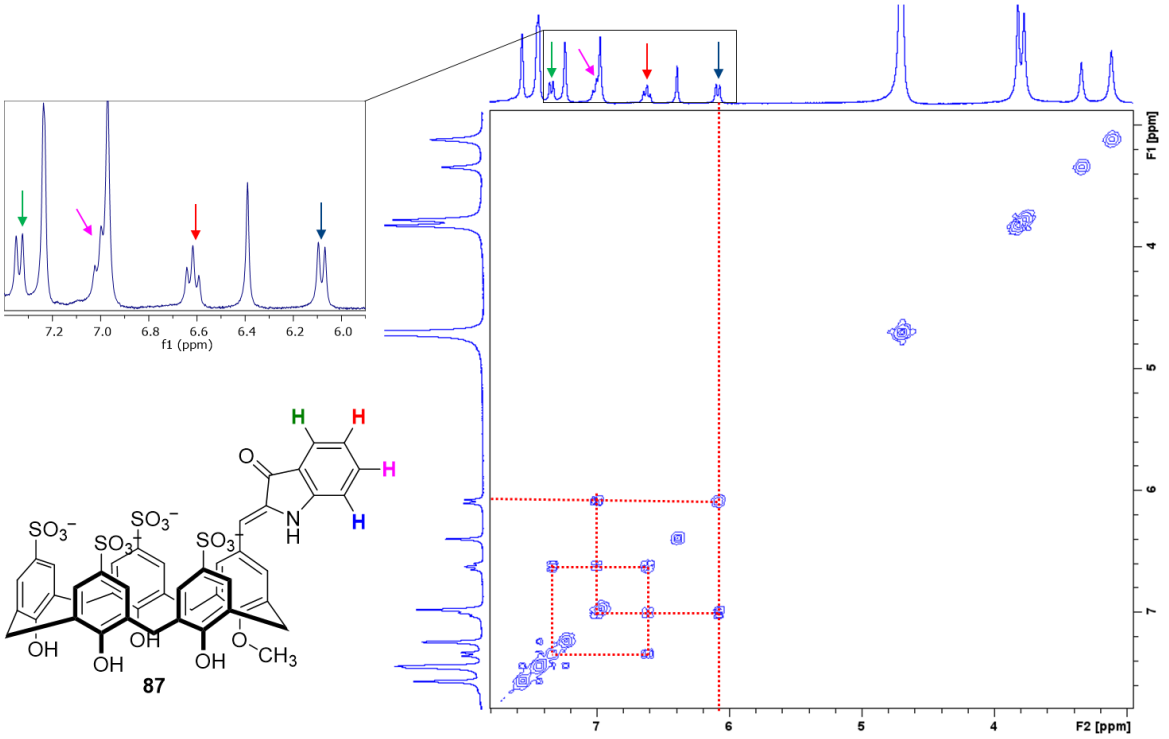

*Figure 3.7. [1]H COSY NMR of hemiindigo **87**.*

In summary, the data arising from COSY allow the definitive assignment of protons in the 1D **[1]**H NMR spectra, which reveal chemical shifts characteristic of dimerization for hemiindigo calix[4]arene **86** and shifts characteristic of monomer for hemiindigo calix[5]arene **87**. Additionally, the DOSY NMR are an orthogonal set of studies reveal hydrodynamic radii that are consistent with

dimerization for the calix[4]arene hemiindigo and monomer formation for the calix[5]arene hemiindigo.

3.3.3 Binding studies

Having cemented our initial guesses about aggregation states of our molecules, we decided to check if it is possible to disrupt the dimer by competition with a small molecule guest. We conducted a series of simple qualitative NMR titrations with a typical cationic guest – choline. It was demonstrated before for similar systems[49,85] that addition of guest can disrupt the dimer formation by the competing process of host-guest complex formation. So, we titrated choline chloride into the solution of hemiindigo calix[4]arene **86** in D_2O. As it can be seen from Figure 3.8., addition of even small amount of guest causes number of resonances to seemingly disappear, such as some aromatic peaks as well as the peaks associated with the shielded part of the hemiindigo pendant arm.

At the same time, methylene bridges are losing their asymmetry pattern and getting sharper, along with the remaining aromatic signals. Such "vanishing" of signals is caused by broadening, which occurs when the frequency of exchange between dimer and host-guest complex being close to frequency difference between their corresponding resonances. This effect is known as coalescence. This confirms that the dimers that exist before addition of choline

are disrupted, but does not allow us to observe the expected host-choline complexes directly.

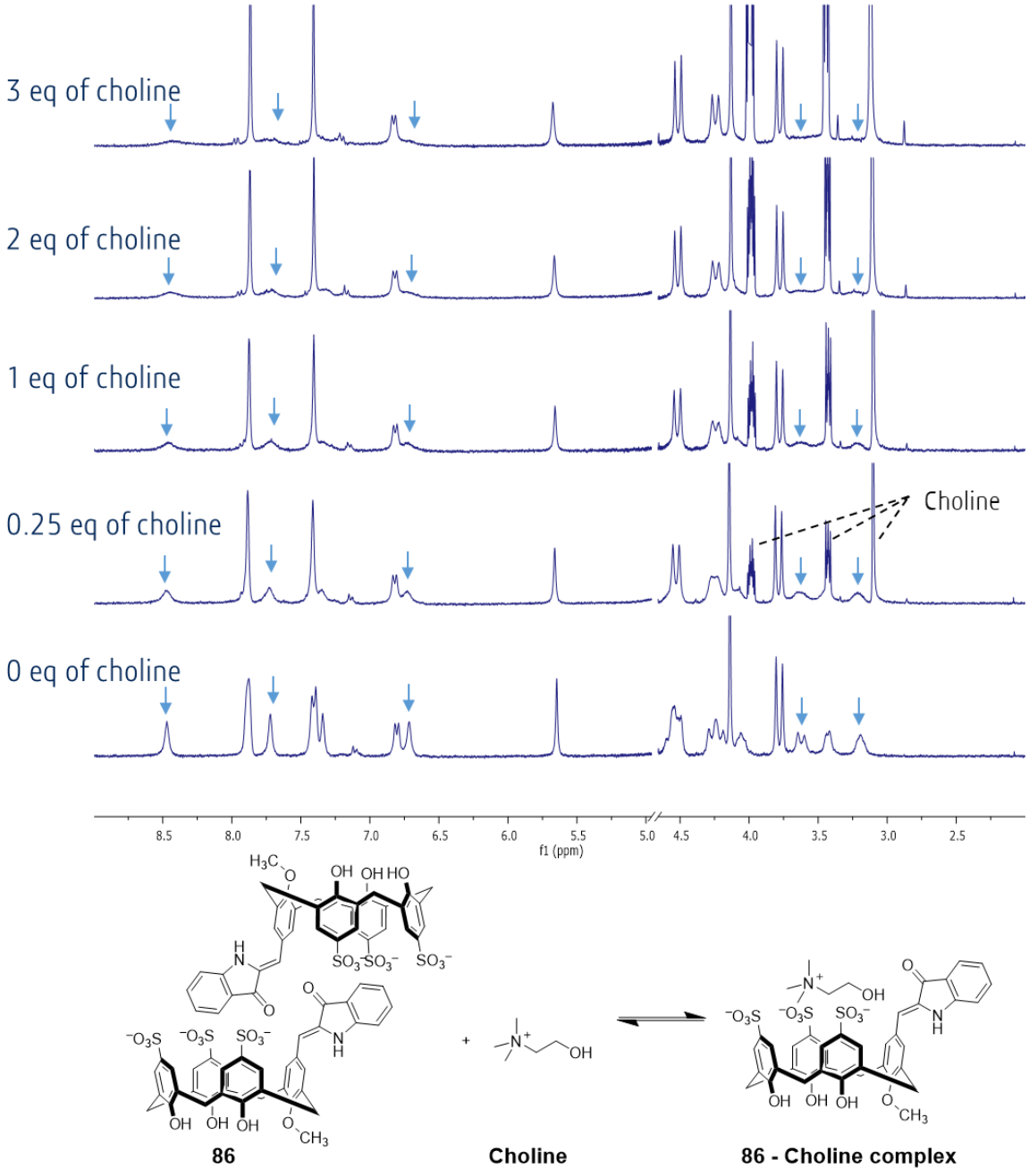

*Figure 3.8. NMR titration of choline to Hemiindig Calix[4]arene **86**.*

Possible ways of solving this problem would be either slowing down exchange by tilting the exchange equilibrium more towards host-guest complex (so it stays in complexed form longer), or changing the temperature, thus increasing or decreasing rate of the reaction. Increasing up to 100 equivalents of choline did not improve our ability to observe the host-guest complex, leaving varying the temperature our only option. But due to generally qualitative nature of the experiment, it was decided that the very presence of coalescence hints towards existence of the exchange and therefore supports the dimer disruption by added guest.

As for calix[5]arene **87**, the same type of experiment produced somewhat different results (Figure 3.9). If the host does not form disruptable dimers, the only exchange happening is between free and bound host and guest molecules.[9] While choline binding affects chemical shifts to some degree, the frequency difference is usually small, and exchange is fast, so NMR can detect it. As a result, we don't see the coalescence of signals, instead they shift in small increments either upfield or downfield. Such behavior reinforces our claim that hemiindigo calix[5]arene **87** exists as a monomer in aqueous solutions.

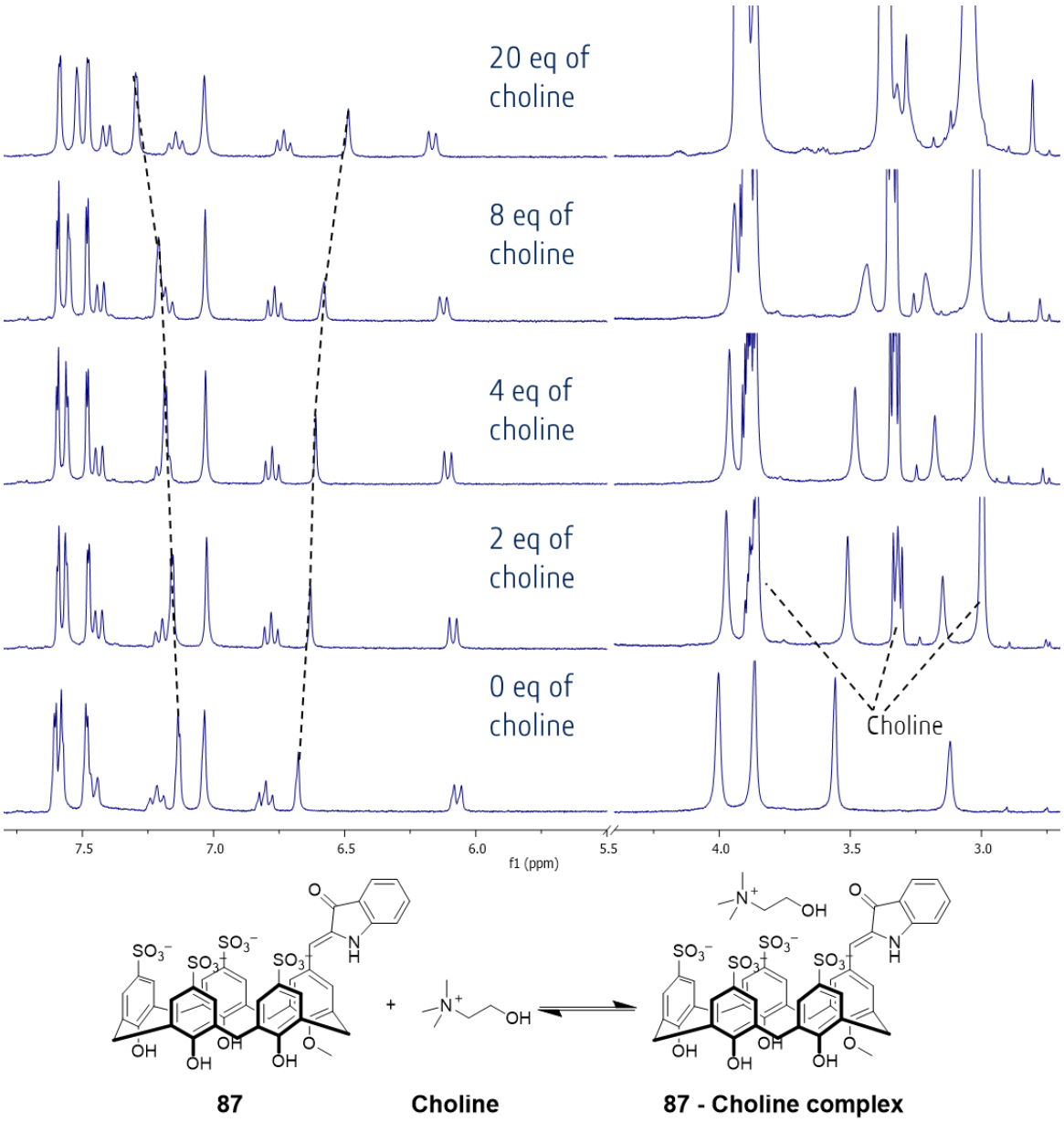

*Figure 3.9. NMR titration of choline into hemiindigo calix[5]arene **87**.*

3.3.4 NOESY studies

Finally, we used NOESY to find out if we can get more detailed structural information about the dimers. While we did not see any correlations that would correspond to intermolecular interactions between monomers we were able to detect unusually strong correlation between two aromatic protons at 8.4 ppm

and 7.65 ppm (Figure 3.10). Since the strength of NOE is extremely unlikely to reach 100%, we made a conclusion that it is in fact arising from chemical exchange. In fact, the NMR pulse sequence for a technique called Exchange Spectroscopy (EXSY) is the same as that for NOESY experiments. This is because, once a spin is polarized, it can transfer either to a new nucleus via Nuclear Overhauser Effect (NOE, see above) or by exchanging identities with a different nucleus, when such an exchange is possible due to a chemical exchange process between the two specific nuclei involved.

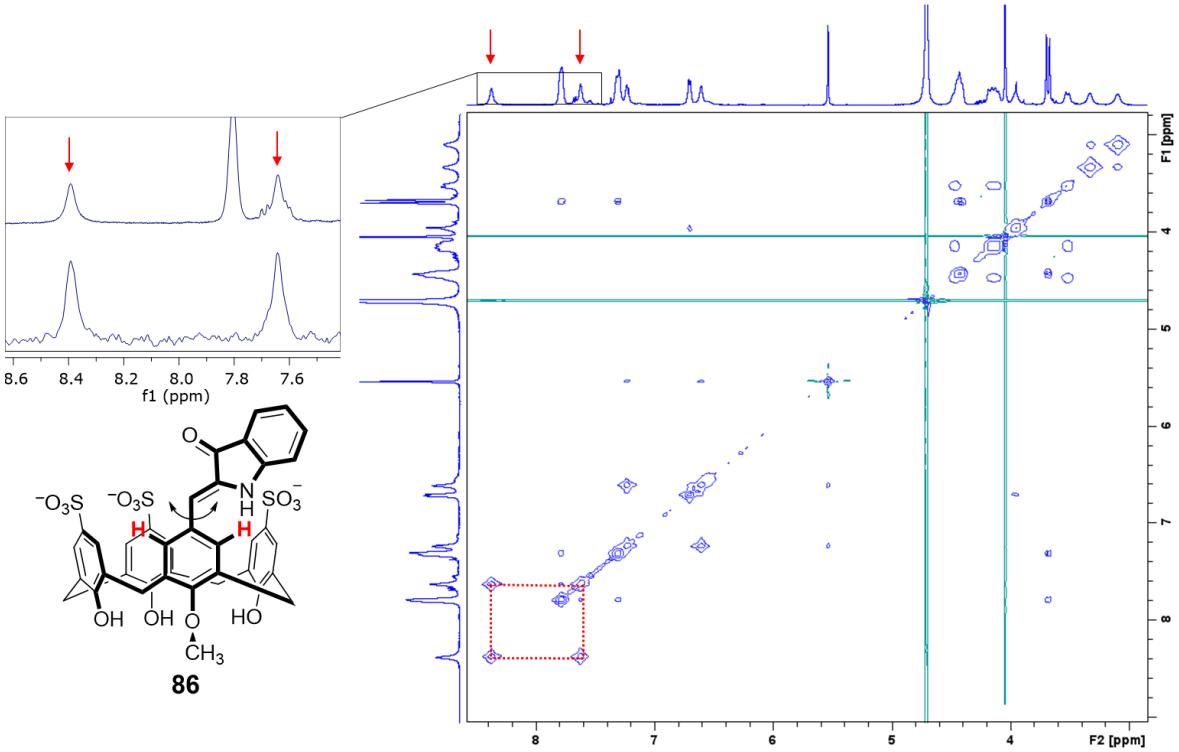

Figure 3.10. 2D NOESY spectra of ***86.*** *Lower part of zoomed up fragment represents a 1D NOESY slice of the region.*

The two resonances that we propose exchange with each other are the aromatic protons indicated in red in Figure 3.10. This assignment and EXSY result aligns well with our suggested structure (Figure 3.6), where the hemiindigo pendant arm lies in the same plane as the benzene ring to which it is attached. When that pendant arm makes its 180° rotation slow enough to give two distinctive NMR signals, but fast enough for the two protons to exchange identities on the time scale of an EXSY experiment. It worth mentioning that this effect probably arises because this rate of exchange depends on the dissociation rate of dimer, rather than the rate of rotation itself. While rotations around single sp^3-sp^2 bond are generally slower than rotations around sp^3-sp^3 bond they are still much faster compared with dimer exchange. In the dimer the conformation rotation is strictly locked, but once it spontaneously dissociates the ability to rotate freely is recovered until the next act of aggregation. While it is not possible based on the present data to make solid conclusion on the exact rate of this exchange *k*, or, in other words about lifetime of dimers τ_s, we can still make some estimations and at least draw some boundaries. The mixing time for an EXSY experiment, D8 was chosen to be 0.5 seconds, which gives the upper limit of said lifetime. The presence of two fairly resolved and sharp resonances allows us to classify it as a slow-intermediate exchange regime (1 Hz $<k<$100 Hz). We can also make some conclusions from Figure 3.8 now that we know which exact protons are exchanging. The rate of exchange at the coalescence

point k_c depends on the difference in resonance frequencies of exchanging nuclei v_{AB} in Hz and is given by Equation 3.7.[125]

$$k_c = \frac{\pi \Delta \nu_{AB}}{\sqrt{2}} \sim 2.2 \Delta \nu_{AB} \quad (3.7)$$

The difference between two resonances denoted in red in Figure 3.10 is ~ 225 Hz (on 300 MHz spectrometer), which gives value for $k_c \sim 500$ Hz for the exchange in presence of the excess guest, which corresponds to intermediate exchange regime ($1<k<10^4$). The lifetimes of states τ_s are inversely proportional to k (Equation 3.8), which means that for slow exchange without guest 2 ms.< $\tau_s \leq 500$ms., while in the presence of choline it plummets to $\tau_s \sim 2$ ms.

$$\tau_s = \frac{1}{k_c} \quad (3.8)$$

Of course, it must be said that this approach does not take into the account the change in resonance frequencies of aforementioned protons upon binding, but we can assume that it is negligible, especially in view of qualitative nature of our conclusions in first place.

3.4 Conclusions

We have successfully employed an array of NMR techniques in order to clarify the supramolecular properties of our hemiindigo calixarenes **86** and **87**. Despite the fact that our results were somewhat marred by being unable to isolate separate and study the photoswitched *E*-isomer due to rapid

photodecomposition during its production, we were still able to extract useful information. DOSY was used in conjunction with COSY in order to prove dimer formation in water for hemiindigo calix[4]arene **86**. We have shown, that despite structural similarities, the same is not true for calix[5]arene analogue **87**. It might be attributed to larger cavity of calix[5]arenes which provides a looser fit for pendant arm and at the same time allows for more internal flexibility, which further disfavors locked conformation required to adopt a dimeric state. Qualitative NMR titrations were used in order to show a potential ability of both hosts to bind cationic guests, with dimer disruption in the case of calix[4]arene hemiindigo **86**. We have also suggested a 3D structure for hemiindigo calix[4]arene dimer, which aligns with our experimental data.

3.5 Supporting information

3.5.1 General considerations

COSY, NOESY and DOSY NMR experiments were done on Bruker Avance Neo 500 MHz spectrometer, NMR titration was done or Bruker AV300 MHz. Photodegradation studies were done identically to Chapter 2, but concentration of hosts were set to 1 mM, and D_2O was used in place of water. NMR titrations were done by mixing 1mM stock solution of guest with volumes of 1 mM stock solution of guest + 20 eq of choline. Molecular modelling was done using Avogadro 1.2.0, force field used is MMFF94 with steepest descent algorithm.

3.5.2 DOSY procedure

For each DOSY experiment, the 90° pulse is determined by measuring the pulse length at 360° by a zg pulse sequence and dividing by four. The T1 relaxation was estimated through an inversion recovery (t1ir1d) pulse sequence. The relaxation time for each experiment was set to be 10-times the estimated T1. For each experiment, the Δ was set to 50 or 100 ms. The δ was determined by finding a 90-95% intensity difference between the first and last spectra in the power array via a stebpgp1s1d pulse program, see calculations below for δ used for each experiment. The pulse sequences used for 1D DOSY was stebpgp1s. After pre-processing through TopSpin, the diffusion coefficients were calculated with Bruker Dynamic Center by user defined area under the peaks of interest and plotted as a function of the field gradient strength (G). The function fitted is Equation 3.9

$$I = I_0 * \exp(-DG\gamma^2\delta^2\delta\left(\Delta - \frac{\delta}{3}\right)) * 10^4 \qquad (3.9)$$

The average diffusion coefficient was calculated along with an uncertainty. The hydrodynamic radius (r_s) is calculated using the Stokes-Einstein Equation 3.6 along with an uncertainty. k_B is the Boltzmann constant, temperature (T) is 297 K ± 1 K and viscosity (η) of water at 297 K is 8.94 x 10^{-4} ± 2.78 x 10^{-5} Pa·s.

3.5.3 NOESY procedure

Concentrations were chosen to be 7.5 mM due to overall weakness of NOE responses. Solutions were degassed by bubbling argon for a few minutes, after which the tube is closed and sealed with parafilm. The experiments were run with a relaxation time (D1) = 3 sec and mixing time (D8) = 0.5 sec.

3.5.4 1D DOSY calculations and data

*Table S3.1. Parameters used for diffusion analysis of **86** and **87**.*

Parameters used during experiment	
used **γ**:	26752 rad/(s*Gauss)
used **δ**:	0.0029000 s
used **Δ**:	0.099900 s
used gradient strength:	variable
Random error estimation of data:	RMS per spectrum (or trace/plane)
Systematic error estimation of data:	worst case per peak scenario
Fit parameter Error estimation method:	from fit using arbitrary *y* uncertainties
Confidence level:	95%
Used peaks:	peaks from peaklist.xml at spectrum
Used integrals:	area integral
Used Gradient strength:	all values (including replicates) used

*Table S3.2 . Diffusion coefficients calculated from indicated resonances for **86.** Peaks **4** and **8** were not used for calculations.*

Peak name	F2 [ppm]	D [m^2/s]*10^{-10}	fitInfo
1	5.56	2.30±0.02	Done
2	8.40	2.28±0.02	Done
3	3.13	2.09±0.08	Done
4	6.85	3.80±0.09	Done
5	7.82	2.27±0.01	Done
6	7.64	2.44±0.02	Done
7	3.71	2.19±0.03	Done
8	1.91	10.74±0.72	Done

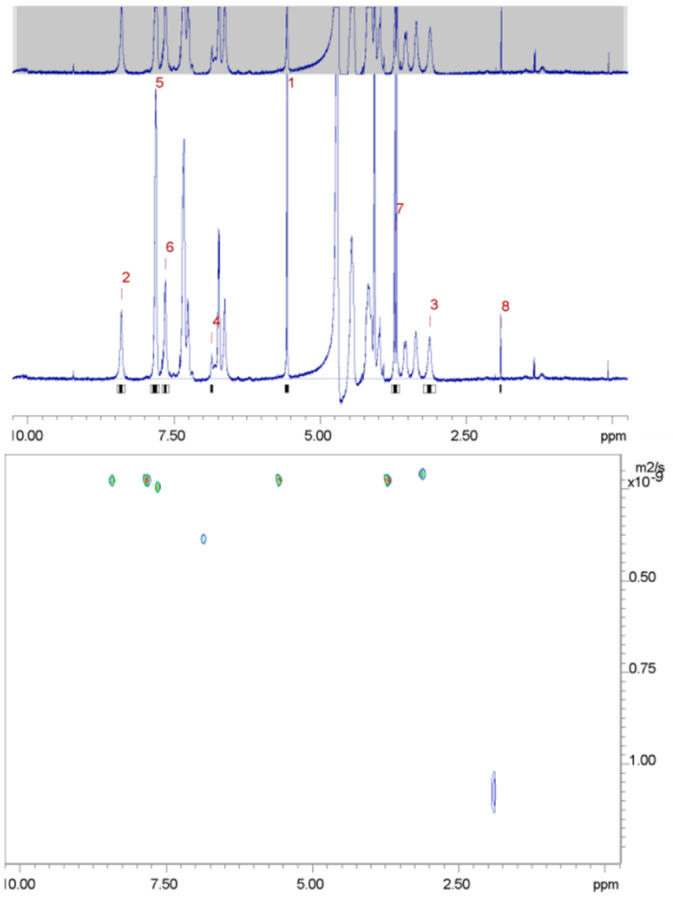

*Figure S3.1. [1]H NMR of **86** with integrals highlighted (gray boxes) used to calculate diffusion coefficients for each resonance along with the corresponding 2D DOSY spectrum.*

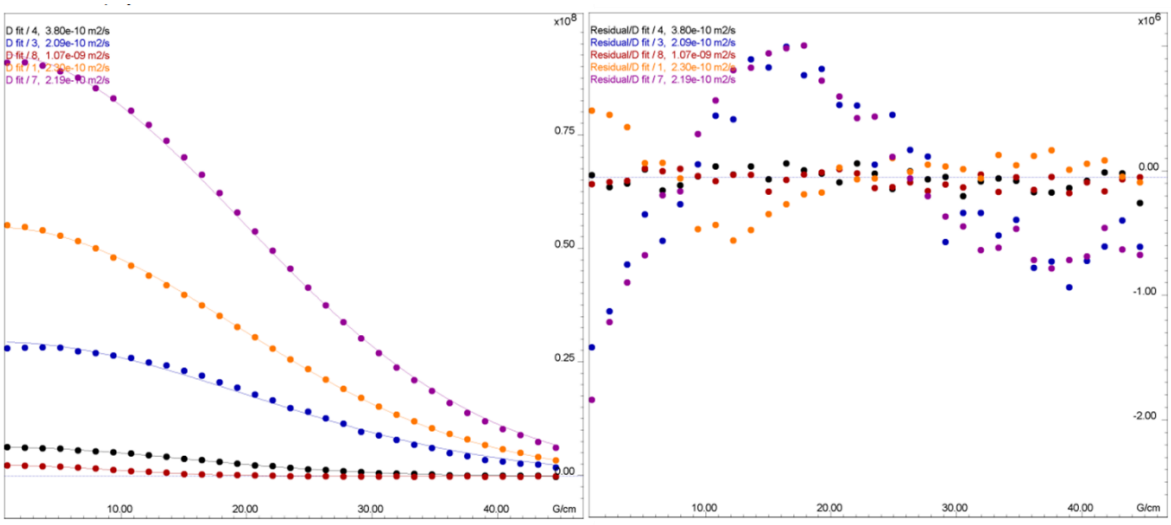

*Figure S3.2. 1D DOSY plots of each integral from **86** along with corresponding residuals.*

Table S3.3. Diffusion coefficients calculated from indicated resonances for ***87.***

Peak name	F2 [ppm]	D [m^2/s]*10^{-10}	fitInfo
1	6.12	2.50±0.02	Done
2	6.55	2.52±0.02	Done
3	6.74	2.52±0.02	Done
5	7.14	2.52±0.02	Done
6	7.22	2.47±0.01	Done
8	7.54	2.44±0.01	Done
9	7.49	2.46±0.01	Done
10	7.62	2.50±0.01	Done

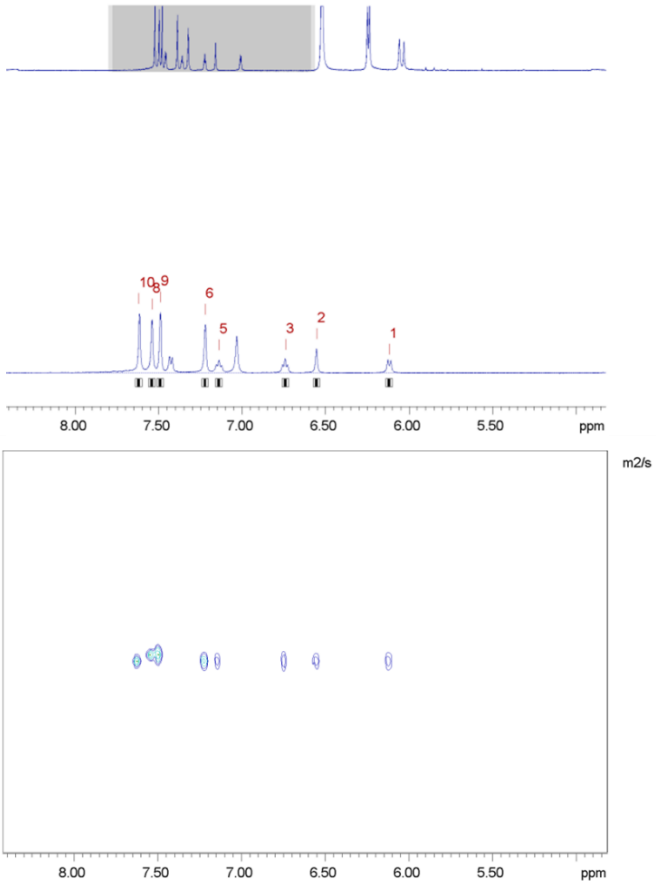

Figure S3.3. ^{1}*H NMR of* ***87*** *with integrals highlighted (gray boxes) used to calculate diffusion coefficients for each resonance along with the corresponding 2D DOSY spectrum.*

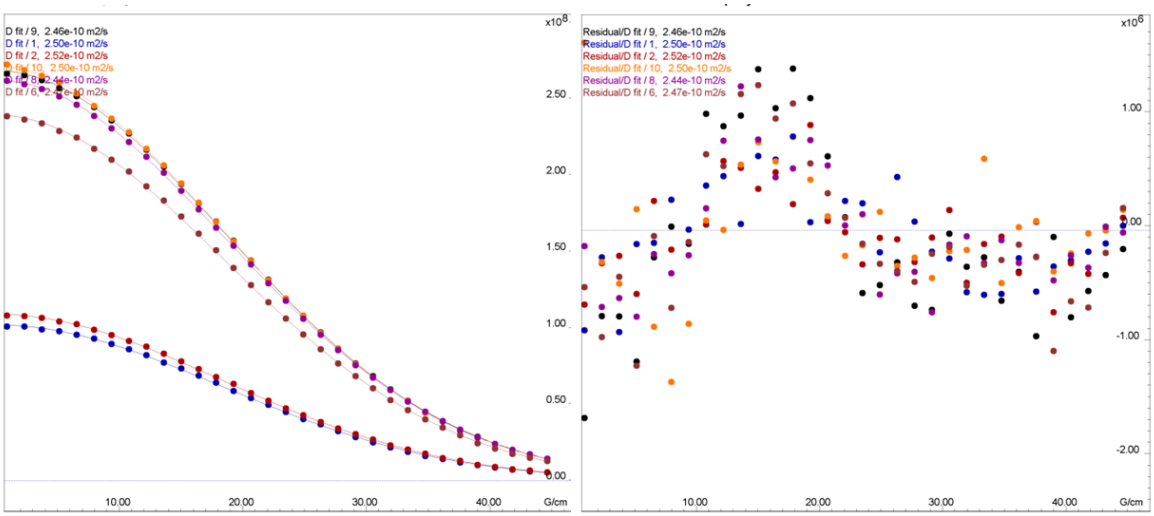

*Figure S3.4. 1D DOSY plots of each integral from **87** along with corresponding residuals.*

3.5.5 2D NOESY data

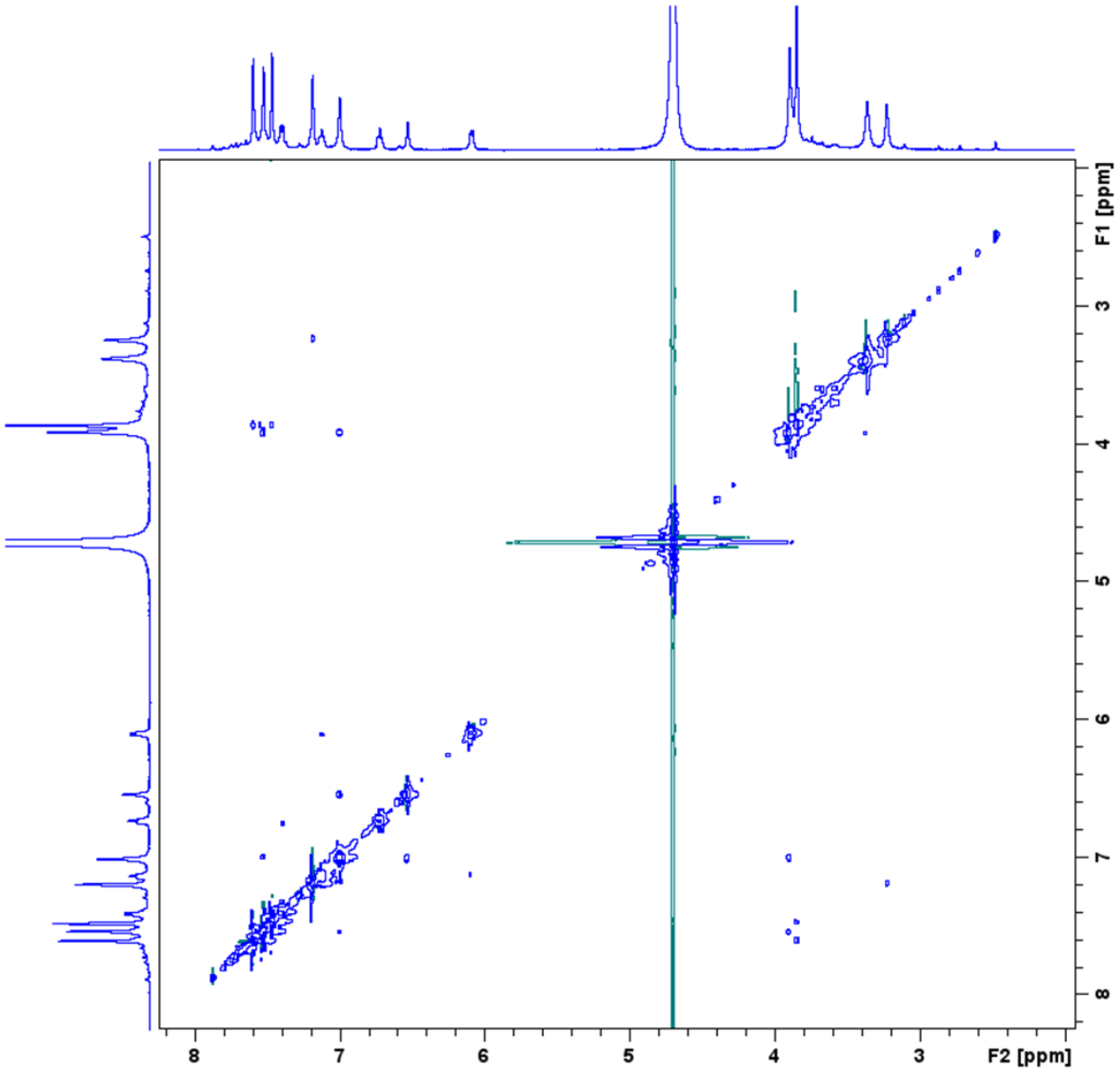

*Figure S3.5. 2D NOESY spectra of **87**.*

References

(1) Yao, C.; Ou, J.; Tang, J.; Yang, D. DNA Supramolecular Assembly on Micro/Nanointerfaces for Bioanalysis. *Acc Chem Res* **2022**, *55* (15), 2043–2054. https://doi.org/10.1021/acs.accounts.2c00170.

(2) Balzani, V.; Credi, A.; Raymo, F. M.; Stoddart, J. F. Artificial Molecular Machines. *Angewandte Chemie - International Edition*. Wiley-VCH Verlag October 2, 2000, pp 3348–3391. https://doi.org/10.1002/1521-3773(20001002)39:19<3348::aid-anie3348>3.0.co;2-x.

(3) Meeuwissen, J.; Reek, J. N. H. Supramolecular Catalysis beyond Enzyme Mimics. *Nat Chem* **2010**, *2* (8), 615–621. https://doi.org/10.1038/nchem.744.

(4) Beatty, M. A.; Selinger, A. J.; Li, Y.; Hof, F. Parallel Synthesis and Screening of Supramolecular Chemosensors That Achieve Fluorescent Turn-on Detection of Drugs in Saliva. *J Am Chem Soc* **2019**, *141* (42), 16763–16771. https://doi.org/10.1021/jacs.9b07073.

(5) Williams, G. T.; Haynes, C. J. E.; Fares, M.; Caltagirone, C.; Hiscock, J. R.; Gale, P. A. Advances in Applied Supramolecular Technologies. *Chemical Society Reviews*. Royal Society of Chemistry February 21, 2021, pp 2737–2763. https://doi.org/10.1039/d0cs00948b.

(6) Böhmer, V. Calixarenes, Macrocycles with (Almost) Unlimited Possibilities. *Angewandte Chemie International Edition in English*. April 13, 1995, pp 713–745. https://doi.org/10.1002/anie.199507131.

(7) Gaeta, C.; Troisi, F.; Neri, P. Endo-Cavity Complexation and through-the-Annulus Threading of Large Calixarenes Induced by Very Loose Alkylammonium Ion Pairs. *Org Lett* **2010**, *12* (9), 2092–2095. https://doi.org/10.1021/ol100578z.

(8) Beatty, M. A.; Hof, F. Host-Guest Binding in Water, Salty Water, and Biofluids: General Lessons for Synthetic, Bio-Targeted Molecular Recognition. *Chemical Society Reviews*. Royal Society of Chemistry April 21, 2021, pp 4812–4832. https://doi.org/10.1039/d0cs00495b.

(9) Shaurya, A.; Garnett, G. A. E.; Starke, M. J.; Grasdal, M. C.; Dewar, C. C.; Kliuchynskyi, A. Y.; Hof, F. An Easily Accessible, Lower Rim Substituted Calix[4]Arene Selectively Binds: N, N -Dimethyllysine. *Org Biomol Chem* **2021**, *19* (21), 4691–4696. https://doi.org/10.1039/d1ob00524c.

(10) Selinger, A. J.; Cavallin, N. A.; Yanai, A.; Birol, I.; Hof, F. Template-Directed Synthesis of Bivalent, Broad-Spectrum Hosts for Neuromuscular Blocking Agents**. **2021**. https://doi.org/10.33774/chemrxiv-2021-zq9z2.

(11) Shinkai, S.; Mori, S.; Tsubaki, T.; Sone, T.; Manabe, O. *NEW WATER-SOLUBLE HOST MOLECULES DERIVED FROM CALIX[ó]ARENE*; 1984; Vol. 25.

(12) Gutsche C. David; Alam Iftikhar. The Complexation and Catalytic Properties of Water Soluble Calixarens. *Tetrahedron* **1988**, *44* (15), 4689–4694.

(13) Shinkai, S.; Nagasaki T.; Arimura T.; Matsuda T. Host-Guest Properties of New Water-Soluble Calixarenes Derived from p-(Chloromethyl)Calixarenes. *J. Org. Chem* **1989**, *54* (3), 3768–3770.

(14) Nagasaki, T.; Sisido, K.; Arimura, T.; Shinkai', S. *Novel Conformational Isomerism of Water-Soluble Calixt4larenes*; 1992; Vol. 48.

(15) Warmerdam, Z.; Kamba, B. E.; Shaurya, A.; Sun, X. X.; Maguire, M. K.; Hof, F. Calix[4]Arene Sulfonate Hosts Selectively Modified on the Upper Rim: A Study of Nicotine Binding Strength and Geometry. *Supramol Chem* **2021**, *33* (4), 88–96. https://doi.org/10.1080/10610278.2021.1873991.

(16) Shinkai S; Kawabata H.; Matsuda T.; Kawaguchi H.; Manabe O. Synthesis and Inclusion Properties of "Neutral" Water-Soluble Calixarenes. *Bull. Chem. Soc. Jpn* **1990**, *63* (4), 1272–1274.

(17) Arduini Arturo; Pochini Andrea; Reverberi Sara; Unagaro Rocco. P-t-Butyl-Calix[4]Arene Tetracarboxylic Acid. A Water Soluble Calixarene in a Cone Structure. *J. CHEM. SOC., CHEM. COMMUN.* **1984**, 981–982.

(18) Shinkai, S.; Kawabata, H.; Arimura, T.; Matsuda, T.; Satoh, H.; Manabe, O. *New Water-Soluble Calixarenes Bearing Sulphonate Groups on the "Lower Rim": The Relation between Calixarene Shape and Binding Ability*; 1989; Vol. 9.

(19) Jose, P.; Menon, S. Lower-Rim Substituted Calixarenes and Their Applications. *Bioinorganic Chemistry and Applications*. 2007. https://doi.org/10.1155/2007/65815.

(20) Daze, K. D.; Ma, M. C. F.; Pineux, F.; Hof, F. Synthesis of New Trisulfonated Calix[4]Arenes Functionalized at the Upper Rim, and Their Complexation with the Trimethyllysine Epigenetic Mark. *Org Lett* **2012**, *14* (6), 1512–1515. https://doi.org/10.1021/ol300243b.

(21) Beatty, M. A.; Pye, A. T.; Shaurya, A.; Kim, B.; Selinger, A. J.; Hof, F. Using Reversible Non-Covalent and Covalent Bonds to Create Assemblies and Equilibrating Molecular Networks That Survive 5 Molar

Urea. *Org Biomol Chem* **2019**, *17* (8), 2081–2086. https://doi.org/10.1039/C8OB02909A.

(22) Beatty, M. A.; Borges-González, J.; Sinclair, N. J.; Pye, A. T.; Hof, F. Analyte-Driven Disassembly and Turn-On Fluorescent Sensing in Competitive Biological Media. *J Am Chem Soc* **2018**, *140* (10), 3500–3504. https://doi.org/10.1021/jacs.7b13298.

(23) Da Silva, E.; Lazar, A. N.; Coleman, A. W. Biopharmaceutical Applications of Calixarenes. *Journal of Drug Delivery Science and Technology*. Editions de Sante 2004, pp 3–20. https://doi.org/10.1016/s1773-2247(04)50001-1.

(24) Da Silva, E.; Coleman, A. W. Synthesis and Complexation Properties towards Amino Acids of Mono-Substituted p-Sulphonato-Calix-[n]-Arenes. *Tetrahedron* **2003**, *59* (37), 7357–7364. https://doi.org/10.1016/S0040-4020(03)01137-2.

(25) Morzherin, Y.; Rudkevich, D. M.; Verboom, W.; Reinhoudt', D. N. *Chlorosulfonylated Calix[4]Arenes: Precursors for Neutral Anion Receptors with a Selectivity for Hydrogen Sulfate*; 1993; Vol. 58.

(26) Makha, M.; Raston, C. L. Direct Synthesis of Calixarenes with Extended Arms: P-Phenylcalix[4,5,6,8]Arenes and Their Water-Soluble Sulfonated Derivatives. **2001**.

(27) Katritzky, A. R.; Wu, J.; Rachwal, S.; Macomber, D.; Smith, T. P. A Novel Method for the Preparation of 3-Amino-4-Hydroxybenzenesulfonamide Precursors of "Acid Alizarin Violet N" Derivatives. *Synth Commun* **1993**, *23* (3), 405–417. https://doi.org/10.1080/00397919308009795.

(28) Alml, M.; Ardulnl, A.; Casnatl, A.; Pochlnr, A.; Ungaro, R. *Chloromethylation of Calixarenes and Synthesis of New Water Soluble Macrocyclic Hosts*; 1989; Vol. 45.

(29) Kalchenko, V. I.; Visotsky, M. A.; Shivanyuk, A. N.; Pirozhenko, V. V.; Markovsky, L. N. Synthesis and Binding Properties of Phosphorus-Containing Calixarenes and Calixresorcinarenes. *Phosphorus, Sulfur and Silicon and Related Elements* **1996**, *109* (1–4), 513–516. https://doi.org/10.1080/10426509608545203.

(30) Gutsche, C. D.; Boschke, F. L.; Ed, ; K H; Muthukrishnan, R. *Calixarenes. 16. Functionalized Calixarenes: The Direct Substitution*; Springer-Verlag, 1985; Vol. 50. https://pubs.acs.org/sharingguidelines.

(31) Shahgaldian, P.; Coleman, A. W.; Kalchenko, V. I. *Synthesis and Properties of Novel Amphiphilic Calix-[4]-Arene Derivatives*; 2001; Vol. 42.

(32) Bayrakc, M.; Ertul, Ş.; Yilmaz, M. Phase Solubility Studies of Poorly Soluble Drug Molecules by Using O -Phosphorylated Calixarenes as Drug-Solubilizing Agents. *J Chem Eng Data* **2012**, *57* (1), 233–239. https://doi.org/10.1021/je200992c.

(33) Arturo Arduini; Andrea Pochini; Sara Reverber; Rocco Ungaro. P-t-Butyl-Calix[4]Arene Tetracarboxylic Acid. A Water Soluble Calixarene in a Cone Structure. *J. CHEM. SOC., CHEM. COMMUN.*, **1984**, 981–982.

(34) C.David Gutsche; Iftikhar Alam. The Complexation and Catalytic Properties of Water Soluble Calixarenes. *Tetrahedron* **1988**, *44* (15), 4689–4694.

(35) C. David Gutsche; Kye Chun Nam. Calixarenes. 22. Synthesis, Properties, and Metal of Aminocalixarenes. *J. Am. Chem. Soc.* **1988**, *110* (18), 6153–6162.

(36) Yilmaz, M.; Vural, U. S. Synthesis of New Substituted Calix[4]Arenes and Their Complexes with Iron(III). *Synthesis and Reactivity in Inorganic and Metal-Organic Chemistry* **1991**, *21* (8), 1231–1241. https://doi.org/10.1080/15533179108020218.

(37) Shahgaldian, P.; Sciotti, M. A.; Pieles, U. Amino-Substituted Amphiphilic Calixarenes: Self-Assembly and Interactions with DNA. *Langmuir* **2008**, *24* (16), 8522–8526. https://doi.org/10.1021/la801083h.

(38) Peters, M. S.; Li, M.; Schrader, T. Interactions of Calix[n]Arenes with Nucleic Acids. *Nat Prod Commun* **2012**, *7* (3), 409–417.

(39) Dudic, M.; Colombo, A.; Sansone, F.; Casnati, A.; Donofrio, G.; Ungaro, R. A General Synthesis of Water Soluble Upper Rim Calix[n]Arene Guanidinium Derivatives Which Bind to Plasmid DNA. *Tetrahedron* **2004**, *60* (50), 11613–11618. https://doi.org/10.1016/j.tet.2004.09.047.

(40) Ak, M. S.; Deligöz, H. Azocalixarenes. 6: Synthesis, Complexation, Extraction and Thermal Behaviour of Four New Azocalix[4]Arenes. *J Incl Phenom Macrocycl Chem* **2007**, *59* (1–2), 115–123. https://doi.org/10.1007/s10847-007-9300-9.

(41) Elçin, S.; Ilhan, M. M.; Deligöz, H. Synthesis and Spectral Characterization of Azo Dyes Derived from Calix[4]Arene and Their Application in Dyeing of Fibers. *J Incl Phenom Macrocycl Chem* **2013**, *77* (1–4), 259–267. https://doi.org/10.1007/s10847-012-0240-7.

(42) Wang, J.; Bodige, S. G.; Watson, W. H.; Gutsche, C. D. Complexation of Fullerenes with 5,5'-Biscalix[5]Arene. *Journal of Organic Chemistry* **2000**, *65* (24), 8260–8263. https://doi.org/10.1021/jo000915w.

(43) Arora, V.; Chawla, H. M.; Santra, A. Synthesis of Selectively Formylated Calixarene Ethers. *Tetrahedron* **2002**, *58* (28), 5591–5597. https://doi.org/https://doi.org/10.1016/S0040-4020(02)00551-3.

(44) Selinger, A. J.; Hof, F. Adaptive Supramolecular Networks: Emergent Sensing from Complex Systems. *Angewandte Chemie International Edition* **2023**. https://doi.org/10.1002/anie.202312407.

(45) Ivanova, E. A.; Prokhorova, P. E.; Mitin, V. V.; Glukhareva, T. V.; Morzherin, Y. Y. Chlorination of Calix[4]Arene Derivatives. *Synth Commun* **2015**, *45* (13), 1592–1597. https://doi.org/10.1080/00397911.2015.1036452.

(46) Gunji, A.; Takahashi, K. Selective and Efficient Iodination of the P-Positions of Calix[4]Arene Derivatives. *Synthetic Communications*. Marcel Dekker Inc. 1998, pp 3933–3941. https://doi.org/10.1080/00397919808004951.

(47) Daze, K. D.; Ma, M. C. F.; Pineux, F.; Hof, F. Synthesis of New Trisulfonated Calix[4]Arenes Functionalized at the Upper Rim, and Their Complexation with the Trimethyllysine Epigenetic Mark. *Org Lett* **2012**, *14* (6), 1512–1515. https://doi.org/10.1021/ol300243b.

(48) Beatty, M. A.; Busmann, J. A.; Fagen, N. G.; Garnett, G. A. E.; Hof, F. A Clip-like Host That Undergoes Self-Assembly and Competitive Guest-Induced Disassembly in Water. *Supramol Chem* **2019**, *31* (3), 101–107. https://doi.org/10.1080/10610278.2018.1494275.

(49) Garnett, G. A. E.; Daze, K. D.; Peña Diaz, J. A.; Fagen, N.; Shaurya, A.; Ma, M. C. F.; Collins, M. S.; Johnson, D. W.; Zakharov, L. N.; Hof, F. Attraction by Repulsion: Compounds with like Charges Undergo Self-Assembly in Water That Improves in High Salt and Persists in Real Biological Fluids. *Chemical Communications* **2016**, *52* (13), 2768–2771. https://doi.org/10.1039/c5cc10527g.

(50) Tabet, S.; Douglas, S. F.; Daze, K. D.; Garnett, G. A. E.; Allen, K. J. H.; Abrioux, E. M. M.; Quon, T. T. H.; Wulff, J. E.; Hof, F. Synthetic Trimethyllysine Receptors That Bind Histone 3, Trimethyllysine 27 (H3K27me3) and Disrupt Its Interaction with the Epigenetic Reader Protein CBX7. *Bioorg Med Chem* **2013**, *21* (22), 7004–7010. https://doi.org/10.1016/j.bmc.2013.09.024.

(51) Ali, M.; Daze, K. D.; Strongin, D. E.; Rothbart, S. B.; Rincon-Arano, H.; Allen, H. F.; Li, J.; Strahl, B. D.; Hof, F.; Kutateladze, T. G. Molecular Insights into Inhibition of the Methylated Histone-Plant Homeodomain Complexes by Calixarenes. *Journal of Biological Chemistry* **2015**, *290* (38), 22919–22930. https://doi.org/10.1074/jbc.M115.669333.

(52) Allen, H. F.; Daze, K. D.; Shimbo, T.; Lai, A.; Musselman, C. A.; Sims, J. K.; Wade, P. A.; Hof, F.; Kutateladze, T. G. Inhibition of Histone Binding by Supramolecular Hosts. *Biochemical Journal* **2014**, *459* (3), 505–512. https://doi.org/10.1042/BJ20140145.

(53) Dudic, M.; Colombo, A.; Sansone, F.; Casnati, A.; Donofrio, G.; Ungaro, R. A General Synthesis of Water Soluble Upper Rim Calix[n]Arene Guanidinium Derivatives Which Bind to Plasmid DNA. *Tetrahedron* **2004**, *60* (50), 11613–11618. https://doi.org/10.1016/j.tet.2004.09.047.

(54) Gordo, S.; Martos, V.; Santos, E.; Mené Ndez §, M.; Bo, C.; Giralt, E.; De Mendoza, J. *Stability and Structural Recovery of the Tetramerization Domain of P53-R337H Mutant Induced by a Designed Templating Ligand*; 2008. www.pnas.org/cgi/content/full/.

(55) Nimse, S. B.; Kim, J.; Ta, V. T.; Kim, H. S.; Song, K. S.; Jung, C. Y.; Nguyen, V. T.; Kim, T. New Water-Soluble Iminecalix[4]Arene with a Deep Hydrophobic Cavity. *Tetrahedron Lett* **2009**, *50* (52), 7346–7350. https://doi.org/10.1016/j.tetlet.2009.10.058.

(56) da Silva, C. M.; da Silva, D. L.; Magalhães, T. F. F.; Alves, R. B.; de Resende-Stoianoff, M. A.; Martins, F. T.; de Fátima, Â. Iminecalix[4]Arenes: Microwave-Assisted Synthesis, X-Ray Crystal Structures, and Anticandidal Activity. *Arabian Journal of Chemistry* **2019**, *12* (8), 4365–4376. https://doi.org/10.1016/j.arabjc.2016.06.013.

(57) Burilov, V.; Makarov, E.; Mironova, D.; Sultanova, E.; Bilyukova, I.; Akyol, K.; Evtugyn, V.; Islamov, D.; Usachev, K.; Mukhametzyanov, T.; Solovieva, S.; Antipin, I. Calix[4]Arene Polyamine Triazoles: Synthesis, Aggregation and DNA Binding. *Int J Mol Sci* **2022**, *23* (23). https://doi.org/10.3390/ijms232314889.

(58) Zhou, H.; Wang, D. A.; Baldini, L.; Ennis, E.; Jain, R.; Carie, A.; Sebti, S. M.; Hamilton, A. D. Structure-Activity Studies on a Library of Potent Calix[4]Arene-Based PDGF Antagonists That Inhibit PDGF-Stimulated PDGFR Tyrosine Phosphorylation. *Org Biomol Chem* **2006**, *4* (12), 2376–2386. https://doi.org/10.1039/b515483a.

(59) Tsou, L. K.; Dutschman, G. E.; Gullen, E. A.; Telpoukhovskaia, M.; Cheng, Y. C.; Hamilton, A. D. Discovery of a Synthetic Dual Inhibitor of HIV and HCV Infection Based on a Tetrabutoxy-Calix[4]Arene Scaffold.

Bioorg Med Chem Lett **2010**, *20* (7), 2137–2139. https://doi.org/10.1016/j.bmcl.2010.02.043.

(60) Martos, V.; Bell, S. C.; Santos, E.; Isacoff, E. Y.; Trauner, D.; De Mendoza, J. *Calix[4]Arene-Based Conical-Shaped Ligands for Voltage-Dependent Potassium Channels*. www.pnas.org/cgi/content/full/.

(61) Roy, R.; Kim, J. M. Amphiphilic P-Tert-Butylcalix[4]Arene Containing Exposed Carbohydrate. *Angew. Chem. Int. Ed* **1999**, *38* (3), 224.

(62) Bagnacani, V.; Franceschi, V.; Fantuzzi, L.; Casnati, A.; Donofrio, G.; Sansone, F.; Ungaro, R. Lower Rim Guanidinocalix[4]Arenes: Macrocyclic Nonviral Vectors for Cell Transfection. *Bioconjug Chem* **2012**, *23* (5), 993–1002. https://doi.org/10.1021/bc2006829.

(63) Kassem, S.; Van Leeuwen, T.; Lubbe, A. S.; Wilson, M. R.; Feringa, B. L.; Leigh, D. A. Artificial Molecular Motors. *Chemical Society Reviews*. Royal Society of Chemistry May 7, 2017, pp 2592–2621. https://doi.org/10.1039/c7cs00245a.

(64) Broichhagen, J.; Frank, J. A.; Trauner, D. A Roadmap to Success in Photopharmacology. *Acc Chem Res* **2015**, *48* (7), 1947–1960. https://doi.org/10.1021/acs.accounts.5b00129.

(65) Li, Q. *Photoactive Functional Soft Materials : Preparation, Properties, and Applications*.

(66) Spiegel, C. A.; Hippler, M.; Münchinger, A.; Bastmeyer, M.; Barner-Kowollik, C.; Wegener, M.; Blasco, E. 4D Printing at the Microscale. *Adv Funct Mater* **2020**, *30* (26). https://doi.org/10.1002/adfm.201907615.

(67) Wang, C.; Liu, Y. Cucurbit[8]Uril-Induced Diarylethene Thermally Activated Delay Fluorescence Supramolecular Switch for Sequential

Energy Transfer. *Mater Today Chem* **2022**, *25*. https://doi.org/10.1016/j.mtchem.2022.100954.

(68) Yang, L.; Li, Y.; Zhang, H.; Tian, C.; Cao, Q.; Xiao, Y.; Yuan, L.; Liu, G. Photoisomerization, Assembling and Fluorescence Photoswitching Behaviors of a Water-Soluble Stiff-Stilbene with Cucurbit[7]Uril. *Chinese Chemical Letters* **2023**, *34* (8). https://doi.org/10.1016/j.cclet.2022.108108.

(69) Baroncini, M.; Gao, C.; Carboni, V.; Credi, A.; Previtera, E.; Semeraro, M.; Venturi, M.; Silvi, S. Light Control of Stoichiometry and Motion in Pseudorotaxanes Comprising a Cucurbit[7]Uril Wheel and an Azobenzene-Bipyridinium Axle. *Chemistry - A European Journal* **2014**, *20* (34), 10737–10744. https://doi.org/10.1002/chem.201402821.

(70) Liu, G.; Zhang, H.; Xu, X.; Zhou, Q.; Dai, X.; Fan, L.; Mao, P.; Liu, Y. Supramolecular Photoswitch with White-Light Emission Based on Bridged Bis(Pillar[5]Arene)s. *Mater Today Chem* **2021**, *22*. https://doi.org/10.1016/j.mtchem.2021.100628.

(71) Qiao, F.; Lian, Z.; Yuan, Z.; Chen, M. N.; Jiang, M.; Wang, R. Z.; Xing, L. B. A Photo-Switchable Supramolecular Hyperbranched Polymer with Aggregation-Induced Emission Based on Host-Guest Interaction. *Dyes and Pigments* **2019**, *163*, 594–599. https://doi.org/10.1016/j.dyepig.2018.12.055.

(72) Xiao, W.; Chen, W. H.; Zhang, J.; Li, C.; Zhuo, R. X.; Zhang, X. Z. Design of a Photoswitchable Hollow Microcapsular Drug Delivery System by Using a Supramolecular Drug-Loading Approach. *Journal of Physical Chemistry B* **2011**, *115* (46), 13796–13802. https://doi.org/10.1021/jp208692c.

(73) Gromov, S. P.; Vedernikov, A. I.; Lobova, N. A.; Kuzmina, L. G.; Dmitrieva, S. N.; Strelenko, Y. A.; Howard, J. A. K. Synthesis, Structure, and Properties of Supramolecular Photoswitches Based on Ammonioalkyl Derivatives of Crown Ether Styryl Dyes. *Journal of Organic Chemistry* **2014**, *79* (23), 11416–11430. https://doi.org/10.1021/jo5018074.

(74) Mukherjee, A.; Seyfried, M.; Ravoo, B. J. Azoheteroarene and Diazocine Molecular Photoswitches: Self-Assembly, Responsive Materials and Photopharmacology. *Angewandte Chemie International Edition* **2023**. https://doi.org/10.1002/anie.202304437.

(75) Basílio, N.; Pischel, U. Drug Delivery by Controlling a Supramolecular Host–Guest Assembly with a Reversible Photoswitch. *Chemistry - A European Journal* **2016**, *22* (43), 15208–15211. https://doi.org/10.1002/chem.201603331.

(76) Liu, G.; Xu, X.; Chen, Y.; Wu, X.; Wu, H.; Liu, Y. A Highly Efficient Supramolecular Photoswitch for Singlet Oxygen Generation in Water. *Chemical Communications* **2016**, *52* (51), 7966–7969. https://doi.org/10.1039/c6cc02996e.

(77) Pipoosananakaton, B.; Sukwattanasinitt, M.; Jaiboon, N.; Chaichit ： , N.; Tuntulani, T. *New Azobenzene Crown P-Tert-Butylcalix[4]Arenes as Switchable Receptors for Na+ and K+ Ions: Synthesis and Isomerization Studies*; 2000; Vol. 21.

(78) Saadioui, M.; Asfari, Z.; Vicens, J. *Synthesis and Characterisation of Two Azobenzene Modified 1,3-Calix[4]-b/s-Crowns as Artificial Potentially Allosteric Systems*; 1997; Vol. 38.

(79) Sukwattanasinitt, M.; Rojanathanes, R.; Tuntulani, T.; Sritana-Anant, Y.; Ruangpornvisuti, V. *Synthesis of Stilbene Crown Ether P-Tert-Butylcalix[4]Arenes*; 2001; Vol. 42.

(80) Grubert, L.; Abraham, W. Photoswitchable Calix[4]Arenes Bearing Dihydroacridine Substituents at the Upper Rim. *Tetrahedron* **2007**, *63* (44), 10778–10787. https://doi.org/10.1016/j.tet.2007.06.126.

(81) Grubert, L.; Hennig, H.; Grummt, U. W.; Abraham, W. Photoswitchable Ionophores Based on 1,3-Alternate Calix[4]Arenes Bearing Acridane Units at the Wide Rim and Bridged at the Narrow Rim by Glycol Chains. *Tetrahedron* **2009**, *65* (40), 8402–8406. https://doi.org/10.1016/j.tet.2009.07.096.

(82) Tsudera, T.; Ikeda, A.; Shinkai, S. *Light-Switched Metal-Tunneling across a π-Basic Tube of 1,3-Alternate-Calix[4]Arenes*; 1997; Vol. 53.

(83) Schäfer, C.; Decker, B.; Letzel, M.; Novara, F.; Eckel, R.; Ros, R.; Anselmetti, D.; Mattay, J. On the Way to Supramolecular Photochemistry at the Single-Molecule Level. In *Pure and Applied Chemistry*; 2006; Vol. 78, pp 2247–2259. https://doi.org/10.1351/pac200678122247.

(84) Serrano, J. L.; Concellón, A.; Marín, I.; Barberá, J.; Marcos, M. Ionic Liquid Crystalline Calixarene with Photo-switchable Proton Conduction. *Helv Chim Acta* **2023**. https://doi.org/10.1002/hlca.202300010.

(85) Beatty, M. A.; Borges-González, J.; Sinclair, N. J.; Pye, A. T.; Hof, F. Analyte-Driven Disassembly and Turn-On Fluorescent Sensing in Competitive Biological Media. *J Am Chem Soc* **2018**, *140* (10), 3500–3504. https://doi.org/10.1021/jacs.7b13298.

(86) Tyson, J. C.; Collard ?, D. M.; Hughes, K. D. *Chromophoric Water-Soluble Tetrakis(4-Carboxyphenylazo)-Calix[4]Arene: Binding of Arylammonium Ions and Benzene*; Kluwer Academic Publishers, 1997; Vol. 29.

(87) Petermayer, C.; Dube, H. Indigoid Photoswitches: Visible Light Responsive Molecular Tools. *Acc Chem Res* **2018**, *51* (5), 1153–1163. https://doi.org/10.1021/acs.accounts.7b00638.

(88) Kink, F.; Collado, M. P.; Wiedbrauk, S.; Mayer, P.; Dube, H. Bistable Photoswitching of Hemithioindigo with Green and Red Light: Entry Point to Advanced Molecular Digital Information Processing. *Chemistry - A European Journal* **2017**, *23* (26), 6237–6243. https://doi.org/10.1002/chem.201700826.

(89) Hean, D.; Alde, L. G.; Wolf, M. O. Photosalient and Thermosalient Crystalline Hemithioindigo-Anthracene Based Isomeric Photoswitches. *J Mater Chem C Mater* **2021**, *9* (21), 6789–6795. https://doi.org/10.1039/d1tc01358k.

(90) Kohl, F.; Gerwien, A.; Hampel, F.; Mayer, P.; Dube, H. Hemithioindigo-Based Trioxobicyclononadiene: 3D Multiswitching of Electronic and Geometric Properties. *J Am Chem Soc* **2022**, *144* (7), 2847–2852. https://doi.org/10.1021/jacs.1c12364.

(91) Berdnikova, D. V. Visible-Range Hemi-Indigo Photoswitch: ON-OFF Fluorescent Binder for HIV-1 RNA. *Chemical Communications* **2019**, *55* (58), 8402–8405. https://doi.org/10.1039/c9cc04270a.

(92) Petermayer, C.; Thumser, S.; Kink, F.; Mayer, P.; Dube, H. Hemiindigo: Highly Bistable Photoswitching at the Biooptical Window. *J Am Chem Soc* **2017**, *139* (42), 15060–15067. https://doi.org/10.1021/jacs.7b07531.

(93) Waldeck, D. H. *Photoisomerization Dynamics of Stilbenes*; 1991; Vol. 91. https://pubs.acs.org/sharingguidelines.

(94) Berdnikova, D. V. Design, Synthesis and Investigation of Water-Soluble Hemi-Indigo Photoswitches for Bioapplications. *Beilstein Journal of Organic Chemistry* **2019**, *15*, 2822–2829. https://doi.org/10.3762/bjoc.15.275.

(95) Garnett, G. A. E.; Daze, K. D.; Peña Diaz, J. A.; Fagen, N.; Shaurya, A.; Ma, M. C. F.; Collins, M. S.; Johnson, D. W.; Zakharov, L. N.; Hof, F. Attraction by Repulsion: Compounds with like Charges Undergo Self-Assembly in Water That Improves in High Salt and Persists in Real Biological Fluids. *Chemical Communications* **2016**, *52* (13), 2768–2771. https://doi.org/10.1039/c5cc10527g.

(96) Thondorf, I.; Brenn, J. *Conformations of Calix[5]Arenes-a Molecular Mechanics Study*; 1997.

(97) Dalgarno, S. J.; Atwood, J. L.; Raston, C. L. Host-Guest Complexes with p-Sulfonatocalix[4,5]Arenes Charged Crown Ethers and Lanthanides: Factors Affecting Molecular Capsule Formation. *Cryst Growth Des* **2006**, *6* (1), 174–180. https://doi.org/10.1021/cg050261q.

(98) Ling, I.; Alias, Y.; Skelton, B. W.; Raston, C. L. Conformationally Flexible P-Sulfonated Calix[5]Arene Binding with Large Bis-Phosphonium Cations. *Cryst Growth Des* **2012**, *12* (3), 1564–1570. https://doi.org/10.1021/cg201615u.

(99) C. David Gutsche*; Lorenz J. Bauer. Calixarenes. 13. The Conformational Properties of Calix[4]Arenes, Calix[6]Arenes, Calix[8]Arenes, And. *J. Am. Chem. Soc.* **1985**, *107*, 6052–6059.

(100) Gutsche, C. D.; Bauer, L. J. Calixarenes. 13. The Conformational Properties of Calix[4]Arenes, Calix[6]Arenes, Calix[8]Arenes, and Oxacalixarenes. *J Am Chem Soc* **1985**, *107* (21), 6052–6059. https://doi.org/10.1021/ja00307a038.

(101) Rehm, M.; Frank, M.; Schatz, J. Water-Soluble Calixarenes—Self-Aggregation and Complexation of Noncharged Aromatic Guests in Buffered Aqueous Solution. *Tetrahedron Lett* **2009**, *50* (1), 93–96. https://doi.org/https://doi.org/10.1016/j.tetlet.2008.10.089.

(102) Basilio, N.; García-Río, L.; Martín-Pastor, M. NMR Evidence of Slow Monomer−Micelle Exchange in a Calixarene-Based Surfactant. *J Phys Chem B* **2010**, *114* (14), 4816–4820. https://doi.org/10.1021/jp910984g.

(103) Bauer, L. J.; Gutsche, C. D. Calixarenes. 15. The Formation of Complexes of Calixarenes with Neutral Organic Molecules in Solution. *J Am Chem Soc* **1985**, *107* (21), 6063–6069. https://doi.org/10.1021/ja00307a040.

(104) Shinkai, S.; Araki, K.; Matsuda, T.; Manabe, O. NMR Determination of Association Constants for Aqueous Calixarene Complexes and Guest Template Effects on the Conformational Freedom. *Bull Chem Soc Jpn* **1989**, *62* (12), 3856–3862. https://doi.org/10.1246/bcsj.62.3856.

(105) Kalchenko, O.; Cherenok, S.; Suikov, S.; Kalchenko, V. Study of Calixarene Complexation with Biologically Active Carboxylic Acids by RP HPLC Method. *J Chem* **2017**, *05* (02), 49–55.

(106) Masci, B.; Finelli, M.; Varrone, M. Fine Tuning of the Cavity Size in Calixarene-like Cyclophanes: A Complete Series of Homooxacalix[4]Arene Ligands for Quaternary Ammonium Ions. *Chemistry - A European Journal* **1998**, *4* (10), 2018–2030.

https://doi.org/10.1002/(sici)1521-3765(19981002)4:10<2018::aid-chem2018>3.0.co;2-i.

(107) Claridge, T. D. W. Introducing Two-Dimensional and Pulsed Field Gradient NMR. In *High-Resolution NMR Techniques in Organic Chemistry*; Elsevier, 2016; pp 171–202. https://doi.org/10.1016/b978-0-08-099986-9.00005-1.

(108) Claridge, T. D. W. Correlations Through the Chemical Bond I: Homonuclear Shift Correlation. In *High-Resolution NMR Techniques in Organic Chemistry*; Elsevier, 2016; pp 203–241. https://doi.org/10.1016/b978-0-08-099986-9.00006-3.

(109) Columbus, I.; Biali, S. E. *Totally and Partially Saturated Calixarene Analogues*; 1998. https://pubs.acs.org/sharingguidelines.

(110) Kliachyna, M. A.; Yesypenko, O. A.; Pirozhenko, V. V.; Shishkina, S. V.; Shishkin, O. V.; Boyko, V. I.; Kalchenko, V. I. Synthesis, Optical Resolution and Absolute Configuration of Inherently Chiral Calixarene Carboxylic Acids. *Tetrahedron* **2009**, *65* (34), 7085–7091. https://doi.org/10.1016/j.tet.2009.06.039.

(111) Bozkurt, S. Calixarene Based Chiral Solvating Agents for α-Hydroxy Carboxylic Acids. *J Mol Struct* **2013**, *1048*, 113–120. https://doi.org/10.1016/j.molstruc.2013.05.032.

(112) Claridge, T. D. W. Correlations Through Space: The Nuclear Overhauser Effect. In *High-Resolution NMR Techniques in Organic Chemistry*; Elsevier, 2016; pp 315–380. https://doi.org/10.1016/b978-0-08-099986-9.00009-9.

(113) Puchta, R.; Clark, T.; Bauer, W. The Formation of Endo-Complexes between Calixarenes and Amines - A Reinvestigation. *J Mol Model* **2006**, *12* (5), 739–747. https://doi.org/10.1007/s00894-005-0079-6.

(114) Gutsche, C. D.; Iqbal, M.; Alam, I. Calixarenes. 20. The Interaction of Calixarenes and Amines. *J Am Chem Soc* **1987**, *109* (14), 4314–4320. https://doi.org/10.1021/ja00248a029.

(115) Syakaev, V. V; Shalaeva, Ya. V; Kazakova, E. Kh.; Morozova, Yu. E.; Makarova, N. A.; Konovalov, A. I. Aggregation and Complexation in a Series of Tetramethylenesulfonate-Substituted Calix[4]Resorcinarenes. *Colloid Journal* **2012**, *74* (3), 346–355. https://doi.org/10.1134/S1061933X12030118.

(116) Syakaev, V. V.; Mustafina, A. R.; Elistratova, J. G.; Latypov, S. K.; Konovalov, A. I. Head-to-Tail Aggregates of Sulfonatomethylated Calix[4]Resorcinarene in Aqueous Solutions. *Supramol Chem* **2008**, *20* (5), 453–460. https://doi.org/10.1080/10610270701310930.

(117) Stilbs, P. Fourier Transform Pulsed-Gradient Spin-Echo Studies of Molecular Diffusion. *Prog Nucl Magn Reson Spectrosc* **1987**, *19* (1), 1–45. https://doi.org/https://doi.org/10.1016/0079-6565(87)80007-9.

(118) Cohen, Y.; Avram, L.; Frish, L. Diffusion NMR Spectroscopy in Supramolecular and Combinatorial Chemistry: An Old Parameter - New Insights. *Angewandte Chemie - International Edition*. January 14, 2005, pp 520–554. https://doi.org/10.1002/anie.200300637.

(119) Claridge, T. D. W. Diffusion NMR Spectroscopy. In *High-Resolution NMR Techniques in Organic Chemistry*; Elsevier, 2016; pp 381–419. https://doi.org/10.1016/b978-0-08-099986-9.00010-5.

(120) Pisagatti, I.; Barbera, L.; Gattuso, G.; Villari, V.; Micali, N.; Fazio, E.; Neri, F.; Parisi, M. F.; Notti, A. Tuning the Aggregation of an Amphiphilic Anionic Calix[5]Arene by Selective Host-Guest Interactions with Bola-Type Dications. *New Journal of Chemistry* **2019**, *43* (20), 7628–7635. https://doi.org/10.1039/c9nj01198f.

(121) Gaeta, C.; Caruso, T.; Mincolelli, M.; Troisi, F.; Vasca, E.; Neri, P. P-Sulfonatocalix[7]Arene: Synthesis, Protolysis, and Binding Ability. *Tetrahedron* **2008**, *64* (22), 5370–5378. https://doi.org/10.1016/j.tet.2008.03.017.

(122) Specht, A.; Ziarelli, F.; Bernard, P.; Goeldner, M.; Peng, L. Para-Sulfonated Calixarenes Used as Synthetic Receptors for Complexing Photolabile Cholinergic Ligand. *Helv Chim Acta* **2005**, *88* (10), 2641–2653. https://doi.org/10.1002/hlca.200590205.

(123) Cohen, Y.; Slovak, S. Diffusion NMR for the Characterization, in Solution, of Supramolecular Systems Based on Calixarenes, Resorcinarenes, and Other Macrocyclic Arenes. *Organic Chemistry Frontiers* **2019**, *6* (10), 1705–1718. https://doi.org/10.1039/c9qo00329k.

(124) Hanwell, M. D.; Curtis, D. E.; Lonie, D. C.; Vandermeersch, T.; Zurek, E.; Hutchison, G. R. SOFTWARE Open Access Avogadro: An Advanced Semantic Chemical Editor, Visualization, and Analysis Platform. *J Cheminform* **2012**, *4*, 17.

(125) Claridge, T. D. W. Introducing High-Resolution NMR. In *High-Resolution NMR Techniques in Organic Chemistry*; Elsevier, 2016; pp 11–59. https://doi.org/10.1016/b978-0-08-099986-9.00002-6.